Skin Electronics: Next-Generation Device Platform for Virtual and Augmented Reality

Article *in* Advanced Functional Materials · February 2021

DOI: 10.1002/adfm.202009602

6 authors, including:

Yan Wang
The University of Tokyo
37 PUBLICATIONS **2,466** CITATIONS
SEE PROFILE

Haoyang Wang
Sungkyunkwan University
10 PUBLICATIONS **316** CITATIONS
SEE PROFILE

Takao Someya
The University of Tokyo
357 PUBLICATIONS **37,181** CITATIONS
SEE PROFILE

ADVANCED FUNCTIONAL MATERIALS
www.afm-journal.de

Skin Electronics: Next-Generation Device Platform for Virtual and Augmented Reality

Jae Joon Kim, Yan Wang,* Haoyang Wang, Sunghoon Lee, Tomoyuki Yokota, and Takao Someya*

Virtual reality (VR) and augmented reality (AR) are overcoming the physical limits of real-life using advances in devices and software. In particular, the recent restrictions in transportation from the coronavirus disease 2019 (COVID-19) pandemic are making people more interested in these virtual experiences. However, to minimize the differences between artificial and natural perception, more human-interactive and human-like devices are necessary. The skin is the largest organ of the human body and interacts with the environment as the site of interfacing and sensing. Recent progress in skin electronics has enabled the use of the skin as the mounting object of functional devices and the signal pathway bridging humans and computers, with opening its potential in future VR and AR applications. In this review, the current skin electronics are summarized as one of the most promising device solutions for future VR/AR devices, especially focusing on the recent materials and structures. After defining and explaining VR/AR systems and the components, the advantages of skin electronics for VR/AR applications are emphasized. Next, the detailed functionalities of skin electronic devices, including the input, output, energy devices, and integrated systems, are reviewed for future VR/AR applications.

1. Introduction

Virtual reality (VR) and augmented reality (AR) are overcoming the physical limits of real life and allow us to experience the digitally modified or substituted reality. In VR and AR, the user is immersed in the virtual space/object without interacting with the real space, or co-interacting with both virtual and real spaces, respectively.[1] The recent development of hardware and software has enabled many applications including healthcare,[2d] manufacturing,[3] entertainment,[4] tourism,[5] construction,[6] and education.[7] In particular, the transportation restrictions from the coronavirus disease 2019 (COVID-19) pandemic are making people more interested in the VR/AR technology based on their intact and spatially unlimited nature.[8] To achieve these secondary experiences and mitigate situational restrictions, VR or AR is selectively used based on their functionality differences. However, conventional VR and AR devices have unfavorable wearing awareness due to their bulkiness, poor adhesion to the body, and overweight. By introducing mechanically complimentary and human-friendly devices, the user discomfort is decreased and consequently, the higher quality of AR/VR experiences can be achieved.

Skin electronics or epidermal electronics refer to a research field associated with the fabrication and utilization of electronic devices that have thinness, lightness, and skin-like functionalities such as softness, flexibility, and stretchability.[9] In general, these devices are noninvasively and conformally mounted on human skin and based on systematically designed materials and structures, generating minimized perceptual differences with the human skin. Therefore, we propose the skin electronic devices as the next-generation devices in AR/VR applications for their skin-like properties and advantageous functionalities compared to the conventional AR/VR devices. As summarized in **Figure 1**, the flexible, thin, and lightweight skin electronic devices are distinguishable from the rigid, thick, and heavy conventional VR/AR devices. This low-wearing discomfort of skin electronic devices is highly beneficial for VR/AR based on the improved user immersion and convenience.[10] In terms of the functionalities, skin electronic devices less-limit the sensing of skin and user physiology compared to the conventional bulky devices. The enhanced device–user interaction in skin electronic VR/AR devices leads to the advanced qualities of the signal acquisition and output feedback. These novel advantages make skin electronics as one of the most important technologies for the next-generation devices in VR/AR applications.

For the successful placement and stable operation on the skin, it is mandatory that the utilized functional materials and device structures constitute similar mechanical properties to the skin. In addition, for the proper sensor and stimulator, appropriate choices of functional optoelectronic and electrochemical materials and robust structures should be considered while maintaining their performance under repetitive bending or stretching. In terms of the system integration, the

Dr. J. J. Kim, Dr. Y. Wang, H. Wang, Prof. S. Lee, Prof. T. Yokota, Prof. T. Someya
Department of Electrical Engineering and Information Systems
School of Engineering
The University of Tokyo
7-3-1 Hongo, Bunkyo-ku, Tokyo 113-8656, Japan
E-mail: jj.kim@ntech.t.u-tokyo.ac.jp; yan.wang@ntech.t.u-tokyo.ac.jp
The ORCID identification number(s) for the author(s) of this article can be found under https://doi.org/10.1002/adfm.202009602.

DOI: 10.1002/adfm.202009602

Figure 1. Schematic illustrations of conventional and skin electronic VR/AR devices and the comparison.

interconnected and integrated approaches in data and power are also necessary for the operation of the VR/AR devices.

However, there has been no representative study reviewing or summarizing the skin electronic devices from the viewpoint of potential application in VR/AR, especially focusing on the highly demanding materials and structural designs. Indeed, there are large technical gaps between the current skin electronics and AR/VR applications. But advanced skin electronic devices are promising alternatives for conventional AR/VR devices. For example, advanced on-skin smart displays directly interfaced on the arm can be used as future AR devices instead of bulky smartphones. In addition, for the audio input and output, the bulky and rigid microphone and headset can be replaced by skin-attached soft electronic counterparts. With these aspects, we believe that skin electronic devices can be used as the advanced devices for the VR/AR applications.

In this review, we present an overview of the advantages and recent progress of skin electronic devices for potential VR/AR applications based on their materials, structures, and functionalities. Section 2 defines and explains the VR/AR system and components, and the necessities of using skin electronics. Sections 3 and 4 explain the input sensor and output stimulator built on the skin, which can be utilized before and after VR/AR processing, respectively. Sections 5 and 6 introduce the on-skin energy sources and the integrated systems necessary for the VR/AR device.

2. VR/AR Systems and Skin Electronics

For the proper application of skin electronics in VR/AR, a fundamental understanding of VR and AR systems and the human sensory system is important. In this section, we will discuss the similarities and differences between VR and AR and investigate how humans perceive the external physical stimuli generated by both physical reality and/or VR/AR output. Based on this understanding, the promising advantages of skin electronics for VR/AR applications will be discussed.

2.1. VR and AR System

In the VR/AR system, the VR/AR components are placed between reality and humans for the additional sensing and stimulating. The VR and AR systems are mainly composed of input devices, output devices, and processors (**Figure 2**).[11] Other components such as blocking/sense-through part, and communication modules are also included. Depending on the usage of VR or AR and its purpose, an appropriate system should be designed and constructed.

2.1.1. Components

Input Device: To initiate the VR/AR process, it is necessary for the devices to obtain information from physical reality and the user. By receiving the external stimuli using detectors, sensors, or transducers, the VR/AR system can acknowledge the relative condition of the user to the surrounding environment for proper interaction. There can be several types of input devices based on the source type and purpose of interaction.[12] 1) First, in the case of external input devices such as a camera or microphone, the information of physical reality is collected and transduced from the specific physical stimuli to

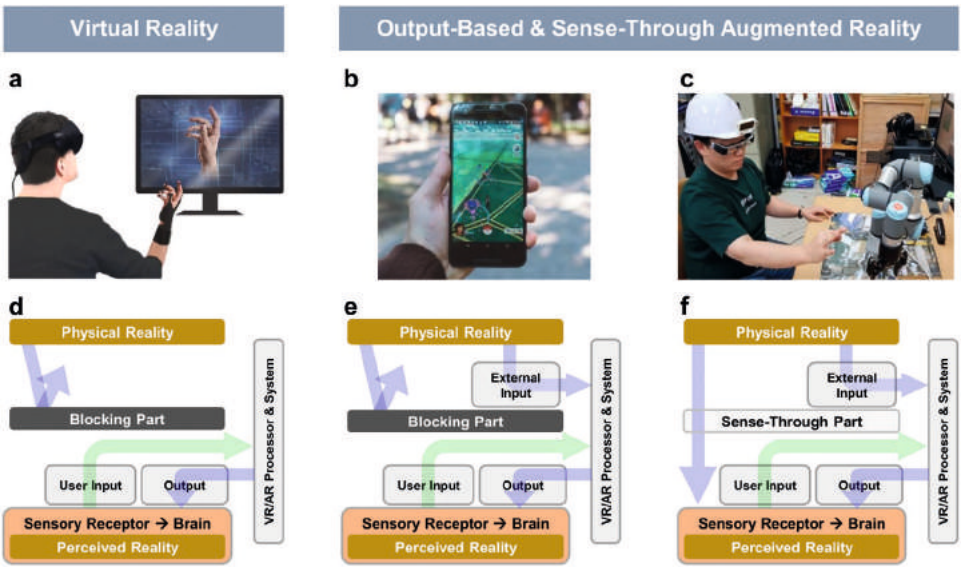

Figure 2. Demonstrations and schematic illustrations of VR and AR. a) VR goggle and glove demonstration. Reproduced under terms of the CC-BY license.[2a] Copyright 2019, Kahye Song, Sung Hee Kim, Sungho Jin, Sohyun Kim, Sunho Lee, Jun-Sik Kim, Jung-Min Park and Youngsu Cha, published by Springer Nature. b) AR game demonstration of Pokemon Go. Reproduced under terms of the CC-BY license.[2b] Copyright 2020, Levente Juhász, Tessio Novack, Hartwig H. Hochmair and Sen Qiao, published by MDPI. c) Smart AR glasses and the demonstration. Reproduced under terms of the CC-BY license.[2c] Copyright 2019, Minseok Kim, Sung Ho Choi, Kyeong-Beom Park and Jae Yeol Lee, published by MDPI. d) The scheme of VR. The reality is exclusively blocked. e,f) The scheme of AR. Stimuli from the physical reality are e) entirely blocked and accepted only by the external sensor in output-based AR or f) accepted both by the external sensor and our sensory organs by the sense-through AR system.

the electrical signal by the corresponding device. 2) Another input device type is the motion tracking device or body position sensor obtaining the exact spatial information of the user. This is especially important for proper definition of the user status and establish the proper user–device interaction. Several types of devices based on magnetic, acoustic, optical, mechanical, and biological mechanisms are being used.[13] 3) Besides the input devices for the external physical information, the biosensors are also used as the input devices of physiological body signals. It provides information to the position or movement of the muscle (by measuring strain or electromyography, EMG) and eyeball (electrooculography, EOG).[14] Additionally, the physiological measurement of health conditions such as electrocardiography (ECG), electroencephalography (EEG), heartbeat, glucose level, and body temperature is crucial to detect and prevent unfavorable sickness during the VR/AR process.[15] 4) Finally, the user input devices are similar, but instead of passively accepting the body signal, these can be used for the interfacing devices of the output from the user.[16] Similar to the case of a keyboard or mouse, these components enable the user to actively interact with the VR/AR environment.

Output Device: The substitution or modification of reality can be achieved by this device–human interactive component. It provides signal or feedback from the processor to stimulate our sensory system by proper signal transduction. Because it requires interaction with human sensory receptors, it can be classified using the vision, auditory, smell, taste haptic, and temperature. The most common and indispensable output devices are wearable displays. Depending on the coverage of view angle and transparency, different kinds of displays such as glasses, head-mounted displays, contact lenses, and portable devices are being used in AR or VR. Auditory sensing is achieved using speakers, and for the proper sense of space and distance, the 3D aspect should be considered. Haptic or touch is another stimulator that is frequently achieved by glove-type devices.[17] Recently, a few examples of temperature, smell, and taste have been demonstrated using portable and wearable devices.[18]

Blocking and Sense-Through Part: To achieve a successful VR or AR experience and create the perception that we are in a real or artificial space, the proper prevention or acceptance of physical reality to our sensory receptors is crucial. In the vision of AR, this allowance of sensory acceptance can be achieved with "video-based AR" (Figure 2b) and another type as "see-through AR" (Figure 2c).[1a] In this review, we extend these concepts to include other sensory systems by define "output-based AR" (Figure 2e) and "sense-through AR" (Figure 2f) depending on whether the user sensed reality comes from all artifacts and whether the physical reality is completely blocked. Especially in visual sensing, this greatly affects the materials, structures, and the design of overall equipment, including the thickness, bulkiness, heaviness, and type of device. For example, the device type of glasses or contact lenses cannot be used for VR because of the lack of the blocking part. For hearing, the blocking is also available by the noise-canceling headset, which removes the external sound input. However, for haptic, taste, and smell sense, it is difficult to block the external signal entirely.[19]

Processors: VR/AR applications ask for the construction of video in display and the processing of camera captured video stream, which usually rely on highly compute-intensive convolutional neural networks.[20] Under these circumstances, the high-performance graphics processing unit (GPU) plays an important role in video data processing.[21] For proper interpretation and feedback to the input signals, processing, and

characterizing, these signals efficiently may require the assistance of advanced machine learning methods such as neural networks. To accelerate this procedure to match the real-time demand in VR/AR, a specially designed neural processing unit (NPU) or tensor processing unit (TPU) can be adopted in the VR/AR system.[22]

Communication Modules: Currently, most VR/AR devices rely on wired connections to transfer data with a display or outside servers, where a high capacity in communication is required. With the evolution of wireless communication technologies, high-speed wireless connection through 5G, Wi-Fi 6, or their future versions has become promising for realizing a fully wireless VR/AR system.[23] Wireless connection to on-skin electronics is also critical for improving imperceptibility and manipulability. Facilitated wireless communication methods such as Bluetooth are preferable here considering the lower data transmission and the requirement of device miniaturization.

2.1.2. VR System

As shown in Figure 2a of the visional VR device, VR blocks user sensing of the external real environment, and instead, the artificially created reality substitutes it.[24] Within this immersion, people perceive themselves as being in a different space that is virtually created. The immersion or isolation from reality gives VR devices different functionalities and requirements from physical reality or AR. Considering the importance of vision in our perception, the VR experience is typically accomplished by a head-mounted display, which completely replaces the user's view of the physical environment with the interactive artificial environment.[11] The demands of both vision blocking and providing a full-angle view for the entire substitution of vision prevent the use of a see-through display system, which allows the acceptance of visual sensing from the environment to our sensory systems, such as glasses or contact lenses in VR.[25] Beyond visual and auditory interactions, other devices using tactic sensory receptors such as haptic gloves and suits have been intensively focused and developed recently.[11] This can be applied to multiple and comprehensive sensing for a higher degree of immersion and for specific applications where user input is crucial such as gaming or virtual medical operation. The VR device demonstration of other kinds of sensing using taste or smell is quite limited.[26] Therefore, for the successful demonstration of VR, not only functional components composing VR such as sensors or stimulators, but also the blocking part without disturbing our natural movement and sense is mandatory.

2.1.3. AR System

In the case of AR, most environmental information is delivered to the human sensory system with only partial substitution or recreation as the purpose of AR.[27] The example of the Pokémon Go game in Figure 2b shows that the image of the game character partially substitutes the real view of the background.[28] This acceptance of environmental information allows people to keep their perception of placement in the real space instead of a virtually made space except for several points of interest.

To achieve this environmentally interactive reality, two methods are utilized depending on the method of delivering environment conditions to the human sensory system, as explained in the previous section.[29] First, in the output-based (video-based) AR, the environmental conditions can be entirely captured by external sensors without human sensing. Instead, the collected and processed signals are given to the human sensor system through the output devices with the corresponding signals matching. For example, as shown in Figure 2b, we accept the external signal using the camera on the portable device. The vision of humans is used only for signal acquisition from the display, not directly to the environment. The game character is added by AR processing and visualized on the view of the environment. This method has an advantage in AR processing because it is easy to add the AR effect on the environmental signal after its capture and digitalization. However, the digitalization can lead to distortion or limit the real environmental conditions that prevent and affect the natural perceptive ability of the user.[30] In addition, as in the case of VR, the necessity of the blocking layer results in the selection of materials and structures being one of the major factors determining the device's weight and bulkiness.

The second sense-through (see-through) AR uses both human sensing and processed output from AR. Similar to the case of AR glasses in Figure 2c, the external visual information is delivered using a visional sensory system and captured by the camera simultaneously, without disturbing our visional sensing. This captured image is sent to the output display after the AR processing, similar to the artificial views on the air in Figure 2c. This technique has advantages in its simplicity of sensing. However, this partial acceptance of the external signal is highly limited by the functionality and/or positioning of the devices, so the distortion of the reality and user inconvenience inevitably occurs. One of the solutions for this is using multiple input devices for integrated sense through.[31] By making a substrate and entire devices including the input device, output device, processor, and connections such as sense through, we can efficiently deliver the external stimuli with minimized distortion, as in the case of AR contact lenses in vision. Likewise, this concept can be expanded to sound, taste, smell, temperature, tactics, and other sensory perceptions. In the case of vision and sound, sophisticated choices of materials and structures are required to achieve see-through or sense-through devices. For chemical sensing such as smelling, tasting, or mechanical sensing such as tactile or kinesthetic, it is extremely difficult to find the materials and structures completely blocking the external signal, so recently developed AR devices having these sensory systems have sense-through properties.[32] Although recent demonstration of AR outputs is extending the user experiences from only vision or audio to touch, temperature, and smell, bulky and heavy equipment are still one of the biggest limiting factors for device development.[33]

Compared with the early stage, there have been huge advances in both VR and AR such as power consumption control, high-resolution visualization, human–machine interaction, and software process.[34] For these advanced functionalities and effective VR/AR, appropriate materials and devices

are mandatory. In addition, the sensing differences between external devices and humans are still exist as one of the biggest bottlenecks. Except for a few examples such as smart contact lenses,[35] the physical volume or weight of equipment give unfavorable discomfort from the additional sense of device wearing and limiting the natural motion.[36] To minimize these device-induced artifacts, more flexible, light, thin, and long-term-applicable devices having higher similarity with the human are favored.

2.2. Advantages of Skin Electronics in VR/AR

Compared with conventional VR/AR devices, skin electronic devices have huge potential in applications based on the advantages of skin-interfacing and skin-like properties as summarized in Figure 1.

2.2.1. Low Wearing Discomfort

Recent advances in soft electronic materials enable the stable mounting and adhesion of devices directly onto the skin by minimizing mechanical mismatch with the skin.[37] The choice of materials having low Young's modulus and intrinsically reorientable structures with partially unfilled voids made the devices skin-like in flexibility and stretchability while maintaining their functionalities. Together with the skin-like mechanical properties, relatively small, ultrathin, and ultralight-weight skin electronic devices do not limit the motion and sense of humans during the VR/AR process, making the mounting of devices with very low wearing discomfort and consciousness. In addition, the permeability to water, air, and sweat created by the voids in the substrates make the long-term usage of devices more applicable.[38]

2.2.2. Maintenance of Skin Sensing

We can take advantage of the functionality of the skin as a haptic and temperature sensor covering most parts of our body. In VR/AR, the recent technical development of both hardware and software in haptic and vibrational feedbacks has opened many applications based on its emotional aspects.[39] The use of skin electronics enables natural skin sensing, including touch, texture, pressure, hardness, and roughness compared to the other devices on a bulk frame or textile. This aspect will be discussed further in the output section.

2.2.3. Minimized Error of Body Position

The small dimension of skin electronic devices minimizes the error of the body position information and can be used for an accurate position input device.[40] The proper acquisition of the body position is tremendously important in VR/AR for proper measurement and reaction to human activity.[11] Compared to the externally mounted thick 3D devices, ultrathin and 2D-like skin electronic devices can be beneficial from the decrease of the measurement error. Compared with clothes or other device systems with limited placement, the skin can be beneficial based on its coverage of the entire body. The intrinsic flexibility and/or stretchability similar to skin can also be beneficial for strain-based motion sensing. Based on the minimized detection errors in body position and the change (motion), skin electronics can successfully improve or deliver the perception of orientation and space.

2.2.4. User-Interactive Physiology and Interfacing

Skin electronic devices can be used as sensors for internal body signals and input devices.[41] The temperature can be acquired with high resolution from the interfacing properties of skin electronics. In addition, many devices enable long-term and real-life monitoring of biological signals. Although these signals are not a part of human sensing, they can be indirectly used because the information tells the status of our body. In the case of the input device, the skin is favorable for inputting the signal of the user using touch and voice without disturbing natural body movement. These advantages allow on-skin devices to have a minimized sense of device perception and accurate measurement of human position and sensing compared with conventional wearable device platforms based on nonflexible and hard materials with 3D structures.[42]

3. Input

Input devices allow us to acquire information from physical reality including the physical conditions of users. Like human sensory organs, the devices receive and detect the stimuli and make VR/AR system to utilize that information to acknowledge the status of the user, surroundings, and their interactions. In particular, huge advances in ultrathin, conformally interfaced, lightweight, soft, and stretchable electronics have significantly reduced mechanical differences between the skin and sensors, allowing the signal acquisition similar to the conditions of human sensory organs and the continuous monitoring of accurate biological signals in a natural state without discomfort. In this section, we describe recent developments in on-skin sensors such as photodetectors, microphones, tactile sensors, kinesthetic sensors, thermal sensors, and electrophysiological sensors as the input devices for the next-generation of VR/AR systems.

3.1. Photodetectors

Considering the huge portion of vision in human sensing system, optical sensors are a crucial part for the successful exhibition of VR/AR. By placing photodetectors onto the skin, we can acquire the environmental information such as orientation and space like our visual sensory system. Also, it can be used for the visual acquisition of the user physiological information by measuring visible light and/or IR. Although the proper acquisition of visual information should be accompanied by integration with other optical components such as the lens and

aperture, the most important part is the photodetector, which transduces optical information (the number and energy of the photon) to the electrical information (current or voltage). In addition, as a fundamental device in electronics with diodes, photovoltaics, and transistors, the photodetector has been developed with various active materials. Inorganic nanomaterials with structures 0D (metal/semiconductor nanoparticles (NPs) and quantum dots (QDs)),[43] 1D (metal/semiconductor nanorods and nanowires (NWs)),[44] and 2D (mono- or multilayer graphene and semiconductors)[45] are applied as their optoelectronic properties. To achieve additional flexibility and stretchability beyond the intrinsic limit of these inorganic materials, strain-relaxing structures such as helical,[46] wavy,[47] wrinkled,[48] nanopatterned,[49] or 3D structures[50] are prepared on prestretched elastomeric substrates. Likewise, thin films of inorganic semiconductors,[51] organic semiconductors of bulk heterojunction blends,[52] and organic–inorganic hybrids[53] are widely employed.

One of the most common applications of photodetectors in skin electronics is photoplethysmography (PPG) obtained by pulse oximetry. The optical difference between oxyhemoglobin (HbO_2) and deoxyhemoglobin (Hb) in the blood is measured as the cardiac cycle by using light sources such as organic light-emitting diodes (OLEDs) and photodetectors. Polat et al.[54] demonstrated multifunctional graphene sensitized with semiconducting QDs photodetectors with broadband wavelength sensitivity (300 to 2000 nm), including ultraviolet (UV), visible light, and infrared (IR). Multilayered chemical vapor deposition graphene and PbS colloidal QDs were prepared on various flexible polymer substrates. After the light illumination, the charges of the electron–hole pairs are generated in the QD layer and separated at the graphene–QD interface. By selective hole-trapping, the resistance and the corresponding photoconductivity changed as "built-in photoconductive gain." This huge photoconductive gain allows the device to communicate wirelessly with extended distance for interaction with data readouts and other devices.

Another advanced example is the image sensor achieved by the integration of arrayed multiple photodetectors. Our group recently reported on-skin flexible image sensors that have a high speed (41 frames per second) and resolution (508 pixels per inch) with an effective sensor area of 12.6×12.8 mm^2 (252×256 cells).[55] The overall thickness of the device is only 15 μm, and the resulting bendability allows successful device attachment onto the skin. The integration of inorganic–organic hybrid systems composed of low-temperature polycrystalline silicon thin-film transistor (TFT) readout circuits and an organic detector made the device highly sensitive in the near-infrared region. Conjugated polymers poly[[2,5-bis(2-hexyldecyl2,3,5,6-tetrahydro-3,6-dioxopyrrolo[3,4-*c*]pyrrole-1,4-diyl]-alt-[3′3″-dimethyl-2,2:5′,2″-terthiophene]-5,5″-diyl] (PMDPP3T)[56] and STD-001 (Sumitomo Chemical Company) were used as the active layer by blending with [6,6]-phenyl C61-butyric acid methyl ester (PCBM). The active layer film was prepared on a 20 nm ZnO layer and showed high detection performance in infrared (the maximum peak at 850 nm), and the 1 μm parylene encapsulation yielded a high air stability. The fabricated image sensors were successfully applied to identify the fingerprint and vein for biometric identification. To further expand color detection, Kim et al.[57] demonstrated a full-color QD photodetector and an array. By integrating various-sized colloidal QDs with thin-film transistors having amorphous indium–gallium–zinc oxide (a-IGZO) semiconductors and introduced chelating ligands, the researchers could achieve full-color light absorption (IR to UV) and highly efficient light detection. Using this method, the authors fabricated a 10 by 10 photodetector array on a polymer substrate and successfully demonstrated light detection by placing it onto the finger skin.

Other than on-skin photodetectors, another important device platform for the optical input is the smart contact lenses.[58] Choi et al. demonstrated the hemispherically curved image sensor using MoS_2–graphene photodetectors.[59] The usage of 2D materials and the fullerene-like truncated icosahedron structure enabled ultrathin (device is 51 nm and encapsulation is 420 nm on both sides) and soft devices having almost complete coverage on the hemispherical surface. The fabricated image sensor array exhibited high-resolution and IR blindness. Based on these advantages, the authors also demonstrated the rental stimulation system using electrical stimulation. The stimulated optic nerves showed similar brain activities with the visual input with bare eyes with proving that the successful input and output using the soft photodetector array. To further understand the implantable or wearable lens and artificial eyes in terms of devices and applications, these reviews can be helpful.[35b,60]

3.2. Microphones

Voice is one of the important methods to deliver the information and is able to provide capability as human–machine interfaces without the limitation of hand/body motions. Also, the integrated and synchronized sound information can be utilized to determine the distance and direction. It is pivotal to guarantee the signal quality of speech recognition/enhancement during VR/AR-based interactions. Therefore, on-skin microphones exhibit an important future direction because of its advantageous features, such as conformability, thinness, softness, and stretchability. With promising features, they are able to produce high-fidelity auditory signals even in noisy environment.[61]

The detection of sound is performed by microphones from the transduction between the mechanical vibration of sound waves propagate through mediums such as air and the electric signals. Piezoelectric materials have a wide frequency range and are suitable for sensing sound waves.[62] For example, Lang et al. proposed polyvinylidene fluoride (PVDF) nanofibers as the active material and sandwiched them within polyethylene terephthalate (PET) substrates having a hole, where the sound waves can be directly transferred to the nanofibers owing to the porous structures.[63] They achieved a sensitivity of 266 mVp-p, which is five times higher than that of commercially available PVDF film devices. Li et al. formed artificial voids inside an 80 μm thick polypropylene layer and incorporated silicate particles to enhance the acoustic sensitivity.[64] Triboelectric-based nanogenerators also possess great potential as flexible acoustic sensors with a high acoustic–electrical conversion efficiency and high mechanical flexibility.[65] In addition, the use of thinner

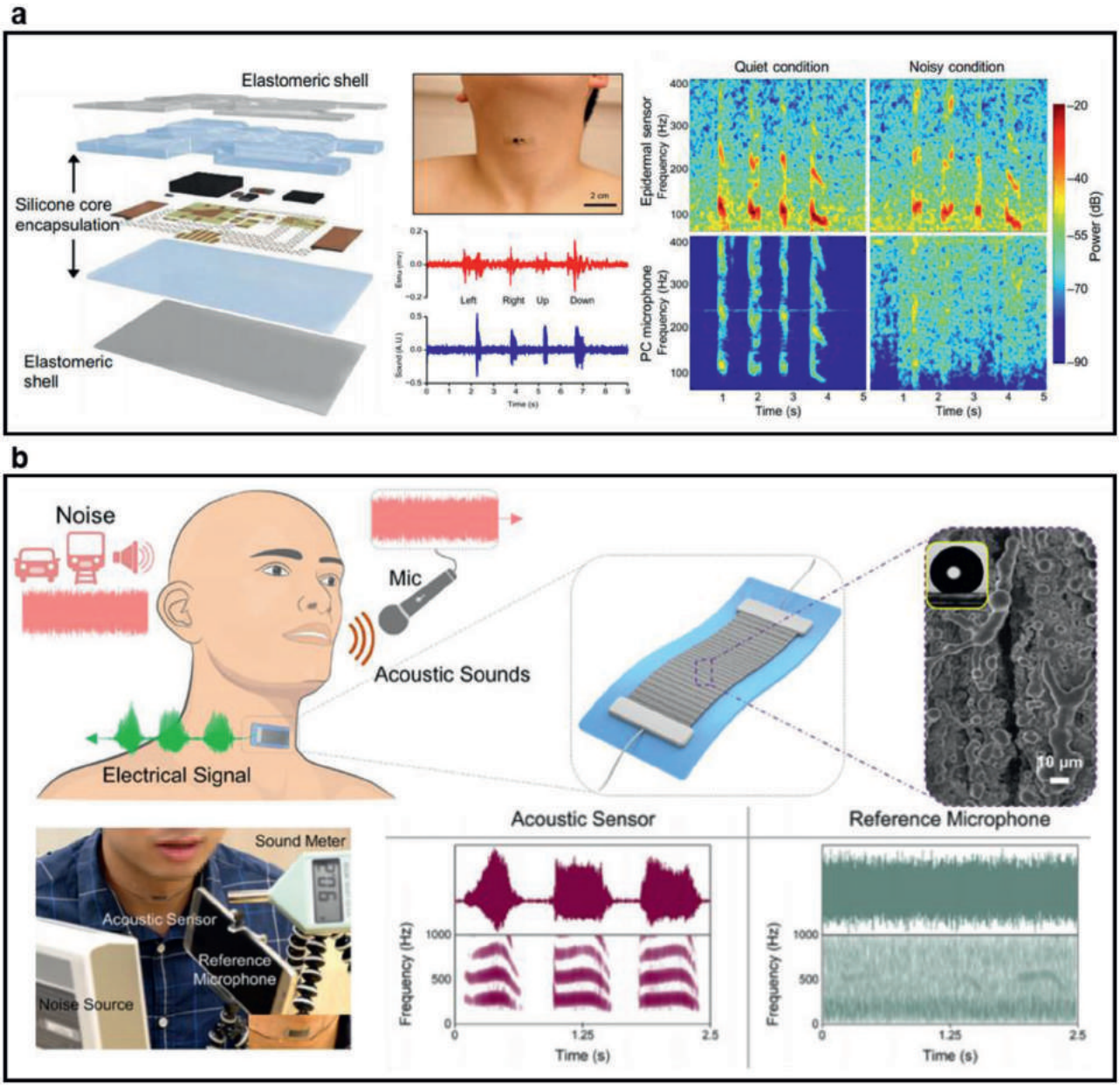

Figure 3. On-skin auditory sensors. a) Accelerometer-based mechanoacoustic sensor. The sensor is capable of detection of voice or heart signal by attaching it to the neck or chest. Reproduced with permission.[68] Copyright 2016, American Association for the Advancement of Science. b) An acoustic sensor with microcracks and hierarchical surface textures. The sensor shows high sensitivity and ultralow detection limit. Reproduced with permission.[61] Copyright 2019, American Chemical Society.

and/or porous sensors enables a larger amplitude of vibrations with the same input signals, which improves the sensitivity of sensors. Fan et al. have demonstrated thin and rollable triboelectric nanogenerators (TENGs) using polytetrafluoroethylene (PTFE) layer and a copper-coated paper substrate that has a porous structure with a diameter of 200 μm.[66] The devices can operate as self-power systems and achieve a volume power density of 1 kW m^{-3} with a sound pressure of 117 dB. Furthermore, the sensors attachable to the skin can detect mechanoacoustic signals through the vibration of the skin.[67] Rogers and co-workers mounted accelerometer-based mechanoacoustic on the skin and successfully monitored the seismocardiography signals.[67a,68] The sensors were fabricated on ultralow-modulus elastomeric substrates (Silbione and Ecoflex with a module of 5 and 60 kPa, respectively) with a total weight of 213 mg and a thickness of 2 mm (**Figure 3**a). To further improve the sensitivity of skin-attachable acoustic sensors, Nayeem et al., proposed all-nanofiber-based acoustic sensors comprising polyurethane nanofibers as a substrate and PVDF nanofibers as an active layer.[69] The introduction of nanoporous substrates with a combination of piezoelectricity and triboelectricity enables a sensitivity as high as 10 050 mV Pa^{-1} and detection of

heart sounds over 10 h with a signal-to-noise ratio (SNR) of over 38.2 dB (Figure 3b). In addition, skin-attachable acoustic sensors allow body acoustic signal detection with high sensitivity, although there are environmental noises. Le et al. proposed a graphene oxide/polydimethylsiloxane (PDMS) composite film with microcracks and hierarchical surface textures.[61] The sensors exhibits a high sensitivity with a gauge factor of 8699 and an ultralow detection limit (ε = 0.000064%) in the audible range (–20 to 20 000 Hz). The sensors are attached to the neck and are able to recognize diverse speech patterns even in noisy environments, where a microphone cannot detect acoustic signals.

3.3. Tactile Sensors

Advances in soft, flexible pressure and thermal sensors have enabled an electrical tactile sensing system on the skin. The low thickness and skin-like mechanical properties supplied by the skin electronic devices can be highly favorable for the natural wearing feeling and accurate on-skin sensing of the pressure. Additionally, their thinness and softness enable to minimize the interference of inherent skin functionalities. For example, on-skin nanomesh pressure sensors have been developed to detect finger manipulation accurately without loss of human sensations.[70] The mechanism to detect the pressure can be categorized into piezoelectric, piezoresistive, and capacitive approaches.[71] Piezoelectric materials generate electronic signals in response to external pressures; therefore, the pressure can be detected by measuring changes in voltage or current. The polarization is proportional to the external pressure due to the distance change between the dipoles. Inorganic piezoelectric materials such as lead zirconate titanate (PZT),[72] AlN,[73] and ZnO[74] have been used because they exhibit a large remanent polarization. Although the mechanical properties of inorganic materials are inferior to those of organic materials, the use of thin and/or stretchable substrates enables mechanically compliant pressure sensors. Because inorganic materials typically require a high-temperature process, transferring to flexible substrate has been proposed after forming the piezoelectric layers on temporary and thermally stable substrates. For example, Dagdeviren et al. fabricated PZT layers on silicon wafers with thermal annealing at 680 °C and then transferred them to elastomeric substrates.[72c] The sensors could be directly mounted on the wrist and used for detecting pulse pressure velocity. In addition, they integrated piezoelectric sensors with transistors and amplified the generated signals. Park et al. also proposed the transfer of PZT layers onto ultrathin (4.8 μm) polyimide (PI) substrates.[75] The PZT layer was manufactured on a sapphire substrate, then it was cut using a XeCl excimer laser. Organic piezoelectric materials, mainly PVDF and PVDF copolymers, have been widely used for realizing flexible piezoelectric pressure sensors.[74f] Organic materials can be easily manufactured on flexible substrates over a large area with relatively low (typically less than 200 °C) fabrication temperatures. In addition, polymers can be made in the form of fibers, which results in the simultaneous achievement of superior flexibility and high sensitivity. Persano et al. proposed aligned poly(vinylidene fluoride-trifluoroethylene) (P(VDF-TrFE)) nanofibers with a detection limit in the pressure of less than 0.1 Pa.[62d] One of the benefits of polymer-based piezoelectric materials is their ability to be directly integrated with transistors or amplified circuits. For example, signals from piezoelectric layers can be used as the gate voltage of transistors or the input voltage of inverter circuits.

Piezoresistive materials change the resistivity in response to external pressures.[76] The materials typically contain an elastomeric matrix and conducting fillers such as graphene,[77] carbon nanotubes (CNTs),[78] and metallic particles,[79] to form an electrical path within the elastomer.[79] The introduction of nano/microstructures[80] and/or porous structures[77b] in active materials is promising to improve the pressure sensitivity.[74f,76b,81] Gong et al. proposed a resistive pressure sensor based on AuNW-incorporated paper.[76b] The sensors are capable of detecting bending and torsional forces with high sensitivity. Jung et al., introduced pores in PDMS matrix using a reverse micelle approach.[82] A mixed solution with an emulsifier (polyoxyethylene nonylphenyl ether), deionized water, and an organic solvent was used. Furthermore, a form in nanofibers is useful to reduce bending-induced stress in an active layer. Lee et al. fabricated graphene and CNTs mixed nanofibers as a piezoresistive material on ultrathin (1.4 μm) PET substrates.[78] Notably, the sensors can detect the external pressures on elastic objects without a performance change, although the sensors are severely bent to a radius of 80 μm (**Figure 4**a).

Capacitive pressures detect the external pressures by measuring the capacitance in a dielectric layer between two electrodes.[83] Unlike piezoresistive sensors, capacitive sensors do not require to use of conductive filler inside the dielectric layer and the characteristics of the sensors are mainly determined by the mechanical properties of the dielectric layer. Because the sensitivity of a capacitive pressure sensor is directly related to the softness of the dielectric layer and soft rubber materials such as Ecoflex have been utilized to increase the sensitivity.[84] To further improve the sensitivity, microstructures,[85] porous structures,[79,86] and nanofibrous structures[87] into the rubber layers[88] along with transistor integration have been reported.[89]

Along with the above approaches, other methods such as triboelectric,[76d,90] optical,[91] and ionic[76d,92] material-based devices, have been demonstrated for detecting pressures. Microfluidics using liquid metal with elastomers can detect external pressures because the resistance of liquid metals changes due to the deformation in the geometric structure of the microfluidic channels when external pressure is applied.[93] Gao et al. proposed a Wheatstone bridge circuit made of Galinstan-based microchannels 70 μm wide and 70 μm high and achieved a sensitivity of 0.0835 kPa^{-1} with high mechanical flexibility (Figure 4b). Sun and co-workers proposed an ionic touch panel consisted of a polyacrylamide hydrogel and lithium (Li) chloride salts.[92a] The touchpoint in the 2D ionic touch panel can be detected by measuring the currents from the four positions of the touch panel (Figure 4c).

A multipoint detection capability is an important feature as it makes it possible to acquire detailed haptic information sensitively. Integration with the transistor matrix array (active matrix) is a promising approach to reduce the number of interconnection wirings.[74b,94] It is also effective to use a virtual ground to suppress crosstalk in the passive capacitance sensor array.[95]

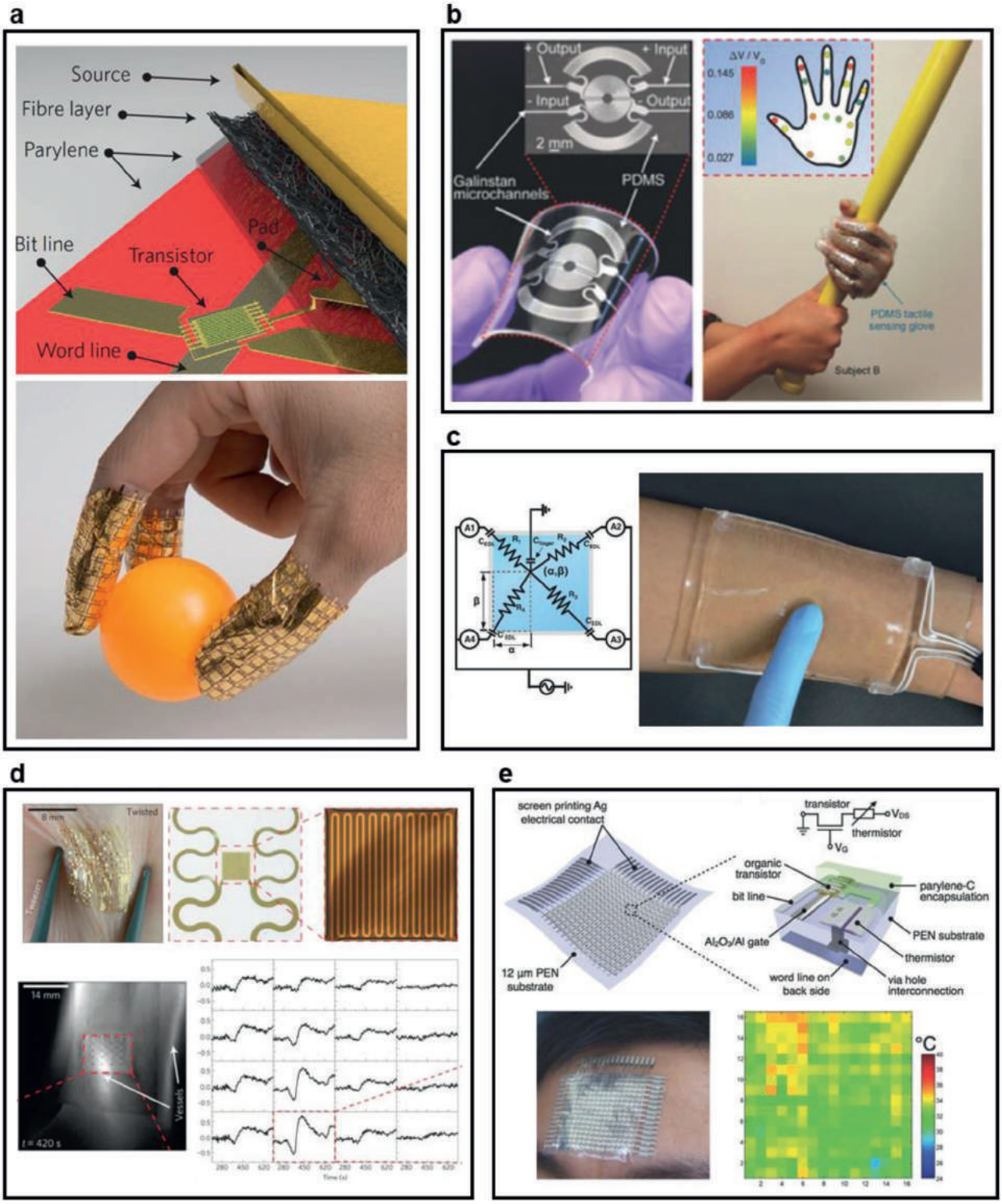

Figure 4. On-skin tactile sensors. a) Capacitive pressure sensor with Ecoflex rubber layer. Reproduced with permission.[78] Copyright 2016, Springer Nature. b) Microfluidic pressure sensor. Reproduced with permission.[93] Copyright 2017, Wiley-VCH. c) Hydrogel-based touch panel. Reproduced with permission.[92a] Copyright 2016, American Association for the Advancement of Science. d) Metal-based thermal sensor on 50 µm thick elastomeric substrate. Reproduced with permission.[96b] Copyright 2013, Springer Nature. e) 16 × 16 thermal sensor array comprising organic thermistors and organic TFTs. Reproduced with permission.[100] Copyright 2016, Wiley-VCH.

Another important human tactile information is temperature. By using on-skin thermal sensors, it is possible to not only measure the skin temperature but also thermal information of other objects. Especially, ultrathin devices mounted on the skin enables the accurate measurement of body temperature with minimized device-induced modification or sensing error. Several methods have been used to realize flexible thermal sensors. One of the important approaches is to use electrical resistive materials, such as metals,[96] semiconductors,[97] and conductive filler-embedded polymers.[98] The conductivity of metals or semiconductors is dependent on temperature because the motion (mobility) of free electrons is affected by phonon scattering due to vibrations of the atomic lattice. The change in conductivity in metals is expressed by the following equation, $dR/R_0 = a(T - T_0)$, where T is the measurement temperature, T_0 is the initial temperature, R is the resistance at temperature T, R_0 is the initial resistance at the temperature T_0, and a is the temperature coefficient of resistance. In particular, serpentine-structured metal layers on ultrathin and stretchable substrates enable stable monitoring of body temperature under the deformation of devices. For example, Webb et al. proposed gold serpentine-structured temperature sensor arrays and demonstrated the detection of the thermal distribution of the skin, which correlated well with those measured by the infrared camera (Figure 4d).[96b] To achieve high sensitivity in the range of body temperature (30–40 °C), semiconductor-based approaches such as thermistors have been proposed, in which the resistance changes exponentially with temperature change. For example, graphene on flexible substrates has been demonstrated for realizing thermistor-based temperature sensors owing to its extraordinary thinness and superior mechanical properties. Yan et al. demonstrated a stretchable temperature sensor by transferring the crumpled graphene to PDMS substrates with Ag NW electrodes as stretchable electrodes.[97d] The sensor is mechanically robust and functional although mechanical deformations, such as twisting and stretching, are applied to the sensor. Organic semiconductor-based thermistors, such as poly(3,4-ethylenedioxythiophene) polystyrene sulfonate (PEDOT:PSS)[99] and pentacene[100] are also widely used owing to their high mechanical flexibility and high thermal sensitivity. To tune and improve the sensitivity, Chan and co-workers introduced AgNPs into pentacene and achieved higher a activation energy of 613 mV in the Arrhenius plot than 157 mV of pure pentacene thin film, resulting in a temperature coefficient of resistance of 0.044.[100] They also integrated the organic thermistors with 16 by 16 organic TFT active-matrix arrays comprising dinaphtho[2,3-*b*:2′,3′-f]thieno[3,2-*b*]thiophene and Al_2O_3/self-assembled monolayer hybrid dielectric and demonstrated acquisition of spatial mapping of skin temperature. To further improve the sensitivity of sensors and/or a readout of measured signals, it is useful to connect the sensors with transistors/circuits or to directly fabricate temperature-sensitive circuits. Zhu et al. demonstrated stretchable temperature sensors with differential sensing circuits based on CNT transistors.[101] The transistors are made of supramolecular-polymer-sorted single-walled CNTs as a semiconducting layer, unsorted single-walled CNTs as electrodes, and PEDOT:PSS as stretchable interconnections. The differential circuits could be suppressed with a measured inaccuracy of ±1 °C, even though the sensor-integrated circuits were stretched up to 60% (Figure 4e).

3.4. Kinesthetic and Vestibular Sensors

On-skin strain sensors can be directly attached to human skin for continuous monitoring of motion and posture, which has shown advantageous usage in future VR/AR applications.[102] On-skin strain sensors can improve signal accuracy during motion and position monitoring owing to intimate contact between sensor and human skin. By the proper analysis and comparison of the status, we can acquire the advanced information about the body valance and the orientation and direction relative to the space with substituting the human visual and vestibular sensory system. There are several basic requirements for skin strain sensors: thinness, softness, ultraflexibility, stretchability, strain sensitivity, biocompatibility, and durability. The fundamental working principle is to generate reproducible electrical changes while being stretched. Typically, strain sensors are fabricated by depositing electrical fillers of polymeric substrates or by mixing them with polymers. Commonly used intrinsically stretchable fillers include liquid metal,[103] metallic NPs,[104] metallic NWs,[105] graphene,[106] CNTs,[107] hydrogels,[108] ionic liquid,[109] conducting polymers,[110] and hybrids.[111] Various approaches have been explored to obtain thinness geometry and/or high sensitivity and/or high stretchability.[112] A typical approach to increase sensitivity is to generate cracks on the electrically conductive film;[113] strain sensor with a gauge factor of over 2000 could be achieved but with limited stretchability.[114] As for the thickness reduction, ultrathin polymers substrate[115] or substrate-free device[38a] have been developed. Additionally, skin strain sensors with better conformability and functionalities have been extensively developed in recent years owing to the increasing advancements in materials and assembling structures.[106,116]

For example, Wang et al.[117] reported a nanomesh strain sensor that can monitor full-range human movement with minimum mechanical constraints. The device was fabricated by reinforced PU–PDMS nanomeshes. The sensor was lightweight (0.12 mg cm^{-2}) and ultrathin with a thickness of ≈430 nm. It exhibited excellent durability of cycling strain (5000 times) under 60% strain with resistance degradation of only 0.03. In addition, the sensitivity and stretchability of the nanomesh strain gauge can be adjusted by changing the mesh morphologies. The mechanical compliance owing to its thinness and softness enabled minimum mechanical disturbance on skin motions. During the facial strain mapping experiment in speech, the nanomesh sensor-attached face exhibited a strain distribution similar to that of a face without nanomesh sensors (**Figure 5**a). Long-term monitoring was also successfully demonstrated owing to the high durability and breathability of the device. Recently, Ko and co-workers developed a deep-learned skin sensor decoding the epicentral human motions.[118] Unlike traditional approaches that require many sensor networks covering the entire curved surface, they used a single skin sensor decoding dynamic complicated motions generated by five fingers in real time. The skin sensor was fabricated by laser-induced nanoscale cracking, allowing for high sensitivity. Conformability was achieved by consecutive serpentine patterning (Figure 5b). The concept of this system is promising for detecting other physiological information when applied to other body parts.

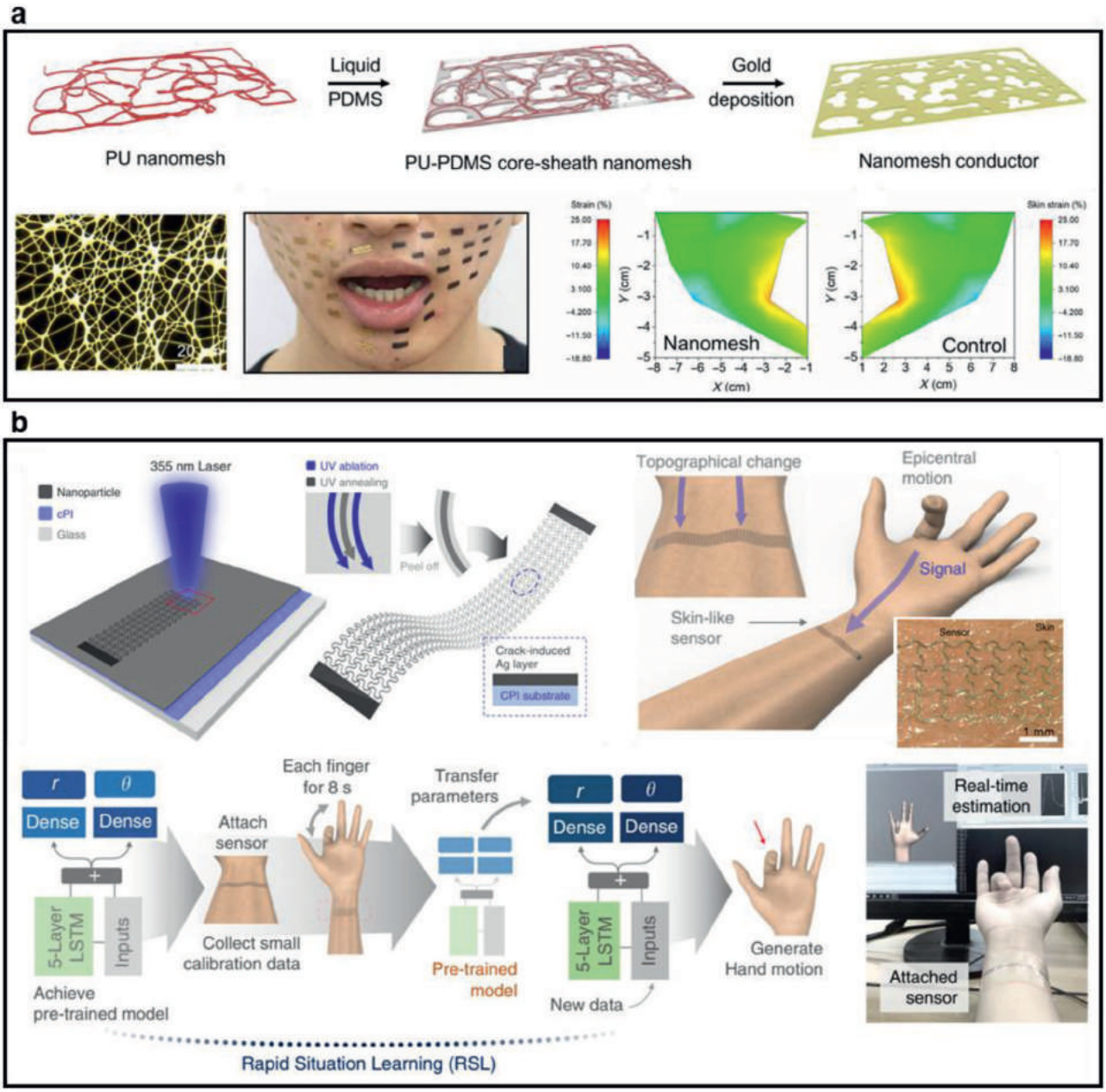

Figure 5. On-skin motion sensors. a) A nanomesh on-skin strain sensor for facial strain mapping during a speech. Reproduced with permission.[117] Copyright 2020, American Association for the Advancement of Science. b) A deep-learned skin sensor decoding the epicentral human motions. Reproduced with permission.[118] Copyright 2020, Springer Nature.

3.5. Electrophysiological Sensor

The neurosystem in the human body generates electricity in the brain (EEG), muscles (EMG), and eyes (EOG). The measurement of these action potentials can be used as the barometer of the human body: the perception and order of movement in the brain, intensity and duration of muscle usage, and direction of eyeball movement.[119] This information is crucial for VR/AR applications by informing clues into user behavior.[120] To capture the action potential invasively, skin electrodes with conductivity, flexibility, and additional stretchability are frequently employed. As the materials, flexible/stretchable conductive polymers with plasticizers,[121] conductive hydrogels,[122] and blending or composite of conductive materials such as conducting polymer,[123] carbon materials (graphene, CNTs),[123b] metal NPs[124] with flexible/stretchable elastomers are demonstrated. Another approach of strain-relaxing 2D or 3D structures such as wavy,[125] ribbon,[126] serpentine,[127] coil,[128] and mesh[129] is attempted using various metals on flexible/stretchable substrates. Someya and co-workers also demonstrated a substrate-free skin electrode by preparing the gold onto the polyvinyl alcohol (PVA) nanomesh and dissolving

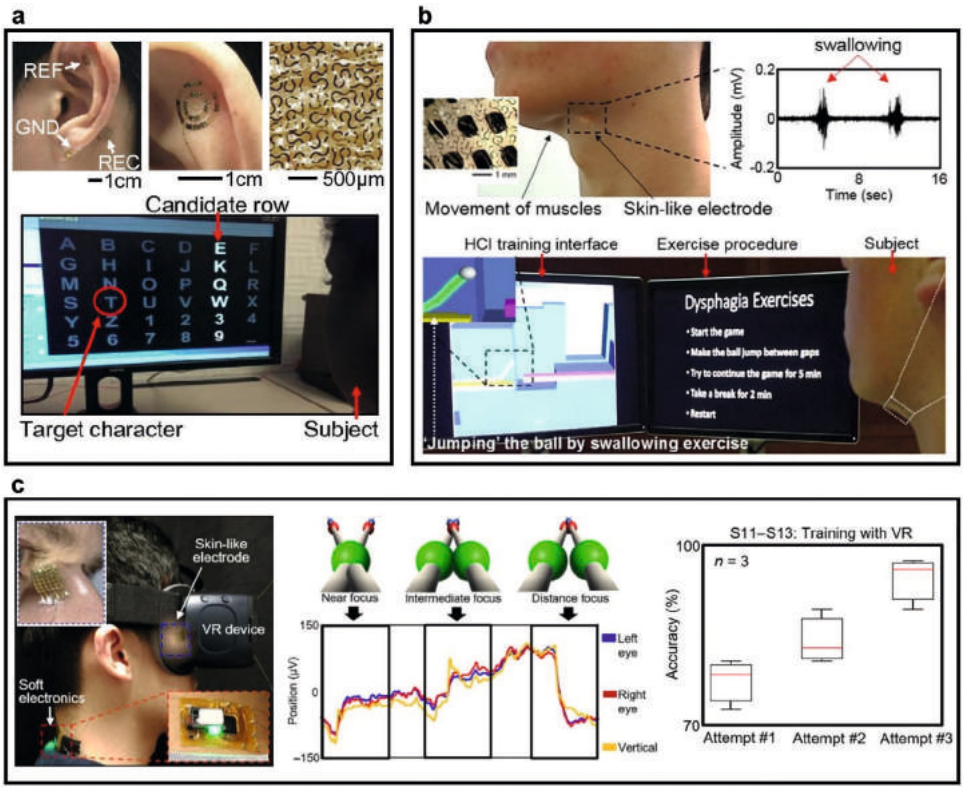

Figure 6. On-skin bioelectric sensors. a) EEG-based text speller. Reproduced with permission.[132] Copyright 2015, National Academy of Sciences. b) EMG-based virtual reality game. Reproduced with permission.[133] Copyright 2017, Springer Nature. c) EOG-based learning in virtual reality. Reproduced with permission.[134] Copyright 2020, American Association for the Advancement of Science.

it on the skin.[38a] In a similar approach, direct deposition of conducting materials on the skin has been demonstrated by using liquid metal[130] or silver ink.[131]

Rogers and co-workers demonstrated human–machine interaction using EEG captured by skin electrodes on the ear (**Figure 6**a).[132] The tripolar concentric ring of the metal and capacitive design of electrodes provided mechanical stability (>180° bendability and >50% stretchability) against long-term and real-life usage conditions. Based on the successful acquisition of EEG action potential, the researchers demonstrated an EEG-activated text speller interface. It can be expected that much advanced brain–machine interaction and VR/AR applications can be produced using EEG measurements. By using an Au nanomembrane with fractal interconnects and circular cells and an elastomer substrate, a highly stretchable (>100%) electrode could be achieved. Figure 6b shows the user-comfortable device–human interaction achieved by attaching the Au nanomembrane to the neck and measuring the muscle usage using an EMG signal.[133] The measured signal was classified by the algorithm and used as the data for the real-time game of a jumping ball in the virtual space. This real-time response of muscle usage can make the user experience the machine–bio interaction, and the usage of a skin-like system gave a higher user satisfaction rating (6.5 out of 7) than the conventional rigid gel electrode (4 out of 7). This game-based biofeedback system accomplished medical rehabilitation by the swallowing training of users.

In addition, the EOG signal could be applied by human–machine interaction. As shown in Figure 6c, the researchers investigated the detection of eye movement in virtual reality and used it to medical applications.[134] The electrode was prepared by aerosol jet printing of silver NPs onto a polyimide substrate. The high thermal stability of PI was enabled by the sintering process at 200 °C, which necessitated the breaking of the capping binder (oleylamine fatty acid), preventing agglomeration. Using these conformally attached electrodes, the sensitive tracking of eye movements (vergence) was achieved in the virtual reality system. In addition, the analysis and computational approach were used for the algorithm of ocular motion classification. With the help of this EOG-based VR system, the users could be trained to enhance their visual activities by providing biofeedback to the vergence motions.

4. Output

For the VR/AR, the output devices making the user to perceive the physical reality as the substituted or modified new reality are mandatory. By the given signal or feedback through displays, loudspeakers, and haptic devices, we can achieve the recreated vision, hearing, and touch, respectively.[135] In this section, we introduce skin electronics (displays, loudspeakers, tactile output, kinesthetic output, and heaters/coolers) which function as stimulators to the human body to provide different sensations such as auditory, visual, and touch for future VR/AR applications.

4.1. Displays

Visual output devices are the key components of standard human–machine interfaces for VR/AR applications. Currently, smart head-mount displays and smart glasses are used for the visual output devices as one of the most primary perceptions. However, the rigidity, bulkiness, and heaviness of these devices interfere with immersive user experiences. Like the skin electronic devices, smart contact lenses are showing their distinctive advantages compared to the conventional bulky displays. Although the quality of output signal is insufficient to substitute to nonwearable or wearable displays for their limited resolution and power/data transmission,[35a,136] it has high potential in future applications for their high user-accessibility. In case of the on-skin displays, even though they have less contribution compared to the wearable displays placed in front of the eyes covering full angle of the human vision, still they can deliver us the perception of physical environment to our eyes.[137] Especially for AR, the on-skin display can be one of the most important future alternatives of portable display devices.

Therefore, in this section, we focus on the materials and structures of the on-skin displays. For the on-skin usage, light-emitting devices are expected to be thin, flexible, and exhibit comparable performance (e.g., high luminance efficiency and color purity) to that of a rigid display.[138] Due to the expeditious development in nanomaterials and assembling technologies, flexible/stretchable electrode materials (e.g., CNTs,[139] graphene,[140] metal NWs,[141] and hybrids[141]), emissive materials (e.g., organic polymers,[142] QDs,[143] and hybrids[144]), and stretchable structures (e.g., island design,[145] "wavy" structure,[146] and composite[147]) have been developed for fabricating high-performance soft displays. In the following, we will introduce representative examples of current on-skin smart displays with various sensing functions.

An ultraflexible and conformable organic photonic skin was fabricated using polymer light-emitting diodes (PLEDs)).[148] The biological information was measured by the optical sensor, and the acquired information was then shown on the skin via PLED (**Figure 7**a). The resultant PLED exhibited excellent flexibility because of its thinness and low rigidness. After laminating on a prestretched acrylic rubber, the device could survive strain up to 67%. Its functionality did not decrease after 1000 cycles of stretching/releasing under 60% strain. Kim and co-workers reported an on-skin EEG monitor using CNT electronics and color-tunable organic LED.[149] P-MOS CNT transistors were used to enable high amplification of the ECG signals. An ultrathin exciton-blocking layer (bis[2-(diphenylphosphino)phenyl]ether oxide) has been developed for color tuning by changing the charge balance between two adjacent emitting layers (bis[2-(4,6-difluorophenyl)pyridinato-C^2,N](picolinato)iridium(III) and bis(2-phenylquinolyl-N,C(2))-iridium(acetylacetonate)). The total thickness of the OLED is ≈366 nm, allowing good wearability and flexibility. After integrated with the EEG sensor and the ultrathin CNT amplifier, cardiac signals could be displayed in real-time through synchronized color changes. The same group further developed a QD-based smart display that could visualize information such as temperature and accelerator retrieved from the wearable sensors.[150] The LED was made of an indium tin oxide (ITO) anode, a Li-Al/Au cathode, and a sandwiched charge transport layer composed of a hole injection layer, hole transport layer, and QD. The resultant LED display was ≈5.5 μm and could conform to human skin. QDs with relatively thick shells were utilized to enhance the brightness up to 44 719 cd m^{-2} at an operation voltage of 9 V by suppressing nonradiative recombination. The integrated wrist-worn smart LED system was fabricated by integrating flexible sensors (touch sensors, temperature sensors, and accelerometer) (Figure 7b). Real-time visualization of the temperature and step counts has been successfully demonstrated while the wearer is at rest or running.

4.2. Loudspeakers

An on-skin loudspeaker is highly desired as sound is another key aspect of any VR/AR environment. Various soft loudspeakers have been developed using advanced technologies and materials in the electronic skin field.[151] The widely used active materials are CNT,[152] graphene,[153] liquid metal,[154] PVDF,[155] metal NWs,[156] metal oxides,[157] and ionic hydrogels.[158] For example, Keplinger et al.[158] reported an ionic hydrogel loudspeaker that can produce sound from 20 Hz to 20 kHz. The ionic loudspeakers exhibited a transmittance of 99.99% at 550 nm and could be stretched beyond 500% (Figure 7c). These active materials have been utilized to design soft loudspeakers based on different mechanisms including electrostatic, piezoelectric, dynamic, and thermoacoustic effects.[151,159] A representative example of a thermoacoustic effect loudspeaker is a CNT thin film developed by Fan and co-workers.[160] The film is lightweight (1.5 μg cm^{-2}) with a thickness of only tens of nanometers. Once applied by electric currents with sound frequency, the thin single-element CNT film could emit loud sounds. The small heat capacity per unit area of CNT films enabled a wide frequency response range and a high sound pressure level (SPL). In addition, the as-fabricated CNT film is stretchable, transparent, freestanding, and can be tuned into arbitrary shapes.

For skin-attachable loudspeakers, it is requisite to achieve lightness, thinness, stretchability, and good conformability. Kang et al.[67c] developed a transparent and conformable loudspeaker based on orthogonal AgNWs/parylene composite. The composite film is as thin as 100 nm and is demonstrated to have increased mechanical properties compared with pure parylene film. These two factors lead to intimate contact with curvilinear surfaces such as human skin. The application of an alternating current (AC) voltage generates thermoacoustic sound by temperature-induced oscillation. The SPL of the output sounds linear as the distance between the hybrid film and the microphone decreases (Figure 7d). In addition, the hybrid speaker generated a much larger SPL in the entire evaluated frequency range compared with the thick-film loudspeakers. They successfully played and recognized music while wearing a hybrid loudspeaker. Besides loudspeakers, AgNW-based nanocomposite films have also been used as microphones in personal voice security systems. These skin-attachable acoustic devices have great potential for VR/AR applications.

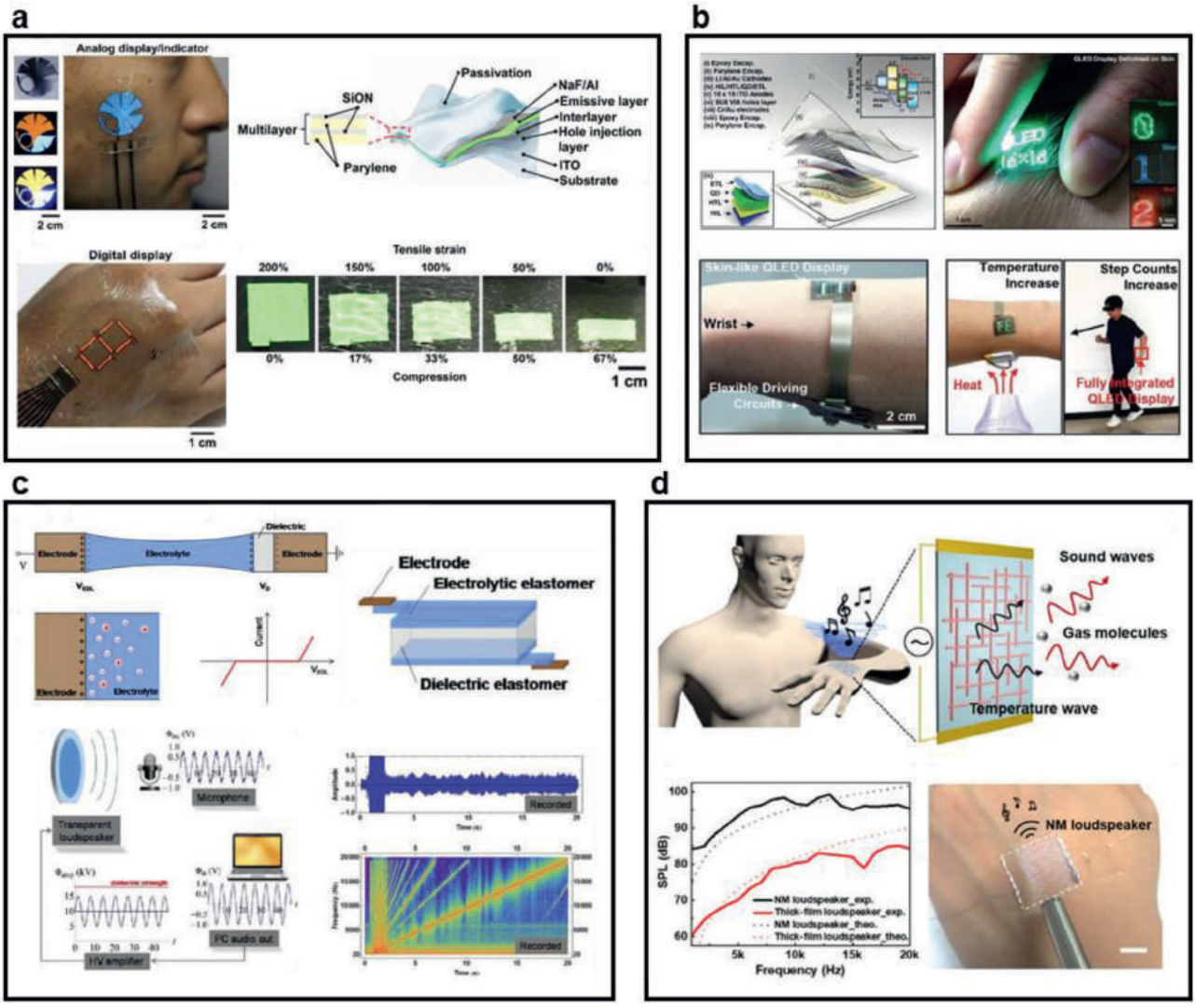

Figure 7. On-skin smart displays and soft loudspeakers. a) An ultraflexible and conformable organic photonic skin. Reproduced with permission.[148] Copyright 2016, American Association for the Advancement of Science. b) A quantum dot-based smart display. Reproduced with permission.[150] Copyright 2017, Wiley-VCH. c) Stretchable, transparent, ionic loudspeakers. Reproduced with permission.[158] Copyright 2013, American Association for the Advancement of Science. d) On-skin loudspeaker based on AgNWs. Reproduced with permission.[67c] Copyright 2018, American Association for the Advancement of Science.

4.3. Tactile Outputs

On-skin tactile devices are one of most important output devices as the skin is the largest sensory organ, where we can immediately and easily discriminate the surface of an object with great acuity.[135,161] Haptic technologies are developed to manipulate the sense of touch and are expected to present dynamic tactile information to the human skin. Although on-skin tactile displays have not been developed the same as on-skin displays, motivation for this research has been driven due to its value in diverse applications including VR and AR. To this end, emerging material technologies have been developed to fabricate on-skin haptic actuators as tactile outputs with high mechanical compliance and flexibility.[135,161] Representative electrode materials such as carbon,[162] Ag,[163] conducting polymers,[163a,164] and dielectric materials such as silicone rubber,[162,164–165] liquid,[166] and PET[164b] have been applied to fabricate tactile actuators. Both single-mode actuating (e.g., dielectric elastomer actuator,[162a] electromagnetic (EM)[165]) and multimode actuating (e.g., hydraulically amplified electrostatic[164b]) are used in haptic actuators.

The ability to place the active components in the same location determines the ability to replicate tactile sensations in a skin haptic device in a VR/AR environment.[164a] A soft-actuator-based wearable tactile display was developed utilizing electroactive polymer as an active tactile stimulator.[162a] An embossed pattern was used to secure the moving direction of buckling. The device exhibits superior adaptability to any contour of the human body due to the softness and flexibility of the device structure. In 2019, Rogers and co-workers reported on-skin haptic interfaces with the wireless and battery-free platform of electronic systems.[165] The developed haptic devices consisted of large arrays of millimeter-scale vibratory actuators in

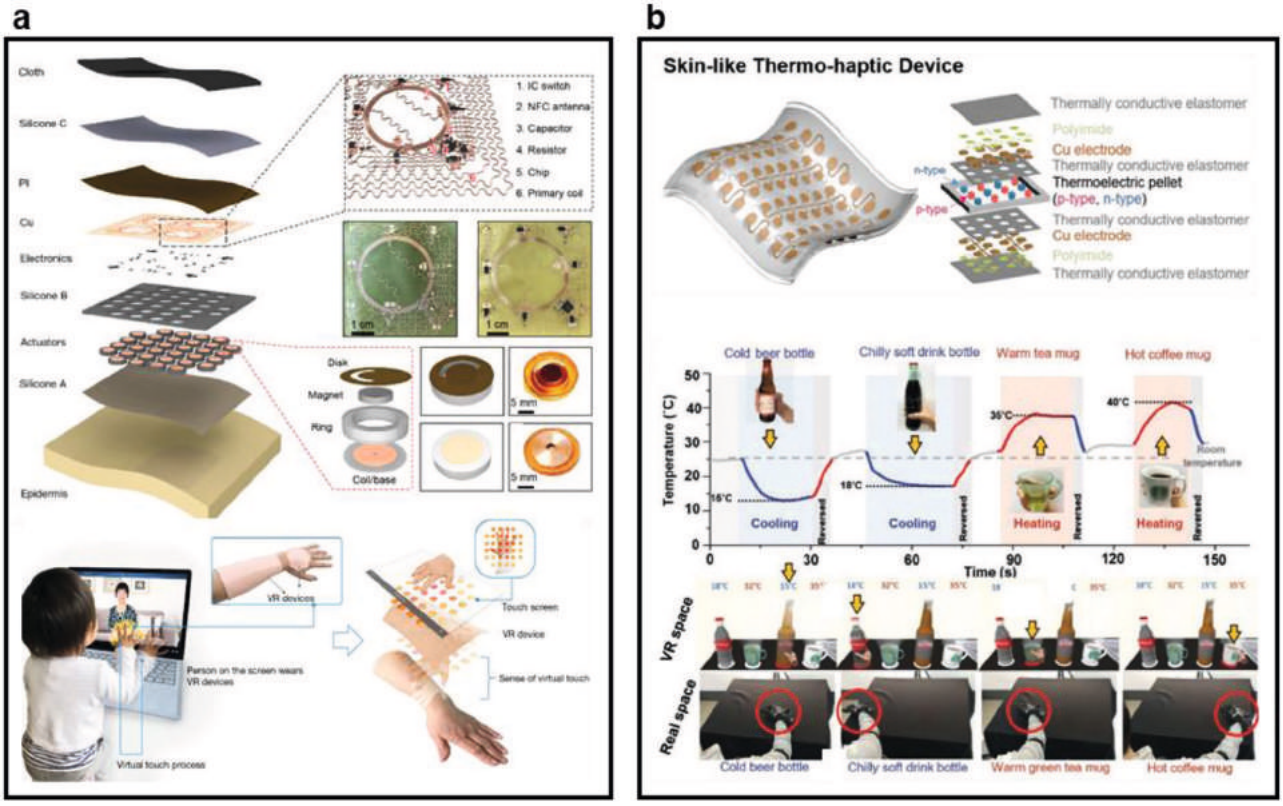

Figure 8. On-skin tactile output. a) Skin-integrated wireless haptic interfaces for VR/AR application. Reproduced with permission.[165] Copyright 2019, Springer Nature. b) Skin-like thermohaptic device. Reproduced with permission.[10a] Copyright 2020, Wiley-VCH.

soft and conformal sheets and enabled direct and noninvasive lamination onto the skin. A single haptic actuator was assembled in the stack by an atop PI disk, a magnet, PDMS ring, and base coil. The ring was used to provide space for the magnet to move freely in the out-of-plane direction (**Figure 8**a). The resonant frequency of the actuator can be tuned to 200 Hz on a skin phantom (Young's modulus: 130 kPa) by changing the angular extent of the slit. The fabricated actuators were connected to other electrical components via conductive traces with a durable and flexible design. Epidermal VR devices have been successfully applied in virtual interactions via social media, tactile feedback, and gaming. This work is promising to scale up for full-body systems and to increase the number of discrete and programmable actuators.

In addition to haptic sensation, thermal sensation by temperature sensing on the skin is an indispensable part along with visual and tactile sensations in everyday life. Therefore, to artificially emulate accurate/controllable thermal sensation tactile information on human skin will certainly be a major research field to regenerate a more realistic VR/AR environment.[10a] In this section, we present the development of on-skin heaters and coolers for future VR/AR applications.

An on-skin heater—a newly emerging functional device—is mainly devoted to offering warmth maintenance and thermal therapy of the human body.[167] Electrically driven resistive heaters are highly suitable for the desired purpose considering the controllable operation, feasible fabrication technique, and efficient power conversion.[168] In general, the structure of soft heaters is simple, and they can be prepared by depositing an electrical layer onto polymer substrates or by embedding electrical fillers into the polymer matrix.[169] As alternatives to ITO, a variety of active materials have been utilized for the fabrication of wearable heaters, such as metal-based materials (e.g., metal films,[97a,170] liquid metal,[171] AgNWs,[172] CuNWs[168]), conducting polymers (e.g., PEDOT:PSS),[173] carbon-based materials (e.g., CNTs,[174] and graphene[175]), and hybrid materials.[176] Various wearable heaters have achieved simultaneous high flexibility and transparency by using low-dimensional nanom aterials.[176b,177] For example, An et al.[178] developed a wearable heater with high transparency (95%) and low sheet resistance (15 Ω sq^{-1}) by supersonically spraying AgNWs onto 3D curvilinear surfaces. The as-prepared heater reached a temperature of 160 °C at a supplied voltage of 8 V. A nanotrough-networked transparent wearable heater was fabricated using electrospun polyvinylpyrrolidone nanofibers, where a sheet resistance of 3.8 Ω sq^{-1} at a transmittance of 90% and a stretchability of 70% strain were achieved. The fabrication techniques of wearable heaters usually involve blending,[173] dipping,[179] printing,[172] transferring,[180] prestrain,[181] spraying,[182] serpentine,[97a] or twisting.[175] To this end, as-developed wearable heaters can be either directly applied to human skin[177a,183] or integrated onto textiles.[167a,176a] Zhang et al.[184] reported a weft-knitted wearable heater with the desired shape and size via carbonization. Additionally, the device could be stretched to 70% strain and exhibited a low operation voltage of 3.5 V driving temperature up to 150 °C.

On-skin coolers, on the other hand, are designed to reduce skin temperature after direct attachment. Passive on-skin coolers using nanoporous textiles or porous electrospun nanofiber mats exhibit effective radiative cooling while still maintaining excellent permeability and mechanical strength for wearability.[185] In the field of skin electronics, thermoelectric materials have been utilized to actively decrease skin temperature. A thermoelectric module can be used as a cooler for cooling when the voltage is added to the two materials, based on the Peltier effect.[186] However, the development of on-skin thermoelectric coolers has been limited owing to insufficient novel materials and assembling technologies.[187] Lee et al.[10a] recently developed a skin-like, soft, and highly stretchable (230% strain) thermo-haptic device that can cool down and heat human skin with a single device structure. As shown in Figure 8b, the device is composed of multiple interfacial materials: Cu/PI electrode, p/n-type bismuth telluride thermoelectric pellets, and Ag flake/Ecoflex thermal conductive elastomer. The fabricated device is able to cool down (thermoelectric cooling) and heat up (Joule heating) human skin by simply changing the direction of electrical current. Reaching a target temperature and returning to the original temperature only takes a few seconds, enabling the realization of desirable fast thermal sensation. In wearable VR applications, three independent devices and wearable heat sinks were integrated with a finger-motion tracking glove. The system reproduced temperatures in real-life virtual situations where the user touched objects with different temperatures. Additionally, electrocaloric materials, such as $Ba_{0.67}Sr_{0.33}TiO_3$ NW arrays have also been used to fabricate wearable coolers.[188]

4.4. Kinesthetic and Vestibular Outputs

Soft actuators can be used to engender various motions, such as contraction, bending, linear extension, and rotary motion, and supply mechanical forces within the desired range.[189] Hence, they play a key role in future VR/AR applications as kinesthetic outputs by simulating the motions of parts of the human body. In this regard, advanced materials and assembling technologies have been developed to construct soft actuators with high mechanical compliance and flexibility/stretchability.[189] The developed actuators exhibit strain of up to 380% in area, stress of up to 7.2 MPa, and elastic energy density of up to 3.4 J cm^{-3}, which already exceeded the performance of natural muscles a decade ago.[190] Emerging materials include soft materials (e.g., gel,[191] liquid and rubber[192]), organic materials,[193] and nanomaterials (e.g., graphene[194] and CNTs[195]), and composites.[196] Based on the working principles, soft actuators can be classified into pneumatic actuators,[197] electroactive polymer actuators,[198] electrostatic force actuators,[199] electromagnetic actuators,[200] fluidic actuators,[201] and liquid crystal elastomeric actuators.[202]

Although soft actuators have been extensively studied over the last two decades, the on-skin haptic actuator for motion output is still limited. Existing wearable actuators are mainly based on bulky design or rigid structures that have been used for joint motion assistance.[203] In order to realize the widespread application of on-skin soft actuators, several challenges have yet to be resolved: miniaturization, low-voltage operation, large-scale production, and integrated sensing to add "smartness" to the wearables.[204] A typical presentation is a skin-stretch device for haptic feedback using twisted and coiled polymer actuators (**Figure 9**a).[205] The device is made of adhesive silicone skin and twisted and coiled polymer actuators, which are soft, lightweight, and finger-worn. This actuator provided lateral skin stretch via ultrahigh molecular weight polyethylene fibers. Recently, Thai et al.[206] reported a soft microtubule muscle-driven triaxial skin-stretch haptic device. The device was driven by hydraulic pressure through direct current micromotors and customized miniature syringes (Figure 9b). Both analytical and kinematic models have been developed to characterize the responses of the soft microtubule muscle output and the motion of the triaxial muscles, respectively. The fabricated muscles could generate displacements of up to 4.5 mm and 1.8 N. The results also show that the device exhibited high speed and good durability.

5. Soft Skin-Like Energy Devices

Soft skin-like wearable energy devices provide power sources for the input and output skin devices introduced in Sections 3 and 4, which expedite the exploration of body-powered electricity or self-powered skin electronic systems in potential VR/AR applications.[207] In this section, we present the recent progress in the development of soft skin-like wearable energy generation devices (solar cells, biofuel cells (BFCs), triboelectric nanogenerators, and piezoelectric nanogenerators (PENGs)) and energy storage devices (supercapacitors and batteries).

5.1. Energy Generation Devices

Recent dramatic technological advances in on-skin healthcare devices (e.g., strain sensors,[208] pressure sensors,[209] sphygmomanometers,[210] blood pressure sensors,[211] PPG sensors,[212] biosensors,[213] and wristbands[214]) have led to the development of new self-sustainable energy harvesting flexible/stretchable devices being developed. Though moisture-based energy-harvesting technologies have emerged in the last decade,[215] these devices exhibit limitations for the applications in soft skin-like wearables. In this section, we discuss three types of soft skin-like energy harvesting devices: 1) scavenging energy from metabolites present in biofluids; 2) conversion of mechanical energy from the daily activities of human into electrical energy using triboelectric nanogenerators and piezoelectric nanogenerators; 3) transforming light energy into electrical energy using solar cells.[207,216]

5.1.1. BFCs

On-body BFCs, a power source constructed from bio-friendly materials, is an effective epidermal energy harvesting device capable of scavenging sufficient energy from metabolites present in biofluids.[217] The performance of BFCs depends strongly on the electron transfer process from an enzyme to the electrode, which is dictated primarily by the strategy of enzyme immobilization.[218] Improved power densities can be realized by effective

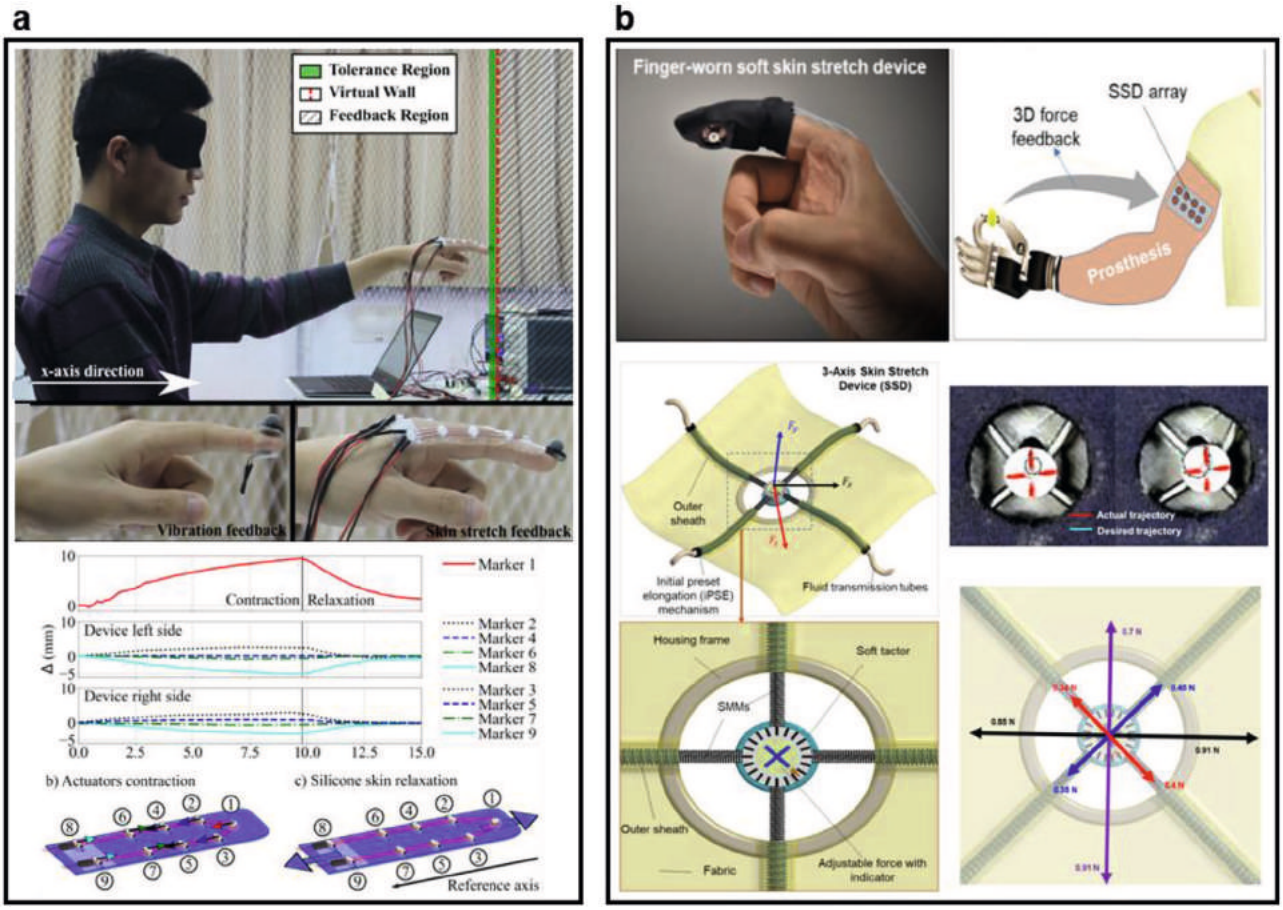

Figure 9. On-skin kinesthetic output. a) Skin-stretch device for haptic feedback using twisted and coiled polymer actuators. Reproduced with permission.[205] Copyright 2019, IEEE. b) Soft microtubule muscle-driven 3-axis skin-stretch haptic devices. Reproduced with permission.[206] Copyright 2020, IEEE.

wiring of an enzyme to the electrode while maintaining high enzyme activity.[217] It predominately relies on the bioelectrocatalytic oxidation of biological fuels, such as lactate or glucose.[219] It is highly required to choose a successful BCF is to select a fuel that can be provided in sufficient abundance. In this regard, human sweat is a promising biofluid, as it is produced in large quantities without invasiveness. In addition, human sweat contains a wide variety of chemicals. Among them, lactate stands out as the biofuel because it is present in abundant levels in human perspiration and can be readily oxidized by commercially available enzymes (lactate oxidase and lactate dehydrogenase).[220]

Wang and co-workers[221] presented the first epidermal BFC harvesting energy from lactate present in the wearer's perspiration during physical activity in a completely noninvasive fashion. The device was based on the oxidation of lactate biofuel, catalyzed by lactate oxidase (LOx) and mediated by tetrathiafulvalene (TTF). The TTF/CNT composite was employed as an efficient electron shuttle between LOx and the electrode. The resultant power density could be as high as 70 μW cm^{-2} from the fabricated tattoo BFC. They further obtained highly stretchable BFCs with a serpentine pattern using specially adjusted screen printable stretchable inks that combined CNTs and PU as a binder up to 500% strain.[222] Furthermore, CNT-based electrochemical sensors and biofuel cells have been realized by building potentiometric ammonium sensors, amperometric enzyme-based glucose sensors, enzymatic glucose biofuel cells, and self-powered biosensor. A high-performance epidermal BFC based on densely packed 3D carbon-nanotube-based bioanode and cathode array was presented in 2017 with an open-circuit voltage (V_{oc}) of 0.5 V and power of 1.2 mW cm^{-2} with the stretchability of up to 50% (**Figure 10**a).[223] Besides glucose[224] and lactate,[225] other vectors, such as hydrogen,[226] have also been utilized as biofuels in BFCs. Meanwhile, considering the advantageous biocompatibility compared to traditional battery energy sources, implanted biofuel cells can be used as the power sources using surrounding biofluids.[217,220a,227]

5.1.2. TENGs

Wang and co-workers first proposed the concept of TENGs in 2012 based on coupled triboelectrification and electrostatic induction.[228] Recently, TENGs have been intensively studied to use mechanical energy from the environment (e.g., water, raindrop, wind, and vibration).[229] While laminating directly on human skin or interfacing with cloths/fabrics or other accessories, TENGs can be used to harvest biomechanical energies from body movement, breathing, and heart beating.[230] Wearable

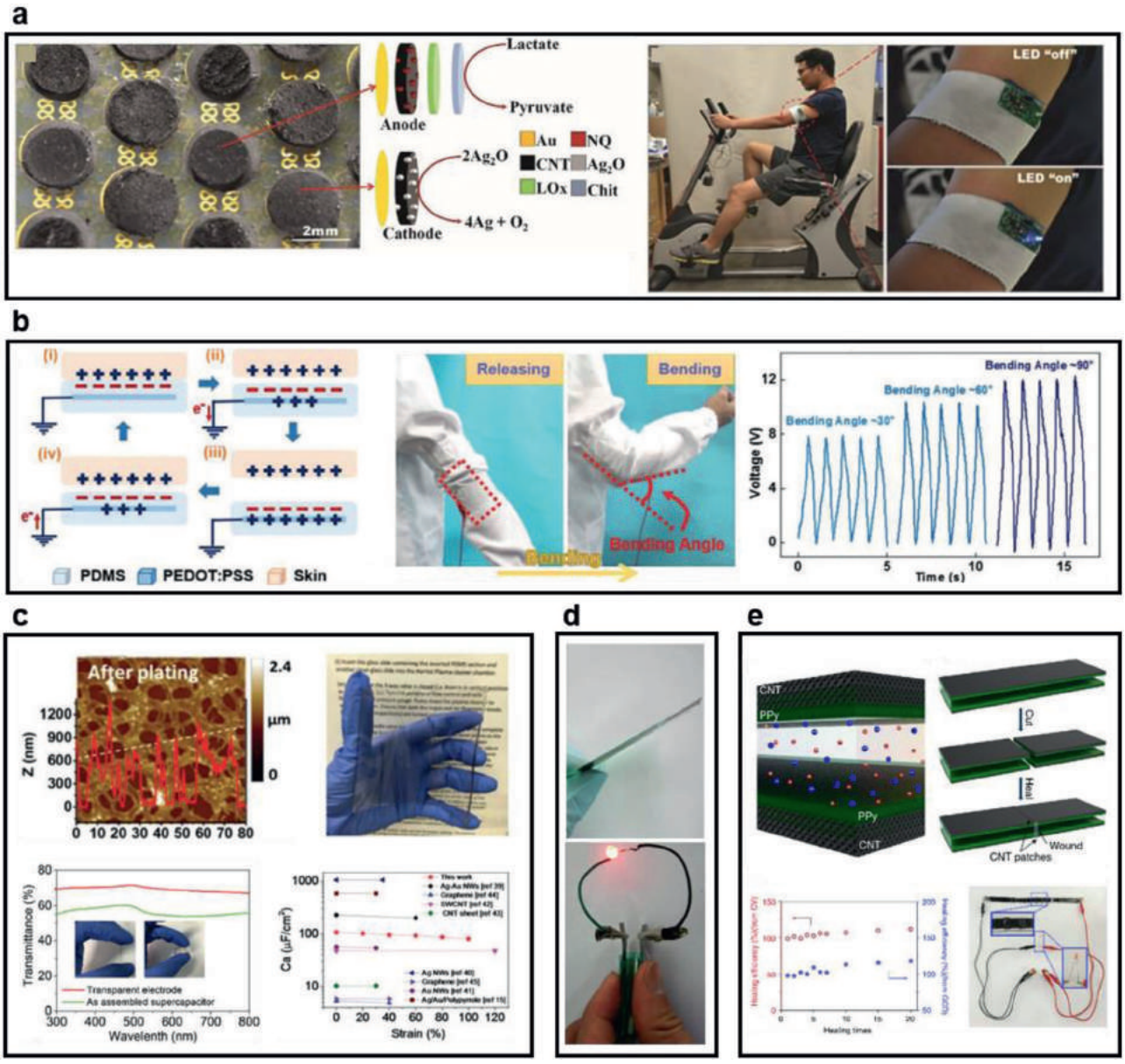

Figure 10. Skin-like energy devices. a) Epidermal biofuel cells. Reproduced with permission.[223] Copyright 2016, Royal Society of Chemistry. b) Wearable TENGs. Reproduced with permission.[236b] Copyright 2017, Elsevier. c–e) Highly transparent (Reproduced with permission.[295b] Copyright 2016, Royal Society of Chemistry.), ultrathin (Reproduced with permission.[296] Copyright 2013, Royal Society of Chemistry.) and self-healable (Reproduced with permission.[298] Copyright 2016, Springer Nature.) flexible supercapacitors.

TENGs have been well proven to be utilized in practical portable electronics as sustainable power sources or self-powered sensors owing to their advantageous characteristics such as low cost, stable output, flexibility, structure diversity, high energy conversion efficiency, and ecofriendly.[231] By using TENGs as self-powered active sensors, researchers have successfully managed to collect biometric information including pulse wave,[232] heart rate,[233] strain,[234] pressure,[235] respiratory rates, cardiac arrhythmias, and human motions[236] as shown in Figure 10b. Moreover, the as-developed TENGs can power liquid crystal displays,[237] smartwatches,[238] commercial LEDs,[239] and calculators.[240] Furthermore, combining TENGs and energy storage technologies is promising to for the development of high-performance wearable self-charging power platforms.[241] Therefore, it is crucial to realize TENG-based electronic skins (i.e., e-skins) in order to add convenience to daily life and health supervision.[242]

TENGs can be categorized into four working principles based on the structure configuration and driving manner: vertical contact/separation mode,[235,243] lateral sliding mode,[244] single electrode mode,[236b,245] and free-standing triboelectric layer mode.[246] For example, Dudem et al.[247] developed a polyaniline (PANI) @worn-out cotton textile-based TENG with a typical vertical contact/separation mode. The PANI@worn-out cotton textile is utilized as a positive triboelectric material

and electrode for TENGs. In the charge generation procedure, the PANI@worn-out cotton textile electrode moves vertically towards and away from other triboelectric materials (e.g., a PTFE film). When the electrode is moving towards the PTFE film, it will contact PTFE. As a result, the PANI@worn-out cotton textile electrode can generate negative tribocharges on the PTFE surface while leaving positive tribocharges. Such accumulation of charges originates from the opposite triboelectric tendencies of PANI@worn-out cotton textile electrodes and PTFE films. Furthermore, the separation can lead to a reduction of positive charges on the electrode surface, and also induce an electrostatic potential difference. Therefore, electrons flow from the ground to the PANI@worn-out cotton textile electrode owing to the potential difference. The electron flow will continue until it reaches an electrostatic equilibrium. When the electrode moves towards the PTFE film, positive tribocharges will be induced on the electrode surface, rendering an equilibrium with the negative tribocharges on the PTFE film. As a result, the electrons flow from the electrode to the ground. With repetitive contact/separation cycles, the TENG can continuously generate electrical flow. The as-obtained dual-electrode mode TENGs exhibit the highest open-circuit voltage (V_{oc}) of ≈350 V, a short-circuit current (I_{sc}) of ≈45 μA, and a power density of up to 11.25 W m^{-2} at an external compression force of 5 N. These values increase as the external force increases. The TENG also showed stable performance under cyclic mechanical deformations of 2000 cycles. In addition, one-electrode TENGs achieved the largest V_{oc} of ≈120 V and I_{sc} of 4.2 μA.

5.1.3. PENGs

Advances in materials science and mechanical engineering enable flexible/stretchable PENGs applicable in energy harvesters from natural motions, actuators for the skin, and in vivo diagnostic kits.[233] Similar to wearable TENGs, wearable PENGs can be applied as power sources or self-powered active sensors in wearable electronics using mechanical energy from diverse body activities.[248] The piezoelectricity is originated from the piezoelectric effects from materials that can produce polarization charges on their surfaces under external stimuli.[248b] Piezotronic effect was first proposed by Wang,[249] which describes the modulation of the band structure and the transport of charge carriers via a deformed piezoelectric semiconductor.[250] Piezotronics has been developing rapidly due to its great potentiality in applications for electronic skins.[250–251]

Piezoelectric materials can be divided into three different categories: inorganic, organic, and organic and composite piezoelectric materials. Typical inorganic nanomaterials with a high piezoelectric effect are ZnO,[252] MoS_2,[253] $BaTiO_3$,[254] PZT,[255] and their composites.[254b,256] For organic piezoelectric materials, PVDF[257] and P(VDF-TrFE)[258] are the most popular polymers due to their promising features such as flexibility, stability, and piezoelectricity. Electrospinning has been proven to be a simple and effective method to produce 1D piezoelectric PVDF and P(VDF-TrFE) nanostructures.[259] Piezoelectric electrospun nanofibers can be easily incorporated into textiles for self-powered wearable electronics.[252a,257a,259b] Gao et al.[260] reported a flexible yarn-shaped PENG from electrospun PVDF nanofibers with a power density average V_{oc} of 0.52 V, I_{sc} of 18.76 nA, and power density of 5.54 μW cm^{-3} under a cyclic compression of 0.02 MPa at 1.85 Hz. In terms of nanocomposite materials, piezoelectric NPs or NWs are integrated with piezoelectric polymers to enhance energy conversion in wearable PENGs.[253,261] For example, a nanocomposite of self-poled electrospun nanofibers of barium titanate NPs/polyurethane (BT NPs–PU) and (P(VDF-TrFE)) was developed to produce a free-standing piezoelectric layer.[262] Packaged with a pair of 3D microstructure graphite/PDMS electrodes, the as-prepared PENGs could achieve a peak V_{oc} of 9.3 V and a I_{sc} of 189 nA. Moreover, the PENG exhibited a high stretchability of 40% and could maintain its performance up to 9000 cycles stretching/releasing under 30% strain with a minimal drop in the output.

5.1.4. Solar Cells

The abundant, clean, and affordable solar power is regarded as the most important renewable energy resource. In this regard, photovoltaics, which convert sunlight into electricity without causing any pollution to our environment, has become one of the most promising technologies to harness solar energy. With the ever-increasing advancement of wearable electronics, flexible/stretchable solar cells have attracted tremendous attention for their promising features such as lightness, thinness, flexibility/stretchability, and adaptability to curvilinear surfaces.[263] Thus far, a various range of wearable solar sources have been reported, for example flexible/stretchable organic photovoltaics (OPVs),[264] flexible/stretchable perovskite solar cells (PSCs),[265] and flexible/stretchable dye-sensitized solar cells (DSSCs).[266] An electron/hole transport layer is utilized in OPVs and PSCs to decrease the recombination of charge, while DSSCs require electrolytes for charge transport and redox reactions.[263c]

Soft skin-like wearable OPVs are known for their excellent characteristics of thinness, high flexibility/stretchability, lightness, good stability, scale-up and solution-processable fabrication, and power conversion efficiency (PCE).[267] The PCE of OPVs was 17.4% in 2020, which is twice as high as it was 10 years ago.[264b] Owing to the advancement in device structure and material exploration, flexible OPVs on ≈100–300 μm thick polymer substrates can tolerate bending radii in the millimeter-scale with PCEs of over 12.5%.[268] The first ultrathin (<10 μm) OPVs was demonstrated by Kaltenbrunner et al.[269] in 2012. It was constructed on 1.4 μm thick PET substrates with a specific weight value of only 10 W g^{-1}. The as-received OPVs have a PCE of 4.2% and can be stretched to more than 300% strain using elastomeric support. Furthermore, a waterproof stretchable OPV was developed by sandwiching an ultraflexible OPV (3 μm thick) between two elastomers with a PCE of 7.9% and a stretchability of 52%.[270] The PCE decreased only by 5.4% after immersion in water for 2 h. Additionally, the efficiency of the device retained 80% of its initial value even after 52% mechanical compression for 20 cycles with 100 min of water exposure.

PSCs were first reported in 2009 with a PCE of 2.81%, and they achieved a record of 22.7% in 2017.[271] Perovskites can be described as ABX_3, where larger A cations are surrounded by anion-constructed cuboctahedrons and smaller B cations

occupy the center anion-constructed octahedrons. The A and B cations are coordinated by 12 and 6 X anions, respectively. A typical ABX_3 is methylammonium lead iodide ($MAPbI_3$).[265b] Recently, soft skin-like PSCs have emerged as a promising candidate for realizing high-quality photovoltaic devices due to its high efficiency, low cost, solution-processability, and low-temperature ability.[263d,272] A PCE of up to 18.1% has been achieved by a flexible PSC made on an ITO/PET surface via a low temperature (≤100 °C) solution procedure in 2017.[273] In 2018, Feng et al.[274] increased the value to 18.4% with good mechanical tolerance using a novel dimethyl sulfide.

In DSSCs, the energy conversion is based on a photoelectrochemical process that involves redox reactions induced by light.[275] A typical DSSC is composed of a large bandgap mesoporous semiconducting film coated with a monolayer of dye molecules and filled in a redox electrolyte.[276] In soft skin-like wearable DSSCs, fullerene is rarely used, carbon-based materials such as CNTs and graphene are usually employed to fabricate fiber-shaped DSSCs and film-type DSSCs.[263a,276a,277] Organic thiolate/disulfide redox couple-based flexible DSSCs has been developed and achieved a PCE of 7.33%, which is higher than that of DSSCs using a conventional I-/I3-redox couple.[278] Fu et al.[279] reported a fiber-shaped DSSC with a record PCE of up to 10%. The DSSCs were fabricated using a new fiber-shaped electrode with a hydrophobic aligned CNT core, which provides both high conductivity and mechanical robustness. The device retained 82% of its initial PCE after bending to 90° for even 2000 cycles and power a pedometer continuously with outdoor sunlight.

5.2. Energy Storage Devices

Recently, soft skin-like energy storage devices have attracted enormous attention due to their advantageous features—low-cost, flexibility, wearability, long cycle life, and high efficiency)—which could be utilized to bridge the energy gap between conventional capacitors and batteries. In this section, we introduce representative examples of soft skin-like supercapacitors and batteries.

5.2.1. Supercapacitors

Soft skin-like wearable supercapacitors have attracted considerable attention owing to their promising features such as ease of fabrication, high energy and power density, superior stability and safety, long cycle life, high efficiency, fast charging/discharging, and excellent mechanical flexibility/stretchability.[280] They are also capable of bridging the power/energy gap between conventional capacitors and fuel cells/batteries. These attributes provide great advantages to power individual skin electronic devices in integrated flexible/stretchable electronics and implantable electronics. Therefore, flexible/wearable supercapacitors are considered one of the most promising energy storage devices for wearable electronics.[281]

A supercapacitor typically consists of two active electrodes, current collectors, an electrolyte, and a separator. From the standpoint of the mechanism of energy storage, supercapacitors can be classified into electrochemical double-layer capacitors (EDLCs), pseudocapacitors, and hybrid capacitors.[282] EDLCs store energy electrostatically at the electrolyte/electrode interface (physical process), whereas pseudocapacitors store charge via fast redox reactions (chemical/Faradaic processes). For EDLCs, carbon-based materials (e.g., graphene, CNTs, graphitic carbon, carbon nanofibers, activated carbon, and carbide-derived carbon) are commonly utilized as electrode materials because of their large surface area, which leads to higher energy densities.[283] Electrode materials for pseudocapacitors are primarily transition metal oxides and hydroxides[284] (e.g., RuO_2, MnO_2, Fe_2O_3, and Nb_2O_5) and conducting polymers (e.g., polypyrrole (PPy), PANI, PEDOT, and polythiophene, which have redox reactions.[280a,285] The working mechanisms of EDLCs have a high energy density and stability but a small capacitance; however, pseudocapacitors exhibit the opposite behavior. Hybrid supercapacitors combine the mechanisms of both EDLCs and pseudocapacitors and show an extended operating window, high energy density, and high capacitance.[286]

Concerning the structure of the electrode materials, supercapacitors can be fabricated into three architectures: 1D fiber/yarn-shaped, 2D planar-type, and 3D sponge-like. In terms of fiber/yarn-shaped supercapacitors, the two yarn/fiber electrodes are assembled in a twisted[287] or parallel model[288] or even packaged into a core-sheath configuration.[289] For a planar supercapacitor, the two electrodes are sandwiched between a solid/gel electrolyte and a separator.[290] In the case of sponge-like supercapacitors, foam materials made from polymers, Nis, free-standing 3D frameworks, and carbon aerogels are used as body materials for the construction of porous flexible supercapacitors. For example, by using PPy conducting polymer as a mediator, Zhao et al.[291] developed an in situ formation of PPy–graphene foam and demonstrated a highly compression-tolerant supercapacitor. PPy was electrodeposited onto 3D graphene, and the freeze-dried PPy–graphene had a specific surface area of up to 463 $m^2\ g^{-1}$. The resultant two-electrode capacitor exhibited ideal capacitive behavior with rectangular cyclic voltammetry (CV) curve. The good performance even retained during 1000 cyclic compressions with a stain of 50%. Furthermore, the normalized volume capacitances are 14 and 28 $F\ cm^{-3}$ for uncompressed and the 50% compressed supercapacitor, respectively. However, the value for a normal 3D graphene supercapacitor is ≈4 $F\ cm^{-3}$.

Soft skin-like wearable supercapacitors are required to maintain high electrical performance under repetitive mechanical deformations, such as bending, twisting, folding, and stretching to adopt them onto the skin.[280a] A key challenge is to archive flexible/stretchable electrode materials with good capacitive behaviors and to assemble them with appropriate electrolytes and separators in a flexible/stretchable and robust configuration.[292] Various highly conductive and flexible/stretchable electrodes have been developed to ensure fast charging/discharging of wearable supercapacitors.[293] These electrodes are either free-standing [286b] or interfaced with flexible metal, paper, and textile substrates.[287c,294] Owing to the technological advances in material and assembling techniques, wearable supercapacitors have become transparent,[293c,295] more stretchable,[290a] and thinner,[286a,296] and display other capabilities such as waterproofing,[297] and self-healability (Figure 10c–e).[298] For instance,

a self-healable supercapacitor has been fabricated using an electrolyte comprising polyacrylic acid dual crosslinked by hydrogen bonding and vinyl hybrid silica NPs. The developed supercapacitor could retain fully even after 20 cycles of cutting/healing and be stretched to 600% strain by simply incorporating wavy electrodes.[298]

5.2.2. Batteries

Batteries, which store electrical energy from redox reactions during the charging/discharging process, are key components as flexible/stretchable power sources in the emerging field of wearable electronics.[299] Compared with supercapacitors, batteries exhibit advantages such as high energy density, lack of a memory effect, long-term stability, and high working voltage.[300] In general, a stretchable battery consists of cathode and anode electrodes, separators and electrolytes, and packaging materials.[301] Based on the device structure, materials for soft skin-like wearable batteries include flexible/stretchable electrode materials and flexible/stretchable electrolyte and separator membrane materials. Among all the components of batteries, the electrode is a key building block for the construction of skin-like wearable batteries. Carbon-based materials, such as graphene,[302] CNTs,[303] and graphite,[304] have been widely employed to fabricate stretchable electrodes owing to their advantageous mechanical and electrical properties. For instance, a highly elastic (100% strain) Li-ion battery was obtained by packaging two aligned CNTs/$Li_4Ti_5O_{12}$ fiber-shaped electrodes with outstanding electrochemical properties (e.g., energy densities of 27 Wh kg^{-1} or 17.7 mWh cm^{-3} and power densities of 880 W kg^{-1} or 0.56 W cm^{-3}).[305] Metals (e.g., aluminum, copper, and stainless steel), conducting polymers (e.g., PPy, PEDOT:PSS) and hybrid materials have also been utilized to fabricate stretchable electrodes of batteries.[301] In order to achieve mechanical flexibility/stretchability, a variety of gel polymer electrolytes (e.g., ethylene carbonate and dimethyl carbonate) and solid polymer electrolytes (e.g., polyethylene oxide and PVA) have been developed to replace the ionic electrolyte used in traditional batteries. In some cases, another stretchable separator membrane is used to enhance the mechanical robustness. For example, a porous separator made of PU/PVDF is able to avoid breakage and elimination under repetitive stretching/releasing cycles.[306] Over the past two decades, Li–S (sulfur) batteries have experienced tremendous development,[232,307] which has led the exploration of new electrode materials (e.g., elements in Group IA and VIA) that share an analogous multielectron chemistry.[302,308]

6. System Integration

For the complete input and output control loop required by VR/AR, signal processing and energy supporting are usually necessary for a complete system of skin electronics (**Figure 11**a). Rigid integrated circuit (IC) chips play an important role in signal processing, communication, and power management. Signals taken by input devices are usually locally amplified, filtered, digitalized, and processed with the assistance of on-skin IC chips.[309] IC chips and their external circuits are also necessary for receiving instructions from external devices and controlling on-skin stimulators.[310] However, to provide an immersive VR/AR and minimize the consciousness of unreality, the most challenging part of skin electronic system integration is how to maintain low wearing discomfort and normal skin sensing ability while using rigid IC chips.

6.1. On-Skin System Integration

To use rigid IC chips for skin electronics, assembling these rigid components onto flexible or stretchable substrates is important (Figure 11b). This decreases the mechanical mismatch between the skin electronics platform and real skin, thus providing a better VR/AR experience. Usually, an island structure is utilized[126,309d,311] where rigid chips as "islands" are assembled soft substrates with stretchable connectors. This method creates a mechanical durable connection between rigid chips and wirings while maintaining the entire system with good flexibility and even stretchability. The substrate of the hybrid system is usually composed of layers of stretchable polymers such as ultrathin polyimide,[309e] PDMS,[126,309f,311c] Ecoflex,[309d] or even just fluid as the filler.[312]

6.1.1. Signal Processing System on Skin

Tiny signal acquisition and processing have been developed in the industry with well-designed analog and digital circuits. However, with respect to skin electronics, the dimension restriction and the demand for soft and biocompatible systems bring challenges in miniaturization.[309c,e] Compared with fully designed industry-level signal processing circuits, on-skin signal processing requires a rigorous system size reduction, accompanied by a decrease in active and passive components, loss of interconnection conductivity, and shrinking in antenna design. These requirements cause a sacrifice in system functionality, performance, and robustness. Under these circumstances, the circuit design rule of an on-skin VR/AR system should focus on maintaining the integrity and stability of body signal acquisition and the effectiveness of stimulator driving, while leaving the compute-intensive data processing task to the external off-skin devices.

Understanding the spectrum and driving ability of designated body signals helps the appropriate design of the filter passband and the input impedance of the amplifier or directly connected analog-to-digital converter (ADC) (Figure 11c).[309a] Signals are in various forms such as voltage, current, resistance, or capacitance, showing a distinct region of interest in the spectrum, and having different output impedances. For signals of different types, the specific design of the circuit topology plays an important role in reducing noise from device deformation, body movement, body potential change, signal crosstalk, power supply, and radio frequency (RF) interference, while maintaining the quality of signal acquisition.

It should be pointed out that, as a system on the skin that suffers bending and stretching, unconscious body movement and intentional interaction with humans contribute a huge part

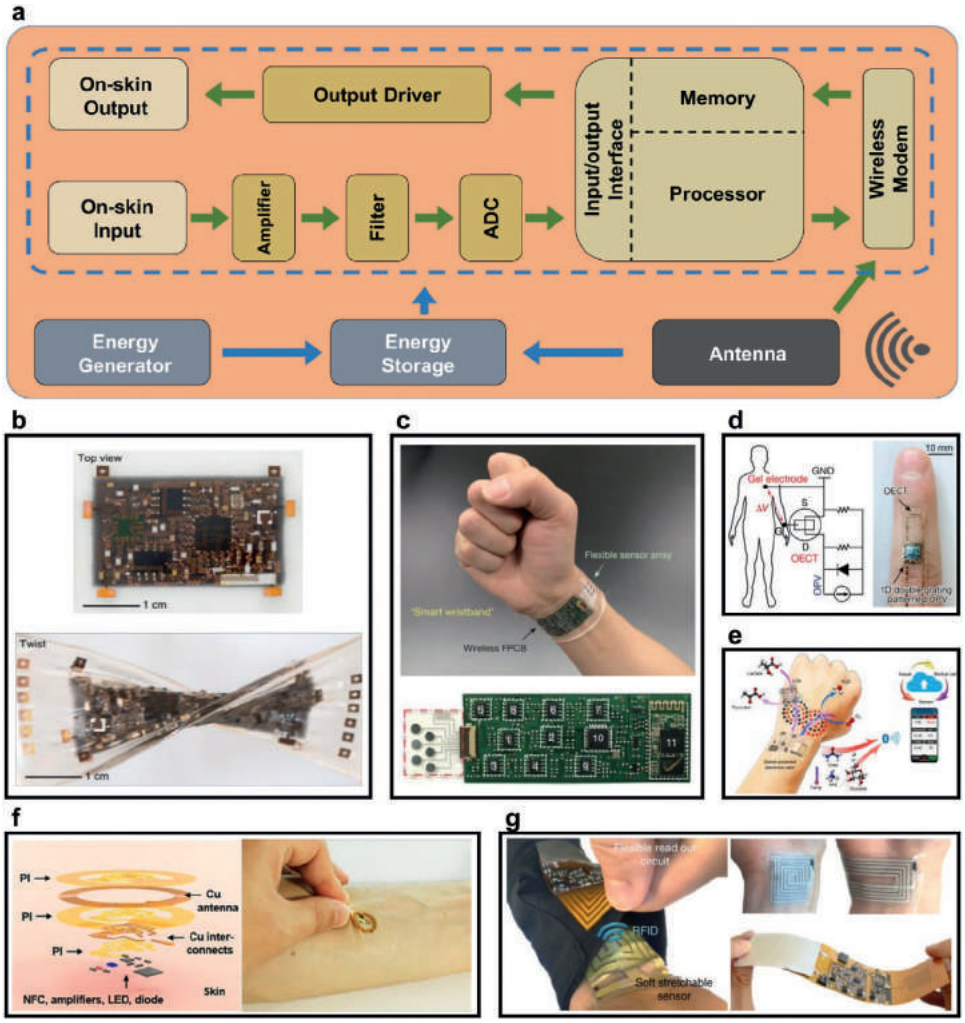

Figure 11. System integration of skin electronics. a) Schematic diagram of typical on-skin systems. This system includes an on-skin signal processing part that acquires input signals or controls outputs, a wireless communication part that synchronizes on-skin data with external processers, and an energy supporting part that uses on-skin energy generators or wireless energy transmission. b) Multilayered stretchable electronics by assembling IC chips on a stretchable substrate. Reproduced with permission.[309c] Copyright 2018, Springer Nature. c) A "smart wristband" with specifically designed readout circuits for on-skin input devices. Reproduced with permission.[309a] Copyright 2016, Springer Nature. d) A self-powered electrochemical sensing system powered by using flexible photovoltaic. Reproduced with permission.[316] Copyright 2018, Springer Nature. e) A biofuel-powered integrated e-skin with multimodal sensors and Bluetooth low energy for communication. Reproduced with permission.[309f] Copyright 2020, American Association for the Advancement of Science. f) A stretchable optoelectronic system using wireless power transmission and near-field communication. Reproduced with permission.[309g] Copyright 2016, American Association for the Advancement of Science. g) On-skin stretchable sensors and on-textile readout circuits and communication terminals to form a body area network. Reproduced with permission.[325a] Copyright 2019, Springer Nature.

of the signal interference. Adding electromagnetic shielding[313] and shortening the connection distance by a vertically stacked configuration[309c,314] have been demonstrated to relieve the interference.

In addition to rigid IC chips, voltage amplification in on-skin sensors by intrinsically flexible or stretchable TFTs has also been reported.[315] For example, by using mismatch compensation and load circuits with high gain and wide input range, Sugiyama et al.[315c] achieved a differential amplifier composed of organic TFTs showing good noise suppressed voltage amplification even when bending to ≈50 µm. This organic differential amplifier provides a high input impedance on the order of MΩ, which enables it for weak and small body signal detection. By attaching this flexible signal processing film to human skin, an ECG signal amplification is demonstrated with an output SNR of 34 dB.

6.1.2. On-Skin Energy System

As introduced in Section 5, energy harvesting is usually realized by piezo/triboelectricity, photovoltaic, and biofuel cells. With energy from local, interference to body signal measured from energy transmission is also suppressed,[316] and high-quality body signals can be collected for the VR/AR system (Figure 11d,e).

Hwang et al.[317] a self-powered integrated system with an all-in-one e-skin patch consisting of a TENG, supercapacitor, and resistive strain sensor stacked together. In this system, the energy harvested by a TENG is rectified and stored in a supercapacitor. With the supercapacitor as the current supply, they successfully demonstrated a resistive strain sensor for detecting human activities. As a comparison, the measured signal shows high consistency when using an external commercial source measurement unit.

Because the output of the piezo/triboelectric nanogenerator is in AC form, it is essential to rectify the current to DC form for energy storage and usage. In addition to using rigid chips or nanomembranes to realize rectification, flexible rectifying diodes for skin electronics are also demonstrated.[318] Lin et al.[318a] reported a polymer-based rectifying diode with an operation frequency of over 14 MHz. They demonstrated that the appropriate conductivity of intermediate layers and the purification of polymer semiconductor materials are critical to the high rectification ratio and operation frequency. With the rise of metal oxide semiconductors, e-skin flexible rectifying diodes with extremely high performance such as operating frequency reaching 6.3 GHz and rectification ratio over 108 are also proposed.[318b,c] To reduce the system complexity, a PENG/TENG with asymmetric output is also invented to directly charge a supercapacitor without current rectification. By introducing a redox reaction, Rasheed et al.[319] achieved a rectifier-free piezoelectric nanogenerator that can be directly integrated with a supercapacitor. This nanogenerator shows asymmetric piezoelectric potential change during compressing and releasing due to the carrier migration caused by the redox reaction, leading to an efficient piezoelectric energy harvesting and storage even without rectification.

Even with possessing of DC output, photovoltaic, biofuel cell, or thermoelectricity usually cannot afford a sufficiently high voltage level to drive many components on e-skin systems. Voltage boosting can be realized by simply making a series connection between energy harvesters[320] or utilizing an external voltage regulator.[309f,321] The latter can especially provide a stable output voltage level, which may be necessary for some stimulator control and ADC processing.

6.2. Wireless System Integration

In VR/AR applications, an external device may contain high-performance processors, off-skin sensors, and simulators as well as an energy source, which will frequently communicate with the on-skin system and even provide energy support. Beyond the connection with wires, a wireless connection can provide better convenience and device flexibility, and is usually preferred.

6.2.1. Wireless Connection Method

Wireless connection through an EM field is a potential solution for the access of the on-skin system to external devices. This approach can be used for both data and power transmission by bringing the convenience of getting rid of wires. From the perspective of connection form, the EM wireless connection can be categorized as a nonradiative connection and a radiative connection.

The nonradiative connection is realized by coupled magnetic resonances, through well-coupled coils between the transmitter and receiver. In most cases, this coupling can only be built effectively in the near-field range, with a wireless connection distance within several centimeters. By finely designing the antenna, a strong coupling can be achieved with a connection distance several times of the coil dimension.[322] In the skin electronics scenario, this can be referred to as a middle-field connection between tens of centimeters.[323] To extend the connection distance, the far-field connection is realized by the radiative EM field. In this range, the EM field dramatically attenuates with increasing distance. For an efficient wireless connection, well-designed antennas and strict impedance matching are critical.[324]

6.2.2. Wireless Communication

With the bloom of the Internet of Things (IoT), wireless digital communications with simple and tiny terminal devices based on a star topology have shown great demand. Many communication protocols such as cellular networks, Wi-Fi, Bluetooth, near-field communication (NFC), and ZigBee have been developed to meet different wireless communication requirements. For skin electronics, NFC and Bluetooth are the most widely used wireless communication methods (Figure 11e,f), as they can be simply realized by a tiny single-chip IC with low power consumption.[309e,f,310,325] With the idea of a system on a chip, most of the units for signal processing, such as general-purpose input/output, ADC, processor, memory, and a wireless modem can all be integrated on a single chip, making it possible to realize a complete on-skin system with only a few rigid components.[309g,326] By attaching such a chip with flexible on-skin sensors, stimulators, energy sources, and the antenna, a fully functional on-skin system can be realized with good flexibility and convenience.

Compared with Bluetooth, the NFC system only requires very low power support, which is usually realized by all passive components with wireless energy transmission through coupled coils. NFC has a limited data transmitting rate of only no more than 424 kbit s^{-1}, but this usually is not a bottleneck to skin electronics for VR/AR, which only requires a small capacity for data transmission. Another drawback of NFC is the wireless connection distance, as the effective coil coupling usually only exists at an almost touching distance, it adds some difficulties to the external terminals connecting with the on-skin device. On the other hand, Bluetooth connection has a built-in meter range, but needs higher power consumption; therefore, a more sustainable local power supply is required.[309a,b,314,327] Bluetooth low energy (BLE) is a new protocol from Bluetooth 4.0 endowed with very low power requirements. With a delicate system design, an on-skin BLE system powered by wireless energy transmission is also achieved.[309d]

While long-distance connection brings convenience, the security of wireless communication also causes people's concerns. Regarding this issue, Tian et al. invented an on-skin system with BLE wireless communication by radio

surface plasmons propagating on textiles. This method confines wireless communication to within 10 cm of the body, making wireless connections to external devices convenient and secure.[328]

In addition to using standard wireless digital communication based on rigid IC chips, another promising wireless data transmission method from an on-skin system to external devices is by measuring the LCR resonance through inductively coupled coils.[329] This method takes advantage of using all flexible components based on passive inductive coupling where no other energy source is needed. However, user-activated LCR resonance measurement by an external device is usually required. To overcome this, Bao and co-workers[325a] constructed a body area sensor network using a textile-based resonance analyzer with on-skin sensors and LCR resonators with the concept of bodyNET.[330] In this system, each resonance analyzer on clothes is connected by Bluetooth to a central hub device, which performs further communication with external devices (Figure 11g).

6.2.3. Wireless Energy Transmission

Wireless energy transmission through coupled coils in the near-field range has already been commercialized in the wireless powering of smartphones and other portable electronics. With the EM wave restricted between coupled coils, this approach can afford a high transmission power efficiently with even simple designed antennas and is widely used in wirelessly connected on-skin systems (Figure 11f).[309d,e,g,310,326,331] The transmitted power is even high enough to drive an array of 32 actuators that consumes more than 50 mW from a distance of 80 cm.[310] However, although middle-field energy transmission based on coil coupling is demonstrated even in the deep tissue range,[323] the high direction dependency and still disquieting transmission distance bring difficulties to the design of energy support on both the e-skin system and the corresponding external device.

Based on the fact that skin electronics usually do not consume high power, far-field RF power transmission also becomes possible. As the power of RF is strictly limited considering human safety, challenges come out in the design of efficient on-skin antennas even under deformation. By using a well-designed antenna with low resistance and wide bandwidth to reduce loss from RF power harvesting, as well as using impedance matcher, rectifier, and voltage doubler based on Si nanomembranes with high performance to realize efficient rectification, Huang et al. achieved an RF powered on-skin system that can harvest sufficient power to operate an LED while the antenna is stretched.[324b]

7. Conclusions and Perspectives

Recent advances in skin electronics allow us to consider their future application in VR and AR as an alternative to conventional bulky and heavy devices. Ultrathin, ultralight, and flexible/stretchable skin electronic devices are conformally attached to skin, exhibiting intrinsic advantages such as low wearing discomfort, maintenance of skin sensing, minimized change in body position, and user-interactive physiology and interfacing. Recently, there are also review papers focusing on the topic of VR/AR topic using soft electronics, such as textile,[332] skin-integrated vibrohaptic interfaces,[333] and wearable electronics.[334] The demonstrations of skin electronics in this review, including input and output devices, energy devices, and system integration components, have great potentiality to partially or fully substitute conventional VR/AR devices.

Nonetheless, many technical challenges and tasks still exist for the real application of skin electronics for advanced VR and AR.

7.1. Perceptional Differences

Although many on-skin devices show performances corresponding to the range and sensitivity of the human sensory system, there are still many gaps in both input and output devices. The inevitable usage of soft materials further broadens the gap between human perception and devices. It is necessary to develop devices with both high performance and mechanical stability based on a better understanding of the human sensory system.

7.2. Varieties in Input and Output Devices

There have been many research approaches to mimic or alternate the haptic sensing of skin. However, many other input and output devices, such as taste and olfaction, are still insufficiently investigated in skin electronics. Although some sense can be substituted with the aid of wearable components such as contact lenses or smart glasses, more investigation into the less-focused sensory parts is required. To achieve this in the form of skin-like devices, advances in functional materials and structures are highly desired.

7.3. Synchronization of Multiple Input and Output

Considering that human perception is an inevitable result of multiple sensing, the synchronization of multiple sensory systems is necessary. This should be applied to spatially differentiable multiple devices of the same sensory system, such as auditory or visual perception, including their spatial resolution and directional resolution. Although this can be partially modified by software processing, the consideration of synchronization at the device level is highly desirable for real-time AV/VR processing.

7.4. Limitations of Energy System

The huge amount of signal processing and frequent data communication require a continuous and powerful energy supply. Although blooming in recent years, current on-skin energy generation solutions still cannot afford very large power for several circuit applications. Energy harvesting using human sweat, motion, or light is highly dependent on the environment, thus

leading to instability. On the other hand, wireless energy transmission usually has strict limitations on transmission distance, direction, and human safety, where more reliable and general approaches are still expected.

7.5. Block or Acceptance of Human Sensing

For an ideal VR or AR, the total block out or permission of the external physical stimuli is desired, respectively. In that sense, many conventional ultrathin and flexible/stretchable skin electronic devices can be more beneficial for AR, without allowing the total blocking out. Therefore, both directions of effort based on the advances in materials and structures are demanded. For AR, the minimization of the loss or distortion of external physical stimuli should be pursued; for VR, the maximization of the absorption or reflection of physical stimuli while maintaining the ultrathin and ultralight properties of components should be invented. In an ideal case, the conversion between blocking out and sensing-through through the transformation of a single device can be considered.

7.6. System Composition and Maintenance

Although several approaches are showing the integrated system of input, output, and energy/signal transporting devices, most of the research on skin electronics is still limited to the demonstration of single components. To cope with this, both approaches of placing whole components onto skin or using wireless data/energy transportation should be considered, depending on the targeted application. In terms of maintenance, the rigid interconnection of components and adhesion to the skin under both relaxed and bent/stretched conditions are required. More technical challenges in real usage such as sweating, skin-to-skin difference, reusability, and long-term stability are also further considered.

7.7. Mixed Reality

Mixed reality is an emerging topic in the field of VR and AR with demanding the interaction with both physical and virtual realities. To archive this mixture of VR and AR simultaneously, the advanced devices are highly demanded with high resolution and partially sense-through functionality. Like in the case of AR, the advantages such as low wearing perception and maintenance of skin sensing in skin electronics can be beneficial to have the partially substituted mixed reality without feeling discomfort in the perception.

7.8. Smart Contact Lenses

One of the technologies that skin electronics can be applied directly and compensatory is the smart contact lenses. Due to the similarities in the technical demands such as softness, biocompatibility, thinness, and damage-free attachment/detachment, it is expected that many materials and structures of skin electronic devices can be used to construct smart contact lenses and vice versa. As the next-generation device platforms, both skin electronic devices and smart contact lenses are crucial for the future VR/AR devices.

The development of materials and structures based on the proper understanding of human–machine interactions will open more new opportunities on skin electronics for VR and AR applications as one of the most important future directions of the field. Furthermore, interdisciplinary research approaches to hardware and software will narrow down the technical difficulties for the realization of the alternation of human perception.

Acknowledgements

J.J.K. and Y.W. contributed equally to this work. J.K., the International Research Fellow of Japan Society for the Promotion of Science, acknowledges the support from the Japan Society for the Promotion of Science (JSPS) Postdoctoral Fellowships for Research in Japan.

Conflict of Interest

The authors declare no conflict of interest.

Keywords

augmented reality, on-skin input devices, on-skin output devices, skin electronics, virtual reality

Received: November 10, 2020
Revised: January 12, 2021
Published online:

[1] a) P. Milgram, H. Takemura, A. Utsumi, F. Kishino, *Telemanipulator and Telepresence Technologies*, Proc. SPIE, Vol. *2351*, SPIE, Bellingham, WA **1995**; b) R. T. Azuma, *Presence: Teleoperators Virtual Environ.* **1997**, *6*, 355.
[2] a) K. Song, S. H. Kim, S. Jin, S. Kim, S. Lee, J. S. Kim, J. M. Park, Y. Cha, *Sci. Rep.* **2019**, *9*, 8988; b) L. Juhsz, T. Novack, H. H. Hochmair, S. Qiao, *ISPRS Int. J. Geo-Inf.* **2020**, *9*, 197; c) M. Kim, S. H. Choi, K.-B. Park, J. Y. Lee, *Appl. Sci.* **2019**, *9*, 3171; d) J. Dascal, M. Reid, W. W. IsHak, B. Spiegel, J. Recacho, B. Rosen, I. Danovitch, *Innovations Clin. Neurosci.* **2017**, *14*, 14.
[3] A. Seth, J. M. Vance, J. H. Oliver, *Virtual Reality* **2011**, *15*, 5.
[4] C. T. Tan, D. Soh, in *Proc. of GAMEON-ARABIA*, EUROSIS **2010**.
[5] R. Yung, C. Khoo-Lattimore, *Curr. Issues Tourism* **2019**, *22*, 2056.
[6] X. Li, W. Yi, H.-L. Chi, X. Wang, A. P. Chan, *Autom. Constr.* **2018**, *86*, 150.
[7] L. Freina, M. Ott, in *The 11th Int. Scientific Conf. eLearning and Software for Education*, National Defence University Publishing House **2015**.
[8] a) J. Iwanaga, M. Loukas, A. S. Dumont, R. S. Tubbs, *Clin. Anat.* **2020**, *34*, 108; b) E. Mantovani, C. Zucchella, S. Bottiroli, A. Federico, R. Giugno, G. Sandrini, C. Chiamulera, S. Tamburin, *Front. Neurol.* **2020**, *11*, 926.
[9] a) D.-H. Kim, N. Lu, R. Ma, Y.-S. Kim, R.-H. Kim, S. Wang, J. Wu, S. M. Won, H. Tao, A. Islam, *Science* **2011**, *333*, 838; b) M. L. Hammock, A. Chortos, B. C. K. Tee, J. B. H. Tok, Z. Bao,

Adv. Mater. **2013**, *25*, 5997; c) T. Someya, M. Amagai, *Nat. Biotechnol.* **2019**, *37*, 382.
[10] a) J. Lee, H. Sul, W. Lee, K. R. Pyun, I. Ha, D. Kim, H. Park, H. Eom, Y. Yoon, J. Jung, *Adv. Funct. Mater.* **2020**, *30*, 1909171; b) M. Kaltenbrunner, T. Sekitani, J. Reeder, T. Yokota, K. Kuribara, T. Tokuhara, M. Drack, R. Schwödiauer, I. Graz, S. Bauer-Gogonea, *Nature* **2013**, *499*, 458.
[11] G. C. Burdea, P. Coiffet, *Virtual Reality Technology*, John Wiley & Sons, Hoboken, NJ **2003**.
[12] F. Zhou, H. B.-L. Duh, M. Billinghurst, in *2008 7th IEEE/ACM Int. Symp. on Mixed and Augmented Reality*, IEEE, Cambridge, UK **2008**, pp. 193–202.
[13] A. B. Craig, W. R. Sherman, J. D. Will, *Developing Virtual Reality Applications: Foundations of Effective Design*, Morgan Kaufmann, Burlington, MA **2009**.
[14] L. Pugnetti, M. Meehan, L. Mendozzi, *Presence: Teleoperators Virtual Environ.* **2001**, *10*, 384.
[15] a) S. Wibirama, H. A. Nugroho, K. Hamamoto, *Entertain. Comput.* **2018**, *26*, 117; b) M. Malińska, K. Zużewicz, J. Bugajska, A. Grabowski, *Int. J. Occup. Saf. Ergon.* **2015**, *21*, 47.
[16] S. H. Nam, J. Y. Lee, J. Y. Kim, *J. Sens.* **2018**, *2018*, 9054758.
[17] C. Pacchierotti, S. Sinclair, M. Solazzi, A. Frisoli, V. Hayward, D. Prattichizzo, *IEEE Trans. Haptics* **2017**, *10*, 580.
[18] a) J. Sardo, J. Semião, J. Monteiro, J. A. Pereira, M. A. de Freitas, E. Esteves, J. M. Rodrigues, *INCREaSE*, Springer, Cham **2017**; b) T. Murakami, T. Person, C. L. Fernando, K. Minamizawa, in *ACM SIGGRAPH 2017 Posters*, ACM, Los Angeles **2017**, pp. 1–2.
[19] C.-C. Liao, H. Koike, T. Nakamura, in *Extended Abstracts of the 2020 CHI Conference on Human Factors in Computing Systems*, ACM, Hololulu **2020**.
[20] a) I. Goodfellow, J. Pouget-Abadie, M. Mirza, B. Xu, D. Warde-Farley, S. Ozair, A. Courville, Y. Bengio, in *Advances in Neural Information Processing Systems 27 (NIPS 2014)*, Morgan Kaufmann Publishers Inc. **2014**; b) J. Redmon, S. Divvala, R. Girshick, A. Farhadi, in *Proc. of the IEEE Conf. on Computer Vision and Pattern Recognition*, IEEE, Las Vegas **2016**, pp. 779–788.
[21] J. Schmidhuber, *Neural Networks* **2015**, *61*, 85.
[22] S. Cass, *IEEE Spectrum* **2019**, *56*, 16.
[23] a) J. Chakareski, in *Proceedings of the Workshop on Virtual Reality and Augmented Reality Network 2017*, ACM, Los Angele **2017**, pp. 36–41; b) I. Selinis, K. Katsaros, M. Allayioti, S. Vahid, R. Tafazolli, *IEEE Access* **2018**, *6*, 56598.
[24] a) R. Pausch, D. Proffitt, G. Williams, in *Proc. of the 24th Annual Conf. on Computer Graphics and Interactive Techniques*, ACM, New York **1997**, pp. 13–18; b) D. A. Bowman, R. P. McMahan, *Computer* **2007**, *40*, 36.
[25] F. Argelaguet, A. Kulik, A. Kunert, C. Andujar, B. Froehlich, *Int. J. Hum-Comput. Stud.* **2011**, *69*, 387.
[26] a) A. D. Cheok, K. Karunanayaka, *Virtual Taste and Smell Technologies for Multisensory Internet and Virtual Reality*, Springer, Cham **2018**; b) N. Ranasinghe, K. Karunanayaka, A. D. Cheok, O. N. N. Fernando, H. Nii, P. Gopalakrishnakone, in *BodyNets '11: Proc. of the 6th Int. Conf. on Body Area Networks*, ACM, New York **2011**.
[27] O. Bimber, R. Raskar, *Spatial Augmented Reality: Merging Real and Virtual Worlds*, CRC Press, Boca Raton, FL **2005**.
[28] T. Baranowski, E. J. Lyons, *Games Health J.* **2020**, *9*, 71.
[29] S. Sharples, S. Cobb, A. Moody, J. R. Wilson, *Displays* **2008**, *29*, 58.
[30] D. Drascic, P. Milgram, *Stereoscopic Displays and Virtual Reality Systems III*, Proc. SPIE, Vol. *2653*, SPIE, Bellingham, WA **1996**.
[31] D. Schmalstieg, T. Hollerer, *Augmented Reality: Principles and Practice*, Addison-Wesley Professional, Boston, MA **2016**.
[32] A. B. Craig, *Understanding Augmented Reality: Concepts and Applications*, Newnes, Oxford **2013**.
[33] D. van Krevelen, R. Poelman, *Int. J. Virtual Reality* **2010**, *9*, 1.
[34] R. Azuma, Y. Baillot, R. Behringer, S. Feiner, S. Julier, B. MacIntyre, *IEEE Comput. Graphics Appl.* **2001**, *21*, 34.
[35] a) J. Park, J. Kim, S.-Y. Kim, W. H. Cheong, J. Jang, Y.-G. Park, K. Na, Y.-T. Kim, J. H. Heo, C. Y. Lee, *Sci. Adv.* **2018**, *4*, eaap9841; b) J. Kim, E. Cha, J. U. Park, *Adv. Mater. Technol.* **2020**, *5*, 1900728.
[36] D. Wagner, D. Schmalstieg, in *IEEE Virtual Reality Conf. (VR 2006)*, IEEE, Piscataway, NJ **2006**, p. 321.
[37] a) S. Choi, H. Lee, R. Ghaffari, T. Hyeon, D. H. Kim, *Adv. Mater.* **2016**, *28*, 4203; b) T. Someya, Y. Kato, T. Sekitani, S. Iba, Y. Noguchi, Y. Murase, H. Kawaguchi, T. Sakurai, *Proc. Natl. Acad. Sci. USA* **2005**, *102*, 12321; c) T. Someya, T. Sekitani, S. Iba, Y. Kato, H. Kawaguchi, T. Sakurai, *Proc. Natl. Acad. Sci. USA* **2004**, *101*, 9966.
[38] a) A. Miyamoto, S. Lee, N. F. Cooray, S. Lee, M. Mori, N. Matsuhisa, H. Jin, L. Yoda, T. Yokota, A. Itoh, M. Sekino, H. Kawasaki, T. Ebihara, M. Amagai, T. Someya, *Nat. Nanotechnol.* **2017**, *12*, 907; b) B. Sun, R. N. McCay, S. Goswami, Y. Xu, C. Zhang, Y. Ling, J. Lin, Z. Yan, *Adv. Mater.* **2018**, *30*, 1804327.
[39] a) D. Bonnet, M. Ammi, J.-C. Martin, in *2011 IEEE Int. Workshop on Haptic Audio Visual Environments and Games*, IEEE, Piscataway, NJ **2011**, pp. 81–87; b) E. Gatti, G. Caruso, M. Bordegoni, C. Spence, in *2013 World Haptics Conf. (WHC)*, IEEE, Daejeon **2013**, pp. 247–252.
[40] a) M. Weigel, A. S. Nittala, A. Olwal, J. Steimle, in *Proc. of the 2017 CHI Conf. on Human Factors in Computing Systems*, ACM, New York **2017**; b) G. S. C. Bermúdez, H. Fuchs, L. Bischoff, J. Fassbender, D. Makarov, *Nat. Electron.* **2018**, *1*, 589.
[41] N. P. Shetti, A. Mishra, S. Basu, R. J. Mascarenhas, R. R. Kakarla, T. M. Aminabhavi, *ACS Biomater. Sci. Eng.* **2020**, *6*, 1823.
[42] T. Someya, S. Bauer, M. Kaltenbrunner, *MRS Bull.* **2017**, *42*, 124.
[43] a) L. Li, L. Gu, Z. Lou, Z. Fan, G. Shen, *ACS Nano* **2017**, *11*, 4067; b) G. Konstantatos, I. Howard, A. Fischer, S. Hoogland, J. Clifford, E. Klem, L. Levina, E. H. Sargent, *Nature* **2006**, *442*, 180.
[44] a) T. Yang, Y. Zheng, Z. Du, W. Liu, Z. Yang, F. Gao, L. Wang, K.-C. Chou, X. Hou, W. Yang, *ACS Nano* **2018**, *12*, 1611; b) C. Soci, A. Zhang, B. Xiang, S. A. Dayeh, D. Aplin, J. Park, X. Bao, Y.-H. Lo, D. Wang, *Nano Lett.* **2007**, *7*, 1003; c) H. Kind, H. Yan, B. Messer, M. Law, P. Yang, *Adv. Mater.* **2002**, *14*, 158.
[45] a) N. Huo, G. Konstantatos, *Adv. Mater.* **2018**, *30*, 1801164; b) M. Long, P. Wang, H. Fang, W. Hu, *Adv. Funct. Mater.* **2019**, *29*, 1803807.
[46] Y. Zhong, T. J. Sisto, B. Zhang, K. Miyata, X.-Y. Zhu, M. L. Steigerwald, F. Ng, C. Nuckolls, *J. Am. Chem. Soc.* **2017**, *139*, 5644.
[47] C.-W. Chiang, G. Haider, W.-C. Tan, Y.-R. Liou, Y.-C. Lai, R. Ravindranath, H.-T. Chang, Y.-F. Chen, *ACS Appl. Mater. Interfaces* **2016**, *8*, 466.
[48] P. Gowda, T. Sakorikar, S. K. Reddy, D. B. Ferry, A. Misra, *ACS Appl. Mater. Interfaces* **2014**, *6*, 7485.
[49] P. Gutruf, E. Zeller, S. Walia, H. Nili, S. Sriram, M. Bhaskaran, *Small* **2015**, *11*, 4532.
[50] G. Hwang, C. Dockendorf, D. Bell, L. Dong, H. Hashimoto, D. Poulikakos, B. Nelson, *Int. J. Optomechatronics* **2008**, *2*, 88.
[51] J. Song, L. Xu, J. Li, J. Xue, Y. Dong, X. Li, H. Zeng, *Adv. Mater.* **2016**, *28*, 4861.
[52] S. Tong, J. Yuan, C. Zhang, C. Wang, B. Liu, J. Shen, H. Xia, Y. Zou, H. Xie, J. Sun, *npj Flexible Electron.* **2018**, *2*, 7.
[53] W. Tian, H. Zhou, L. Li, *Small* **2017**, *13*, 1702107.
[54] E. O. Polat, G. Mercier, I. Nikitskiy, E. Puma, T. Galan, S. Gupta, M. Montagut, J. J. Piqueras, M. Bouwens, T. Durduran, *Sci. Adv.* **2019**, *5*, eaaw7846.
[55] T. Yokota, T. Nakamura, H. Kato, M. Mochizuki, M. Tada, M. Uchida, S. Lee, M. Koizumi, W. Yukita, A. Takimoto, *Nat. Electron.* **2020**, *3*, 113.
[56] W. Li, A. Furlan, K. H. Hendriks, M. M. Wienk, R. A. Janssen, *J. Am. Chem. Soc.* **2013**, *135*, 5529.
[57] J. Kim, S.-M. Kwon, Y. K. Kang, Y.-H. Kim, M.-J. Lee, K. Han, A. Facchetti, M.-G. Kim, S. K. Park, *Sci. Adv.* **2019**, *5*, eaax8801.

[58] a) G. J. Lee, C. Choi, D. H. Kim, Y. M. Song, *Adv. Funct. Mater.* **2018**, *28*, 1705202; b) M. S. Kim, G. J. Lee, C. Choi, M. S. Kim, M. Lee, S. Liu, K. W. Cho, H. M. Kim, H. Cho, M. K. Choi, *Nat. Electron.* **2020**, *3*, 546; c) J. Kim, M. Kim, M.-S. Lee, K. Kim, S. Ji, Y.-T. Kim, J. Park, K. Na, K.-H. Bae, H. K. Kim, *Nat. Commun.* **2017**, *8*, 14997.

[59] C. Choi, M. K. Choi, S. Liu, M. S. Kim, O. K. Park, C. Im, J. Kim, X. Qin, G. J. Lee, K. W. Cho, *Nat. Commun.* **2017**, *8*, 1664.

[60] J.-J. Kim, H. Liu, A. O. Ashtiani, H. Jiang, *Rep. Prog. Phys.* **2020**, *83*, 047101.

[61] T.-S. D. Le, J. An, Y. Huang, Q. Vo, J. Boonruangkan, T. Tran, S.-W. Kim, G. Sun, Y.-J. Kim, *ACS Nano* **2019**, *13*, 7442.

[62] a) I. Graz, M. Kaltenbrunner, C. Keplinger, R. Schwödiauer, S. Bauer, S. P. Lacour, S. Wagner, *Appl. Phys. Lett.* **2006**, *89*, 073501; b) S. Cha, S. M. Kim, H. Kim, J. Ku, J. I. Sohn, Y. J. Park, B. G. Song, M. H. Jung, E. K. Lee, B. L. Choi, *Nano Lett.* **2011**, *11*, 5142; c) T. Inaoka, H. Shintaku, T. Nakagawa, S. Kawano, H. Ogita, T. Sakamoto, S. Hamanishi, H. Wada, J. Ito, *Proc. Natl. Acad. Sci. USA* **2011**, *108*, 18390; d) L. Persano, C. Dagdeviren, Y. Su, Y. Zhang, S. Girardo, D. Pisignano, Y. Huang, J. A. Rogers, *Nat. Commun.* **2013**, *4*, 1633; e) H. S. Lee, J. Chung, G. T. Hwang, C. K. Jeong, Y. Jung, J. H. Kwak, H. Kang, M. Byun, W. D. Kim, S. Hur, *Adv. Funct. Mater.* **2014**, *24*, 6914.

[63] C. Lang, J. Fang, H. Shao, X. Ding, T. Lin, *Nat. Commun.* **2016**, *7*, 11108.

[64] W. Li, D. Torres, R. Díaz, Z. Wang, C. Wu, C. Wang, Z. L. Wang, N. Sepúlveda, *Nat. Commun.* **2017**, *8*, 15310.

[65] a) J. Yang, J. Chen, Y. Liu, W. Yang, Y. Su, Z. L. Wang, *ACS Nano* **2014**, *8*, 2649; b) H. Guo, X. Pu, J. Chen, Y. Meng, M.-H. Yeh, G. Liu, Q. Tang, B. Chen, D. Liu, S. Qi, *Sci. Rob.* **2018**, *3*, 20; c) F. Chen, Y. Wu, Z. Ding, X. Xia, S. Li, H. Zheng, C. Diao, G. Yue, Y. Zi, *Nano Energy* **2019**, *56*, 241.

[66] X. Fan, J. Chen, J. Yang, P. Bai, Z. Li, Z. L. Wang, *ACS Nano* **2015**, *9*, 4236.

[67] a) K. Lee, X. Ni, J. Y. Lee, H. Arafa, D. J. Pe, S. Xu, R. Avila, M. Irie, J. H. Lee, R. L. Easterlin, D. H. Kim, H. U. Chung, O. O. Olabisi, S. Getaneh, E. Chung, M. Hill, J. Bell, H. Jang, C. Liu, J. B. Park, J. Kim, S. B. Kim, S. Mehta, M. Pharr, A. Tzavelis, J. T. Reeder, I. Huang, Y. Deng, Z. Xie, C. R. Davies, et al., *Nat. Biomed. Eng.* **2020**, *4*, 148; b) L.-Q. Tao, H. Tian, Y. Liu, Z.-Y. Ju, Y. Pang, Y.-Q. Chen, D.-Y. Wang, X.-G. Tian, J.-C. Yan, N.-Q. Deng, Y. Yang, T.-L. Ren, *Nat. Commun.* **2017**, *8*, 14579; c) S. Kang, S. Cho, R. Shanker, H. Lee, J. Park, D.-S. Um, Y. Lee, H. Ko, *Sci. Adv.* **2018**, *4*, eaas8772.

[68] Y. Liu, J. J. Norton, R. Qazi, Z. Zou, K. R. Ammann, H. Liu, L. Yan, P. L. Tran, K.-I. Jang, J. W. Lee, D. Zhang, K. A. Kilian, S. H. Jung, T. Bretl, J. Xiao, M. J. Slepian, Y. Huang, J.-W. Jeong, J. A. Rogers, *Sci. Adv.* **2016**, *2*, e1601185.

[69] M. O. G. Nayeem, S. Lee, H. Jin, N. Matsuhisa, H. Jinno, A. Miyamoto, T. Yokota, T. Someya, *Proc. Natl. Acad. Sci. USA* **2020**, *117*, 7063.

[70] S. Lee, S. Franklin, F. A. Hassani, T. Yokota, M. O. G. Nayeem, Y. Wang, R. Leib, G. Cheng, D. W. Franklin, T. Someya, *Science* **2020**, *370*, 966.

[71] T. Q. Trung, N. E. Lee, *Adv. Mater.* **2016**, *28*, 4338.

[72] a) C. Dagdeviren, Y. Shi, P. Joe, R. Ghaffari, G. Balooch, K. Usgaonkar, O. Gur, P. L. Tran, J. R. Crosby, M. Meyer, Y. Su, R. Chad Webb, A. S. Tedesco, M. J. Slepian, Y. Huang, J. A. Rogers, *Nat. Mater.* **2015**, *14*, 728; b) Q.-L. Zhao, G.-P. He, J.-J. Di, W.-L. Song, Z.-L. Hou, P.-P. Tan, D.-W. Wang, M.-S. Cao, *ACS Appl. Mater. Interfaces* **2017**, *9*, 24696; c) C. Dagdeviren, Y. Su, P. Joe, R. Yona, Y. Liu, Y. S. Kim, Y. Huang, A. R. Damadoran, J. Xia, L. W. Martin, Y. Huang, J. A. Rogers, *Nat. Commun.* **2014**, *5*, 4496.

[73] M. Akiyama, Y. Morofuji, T. Kamohara, K. Nishikubo, M. Tsubai, O. Fukuda, N. Ueno, *J. Appl. Phys.* **2006**, *100*, 114318.

[74] a) M. Y. Choi, D. Choi, M. J. Jin, I. Kim, S. H. Kim, J. Y. Choi, S. Y. Lee, J. M. Kim, S. W. Kim, *Adv. Mater.* **2009**, *21*, 2185; b) C. Wang, D. Hwang, Z. Yu, K. Takei, J. Park, T. Chen, B. Ma, A. Javey, *Nat. Mater.* **2013**, *12*, 899; c) C. Pan, L. Dong, G. Zhu, S. Niu, R. Yu, Q. Yang, Y. Liu, Z. L. Wang, *Nat. Photonics* **2013**, *7*, 752; d) W. Wu, X. Wen, Z. L. Wang, *Science* **2013**, *340*, 952; e) R. Bao, C. Wang, L. Dong, R. Yu, K. Zhao, Z. L. Wang, C. Pan, *Adv. Funct. Mater.* **2015**, *25*, 2884; f) J. S. Lee, K. Y. Shin, O. J. Cheong, J. H. Kim, J. Jang, *Sci. Rep.* **2015**, *5*, 7887.

[75] D. Y. Park, D. J. Joe, D. H. Kim, H. Park, J. H. Han, C. K. Jeong, H. Park, J. G. Park, B. Joung, K. J. Lee, *Adv. Mater.* **2017**, *29*, 1702308.

[76] a) B. C. Tee, C. Wang, R. Allen, Z. Bao, *Nat. Nanotechnol.* **2012**, *7*, 825; b) S. Gong, W. Schwalb, Y. Wang, Y. Chen, Y. Tang, J. Si, B. Shirinzadeh, W. Cheng, *Nat. Commun.* **2014**, *5*, 3132; c) Y. Pang, H. Tian, L. Tao, Y. Li, X. Wang, N. Deng, Y. Yang, T. L. Ren, *ACS Appl. Mater. Interfaces* **2016**, *8*, 26458; d) X. Wang, H. Zhang, L. Dong, X. Han, W. Du, J. Zhai, C. Pan, Z. L. Wang, *Adv. Mater.* **2016**, *28*, 2896; e) M. Jian, K. Xia, Q. Wang, Z. Yin, H. Wang, C. Wang, H. Xie, M. Zhang, Y. Zhang, *Adv. Funct. Mater.* **2017**, *27*, 1606066; f) M. A. Darabi, A. Khosrozadeh, R. Mbeleck, Y. Liu, Q. Chang, J. Jiang, J. Cai, Q. Wang, G. Luo, M. Xing, *Adv. Mater.* **2017**, *29*, 1700533; g) B. Lee, J. Y. Oh, H. Cho, C. W. Joo, H. Yoon, S. Jeong, E. Oh, J. Byun, H. Kim, S. Lee, J. Seo, C. W. Park, S. Choi, N. M. Park, S. Y. Kang, C. S. Hwang, S. D. Ahn, J. I. Lee, Y. Hong, *Nat. Commun.* **2020**, *11*, 663.

[77] a) L. Q. Tao, K. N. Zhang, H. Tian, Y. Liu, D. Y. Wang, Y. Q. Chen, Y. Yang, T. L. Ren, *ACS Nano* **2017**, *11*, 8790; b) Y. Guo, Z. Guo, M. Zhong, P. Wan, W. Zhang, L. Zhang, *Small* **2018**, *14*, 1803018.

[78] S. Lee, A. Reuveny, J. Reeder, S. Lee, H. Jin, Q. Liu, T. Yokota, T. Sekitani, T. Isoyama, Y. Abe, Z. Suo, T. Someya, *Nat. Nanotechnol.* **2016**, *11*, 472.

[79] D. Kwon, T. I. Lee, J. Shim, S. Ryu, M. S. Kim, S. Kim, T. S. Kim, I. Park, *ACS Appl. Mater. Interfaces* **2016**, *8*, 16922.

[80] Y. Pang, K. Zhang, Z. Yang, S. Jiang, Z. Ju, Y. Li, X. Wang, D. Wang, M. Jian, Y. Zhang, R. Liang, H. Tian, Y. Yang, T. L. Ren, *ACS Nano* **2018**, *12*, 2346.

[81] a) M. Ha, S. Lim, J. Park, D.-S. Um, Y. Lee, H. Ko, *Adv. Funct. Mater.* **2015**, *25*, 2841; b) J. Park, M. Kim, Y. Lee, H. S. Lee, H. Ko, *Sci. Adv.* **2015**, *1*, e1500661; c) F. Zhang, Y. Zang, D. Huang, C. A. Di, D. Zhu, *Nat. Commun.* **2015**, *6*, 8356; d) H. Park, Y. R. Jeong, J. Yun, S. Y. Hong, S. Jin, S.-J. Lee, G. Zi, J. S. Ha, *ACS Nano* **2015**, *9*, 9974.

[82] S. Jung, J. H. Kim, J. Kim, S. Choi, J. Lee, I. Park, T. Hyeon, D. H. Kim, *Adv. Mater.* **2014**, *26*, 4825.

[83] a) D. J. Lipomi, M. Vosgueritchian, B. C. Tee, S. L. Hellstrom, J. A. Lee, C. H. Fox, Z. Bao, *Nat. Nanotechnol.* **2011**, *6*, 788; b) S. Wan, H. Bi, Y. Zhou, X. Xie, S. Su, K. Yin, L. Sun, *Carbon* **2017**, *114*, 209.

[84] a) S.-J. Woo, J.-H. Kong, D.-G. Kim, J.-M. Kim, *J. Mater. Chem. C* **2014**, *2*, 4415; b) S. Yao, Y. Zhu, *Nanoscale* **2014**, *6*, 2345.

[85] X. Shuai, P. Zhu, W. Zeng, Y. Hu, X. Liang, Y. Zhang, R. Sun, C. P. Wong, *ACS Appl. Mater. Interfaces* **2017**, *9*, 26314.

[86] J. C. Yang, J. O. Kim, J. Oh, S. Y. Kwon, J. Y. Sim, D. W. Kim, H. B. Choi, S. Park, *ACS Appl. Mater. Interfaces* **2019**, *11*, 19472.

[87] W. Yang, N.-W. Li, S. Zhao, Z. Yuan, J. Wang, X. Du, B. Wang, R. Cao, X. Li, W. Xu, Z. L. Wang, C. Li, *Adv. Mater. Technol.* **2018**, *3*, 1700241.

[88] a) G. Schwartz, B. C. Tee, J. Mei, A. L. Appleton, D. H. Kim, H. Wang, Z. Bao, *Nat. Commun.* **2013**, *4*, 1859; b) S. Kang, J. Lee, S. Lee, S. Kim, J.-K. Kim, H. Algadi, S. Al-Sayari, D.-E. Kim, D. Kim, T. Lee, *Adv. Electron. Mater.* **2016**, *2*, 1600356.

[89] Y. Zang, F. Zhang, D. Huang, X. Gao, C. A. Di, D. Zhu, *Nat. Commun.* **2015**, *6*, 6269.

[90] a) F. R. Fan, L. Lin, G. Zhu, W. Wu, R. Zhang, Z. L. Wang, *Nano Lett.* **2012**, *12*, 3109; b) L. Lin, Y. Xie, S. Wang, W. Wu, S. Niu, X. Wen, Z. L. Wang, *ACS Nano* **2013**, *7*, 8266.

[91] a) X. Wang, M. Que, M. Chen, X. Han, X. Li, C. Pan, Z. L. Wang, *Adv. Mater.* **2017**, *29*, 1605817; b) M. Ramuz, B. C. Tee, J. B. Tok, Z. Bao, *Adv. Mater.* **2012**, *24*, 3223.

[92] a) C.-C. Kim, H.-H. Lee, K. H. Oh, J.-Y. Sun, *Science* **2016**, *353*, 682; b) G. Ge, Y. Zhang, J. Shao, W. Wang, W. Si, W. Huang, X. Dong, *Adv. Funct. Mater.* **2018**, *28*, 1802576.
[93] Y. Gao, H. Ota, E. W. Schaler, K. Chen, A. Zhao, W. Gao, H. M. Fahad, Y. Leng, A. Zheng, F. Xiong, C. Zhang, L. C. Tai, P. Zhao, R. S. Fearing, A. Javey, *Adv. Mater.* **2017**, *29*, 1701985.
[94] a) Q. Sun, D. H. Kim, S. S. Park, N. Y. Lee, Y. Zhang, J. H. Lee, K. Cho, J. H. Cho, *Adv. Mater.* **2014**, *26*, 4735; b) S. H. Shin, S. Ji, S. Choi, K. H. Pyo, B. Wan An, J. Park, J. Kim, J. Y. Kim, K. S. Lee, S. Y. Kwon, J. Heo, B. G. Park, J. U. Park, *Nat. Commun.* **2017**, *8*, 14950.
[95] a) S. Pyo, J. Choi, J. Kim, *Adv. Electron. Mater.* **2018**, *4*, 1870006; b) M. Kang, J. Kim, B. Jang, Y. Chae, J. H. Kim, J. H. Ahn, *ACS Nano* **2017**, *11*, 7950; c) B. W. An, S. Heo, S. Ji, F. Bien, J. U. Park, *Nat. Commun.* **2018**, *9*, 2458.
[96] a) C. Yu, Z. Wang, H. Yu, H. Jiang, *Appl. Phys. Lett.* **2009**, *95*, 141912; b) R. C. Webb, A. P. Bonifas, A. Behnaz, Y. Zhang, K. J. Yu, H. Cheng, M. Shi, Z. Bian, Z. Liu, Y.-S. Kim, *Nat. Mater.* **2013**, *12*, 938; c) Y. Chen, B. Lu, Y. Chen, X. Feng, *Sci. Rep.* **2015**, *5*, 11505.
[97] a) J. Kim, M. Lee, H. J. Shim, R. Ghaffari, H. R. Cho, D. Son, Y. H. Jung, M. Soh, C. Choi, S. Jung, *Nat. Commun.* **2014**, *5*, 5747; b) N. T. Tien, S. Jeon, D. I. Kim, T. Q. Trung, M. Jang, B. U. Hwang, K. E. Byun, J. Bae, E. Lee, J. B. H. Tok, *Adv. Mater.* **2014**, *26*, 796; c) S. Harada, W. Honda, T. Arie, S. Akita, K. Takei, *ACS Nano* **2014**, *8*, 3921; d) C. Yan, J. Wang, P. S. Lee, *ACS Nano* **2015**, *9*, 2130; e) J. Yang, D. Wei, L. Tang, X. Song, W. Luo, J. Chu, T. Gao, H. Shi, C. Du, *RSC Adv.* **2015**, *5*, 25609; f) T. Q. Trung, S. Ramasundaram, B. U. Hwang, N. E. Lee, *Adv. Mater.* **2016**, *28*, 502; g) S. Nakata, T. Arie, S. Akita, K. Takei, *ACS Sens.* **2017**, *2*, 443.
[98] a) J. Jeon, H. B. R. Lee, Z. Bao, *Adv. Mater.* **2013**, *25*, 850; b) T. Yokota, Y. Inoue, Y. Terakawa, J. Reeder, M. Kaltenbrunner, T. Ware, K. Yang, K. Mabuchi, T. Murakawa, M. Sekino, *Proc. Natl. Acad. Sci. USA* **2015**, *112*, 14533; c) H. Yang, D. Qi, Z. Liu, B. K. Chandran, T. Wang, J. Yu, X. Chen, *Adv. Mater.* **2016**, *28*, 9175.
[99] T. Vuorinen, J. Niittynen, T. Kankkunen, T. M. Kraft, M. Mäntysalo, *Sci. Rep.* **2016**, *6*, 35289.
[100] X. Ren, K. Pei, B. Peng, Z. Zhang, Z. Wang, X. Wang, P. K. Chan, *Adv. Mater.* **2016**, *28*, 4832.
[101] C. Zhu, A. Chortos, Y. Wang, R. Pfattner, T. Lei, A. C. Hinckley, I. Pochorovski, X. Yan, J. W.-F. To, J. Y. Oh, *Nat. Electron.* **2018**, *1*, 183.
[102] K. Suzuki, K. Yataka, Y. Okumiya, S. Sakakibara, K. Sako, H. Mimura, Y. Inoue, *ACS Sens.* **2016**, *1*, 817.
[103] Y. R. Jeong, J. Kim, Z. Xie, Y. Xue, S. M. Won, G. Lee, S. W. Jin, S. Y. Hong, X. Feng, Y. Huang, *NPG Asia Mater.* **2017**, *9*, e443.
[104] J. Lee, S. Kim, J. Lee, D. Yang, B. C. Park, S. Ryu, I. Park, *Nanoscale* **2014**, *6*, 11932.
[105] K. H. Kim, N. S. Jang, S. H. Ha, J. H. Cho, J. M. Kim, *Small* **2018**, *14*, 1704232.
[106] S. Wan, Z. Zhu, K. Yin, S. Su, H. Bi, T. Xu, H. Zhang, Z. Shi, L. He, L. Sun, *Small Methods* **2018**, *2*, 1700374.
[107] S. J. Park, J. Kim, M. Chu, M. Khine, *Adv. Mater. Technol.* **2016**, *1*, 1600053.
[108] L. Wang, G. Gao, Y. Zhou, T. Xu, J. Chen, R. Wang, R. Zhang, J. Fu, *ACS Appl. Mater. Interfaces* **2018**, *11*, 3506.
[109] Z. Ma, B. Su, S. Gong, Y. Wang, L. W. Yap, G. P. Simon, W. Cheng, *ACS Sens.* **2016**, *1*, 303.
[110] Y. Ding, J. Yang, C. R. Tolle, Z. Zhu, *ACS Appl. Mater. Interfaces* **2018**, *10*, 16077.
[111] a) M. D. Ho, Y. Ling, L. W. Yap, Y. Wang, D. Dong, Y. Zhao, W. Cheng, *Adv. Funct. Mater.* **2017**, *27*, 1700845; b) S. Gong, D. T. Lai, Y. Wang, L. W. Yap, K. J. Si, Q. Shi, N. N. Jason, T. Sridhar, H. Uddin, W. Cheng, *ACS Appl. Mater. Interfaces* **2015**, *7*, 19700.
[112] M. Amjadi, K. U. Kyung, I. Park, M. Sitti, *Adv. Funct. Mater.* **2016**, *26*, 1678.
[113] S. Gong, L. W. Yap, Y. Zhu, B. Zhu, Y. Wang, Y. Ling, Y. Zhao, T. An, Y. Lu, W. Cheng, *Adv. Funct. Mater.* **2020**, *30*, 1910717.
[114] D. Kang, P. V. Pikhitsa, Y. W. Choi, C. Lee, S. S. Shin, L. Piao, B. Park, K.-Y. Suh, T.-i. Kim, M. Choi, *Nature* **2014**, *516*, 222.
[115] Y. Tetsu, K. Yamagishi, A. Kato, Y. Matsumoto, M. Tsukune, Y. Kobayashi, M. G. Fujie, S. Takeoka, T. Fujie, *Appl. Phys. Express* **2017**, *10*, 087201.
[116] G. Ge, W. Huang, J. Shao, X. Dong, *J. Semicond.* **2018**, *39*, 011012.
[117] Y. Wang, S. Lee, T. Yokota, H. Wang, Z. Jiang, J. Wang, M. Koizumi, T. Someya, *Sci. Adv.* **2020**, *6*, eabb7043.
[118] K. K. Kim, I. Ha, M. Kim, J. Choi, P. Won, S. Jo, S. H. Ko, *Nat. Commun.* **2020**, *11*, 2149.
[119] J. Zhang, B. Wang, C. Zhang, Y. Xiao, M. Y. Wang, *Front. Neurorob.* **2019**, *13*, 7.
[120] K. Kansaku, N. Hata, K. Takano, *Neurosci. Res.* **2010**, *66*, 219.
[121] a) Y. Wang, C. Zhu, R. Pfattner, H. Yan, L. Jin, S. Chen, F. Molina-Lopez, F. Lissel, J. Liu, N. I. Rabiah, *Sci. Adv.* **2017**, *3*, e1602076; b) J. Y. Oh, S. Kim, H. K. Baik, U. Jeong, *Adv. Mater.* **2016**, *28*, 4455.
[122] B. Lu, H. Yuk, S. Lin, N. Jian, K. Qu, J. Xu, X. Zhao, *Nat. Commun.* **2019**, *10*, 1043.
[123] a) P. Li, K. Sun, J. Ouyang, *ACS Appl. Mater. Interfaces* **2015**, *7*, 18415; b) M. Chen, T. Tao, L. Zhang, W. Gao, C. Li, *Chem. Commun.* **2013**, *49*, 1612.
[124] S. Choi, S. I. Han, D. Jung, H. J. Hwang, C. Lim, S. Bae, O. K. Park, C. M. Tschabrunn, M. Lee, S. Y. Bae, *Nat. Nanotechnol.* **2018**, *13*, 1048.
[125] W. M. Choi, J. Song, D.-Y. Khang, H. Jiang, Y. Y. Huang, J. A. Rogers, *Nano Lett.* **2007**, *7*, 1655.
[126] D.-H. Kim, J. Song, W. M. Choi, H.-S. Kim, R.-H. Kim, Z. Liu, Y. Y. Huang, K.-C. Hwang, Y.-w. Zhang, J. A. Rogers, *Proc. Natl. Acad. Sci. USA* **2008**, *105*, 18675.
[127] J. A. Fan, W.-H. Yeo, Y. Su, Y. Hattori, W. Lee, S.-Y. Jung, Y. Zhang, Z. Liu, H. Cheng, L. Falgout, *Nat. Commun.* **2014**, *5*, 3266.
[128] T. R. Ray, J. Choi, A. J. Bandodkar, S. Krishnan, P. Gutruf, L. Tian, R. Ghaffari, J. A. Rogers, *Chem. Rev.* **2019**, *119*, 5461.
[129] G. Lanzara, N. Salowitz, Z. Guo, F. K. Chang, *Adv. Mater.* **2010**, *22*, 4643.
[130] Y. Yu, J. Zhang, J. Liu, *PLoS One* **2013**, *8*, e58771.
[131] F. Ershad, A. Thukral, J. Yue, P. Comeaux, Y. Lu, H. Shim, K. Sim, N.-I. Kim, Z. Rao, R. Guevara, *Nat. Commun.* **2020**, *11*, 3823.
[132] J. J. Norton, D. S. Lee, J. W. Lee, W. Lee, O. Kwon, P. Won, S.-Y. Jung, H. Cheng, J.-W. Jeong, A. Akce, S. Umunna, I. Na, Y. H. Kwon, X.-Q. Wang, Z. Liu, U. Paik, Y. Huang, T. Bretl, W.-H. Yeo, J. A. Rogers, *Proc. Natl. Acad. Sci. USA* **2015**, *112*, 3920.
[133] Y. Lee, B. Nicholls, D. S. Lee, Y. Chen, Y. Chun, C. S. Ang, W.-H. Yeo, *Sci. Rep.* **2017**, *7*, 46697.
[134] S. Mishra, Y.-S. Kim, J. Intarasirisawat, Y.-T. Kwon, Y. Lee, M. Mahmood, H.-R. Lim, R. Herbert, K. J. Yu, C. S. Ang, *Sci. Adv.* **2020**, *6*, eaay1729.
[135] D. J. Lipomi, C. Dhong, C. W. Carpenter, N. B. Root, V. S. Ramachandran, *Adv. Funct. Mater.* **2019**, *30*, 1906850.
[136] a) J. De Smet, A. Avci, P. Joshi, D. Schaubroeck, D. Cuypers, H. De Smet, *J. Soc. Inf. Disp.* **2013**, *21*, 399; b) A. R. Lingley, M. Ali, Y. Liao, R. Mirjalili, M. Klonner, M. Sopanen, S. Suihkonen, T. Shen, B. Otis, H. Lipsanen, *J. Micromech. Microeng.* **2011**, *21*, 125014.
[137] a) J. H. Koo, D. C. Kim, H. J. Shim, T. H. Kim, D. H. Kim, *Adv. Funct. Mater.* **2018**, *28*, 1801834; b) M. Vosgueritchian, J. B.-H. Tok, Z. Bao, *Nat. Photonics* **2013**, *7*, 769; c) E. H. Kim, H. Han, S. Yu, C. Park, G. Kim, B. Jeong, S. W. Lee, J. S. Kim, S. Lee, J. Kim, *Adv. Sci.* **2019**, *6*, 1802351; d) C. Zhao, Y. Zhou, S. Gu, S. Cao, J. Wang, M. Zhang, Y. Wu, D. Kong, *ACS Appl. Mater. Interfaces* **2020**, *12*, 47902.
[138] a) T. Q. Trung, C. Kim, H. B. Lee, S. M. Cho, N. E. Lee, *Adv. Mater. Technol.* **2020**, *5*, 1900995; b) M. Choi, S.-R. Bae, L. Hu, A. T. Hoang, S. Y. Kim, J.-H. Ahn, *Sci. Adv.* **2020**, *6*, eabb5898;

c) T. Sekitani, H. Nakajima, H. Maeda, T. Fukushima, T. Aida, K. Hata, T. Someya, *Nat. Mater.* **2009**, *8*, 494.
[139] S. G. R. Bade, X. Shan, P. T. Hoang, J. Li, T. Geske, L. Cai, Q. Pei, C. Wang, Z. Yu, *Adv. Mater.* **2017**, *29*, 1607053.
[140] T.-H. Han, Y. Lee, M.-R. Choi, S.-H. Woo, S.-H. Bae, B. H. Hong, J.-H. Ahn, T.-W. Lee, *Nat. Photonics* **2012**, *6*, 105.
[141] J. Liang, L. Li, K. Tong, Z. Ren, W. Hu, X. Niu, Y. Chen, Q. Pei, *ACS Nano* **2014**, *8*, 1590.
[142] M. Choi, B. Jang, W. Lee, S. Lee, T. W. Kim, H. J. Lee, J. H. Kim, J. H. Ahn, *Adv. Funct. Mater.* **2017**, *27*, 1606005.
[143] M. K. Choi, J. Yang, K. Kang, D. C. Kim, C. Choi, C. Park, S. J. Kim, S. I. Chae, T.-H. Kim, J. H. Kim, *Nat. Commun.* **2015**, *6*, 7149.
[144] C.-L. Tai, W.-L. Hong, Y.-T. Kuo, C.-Y. Chang, M.-C. Niu, M. Karupathevar Ponnusamythevar Ochathevar, C.-L. Hsu, S.-F. Horng, Y.-C. Chao, *ACS Appl. Mater. Interfaces* **2019**, *11*, 30176.
[145] S.-I. Park, Y. Xiong, R.-H. Kim, P. Elvikis, M. Meitl, D.-H. Kim, J. Wu, J. Yoon, C.-J. Yu, Z. Liu, *Science* **2009**, *325*, 977.
[146] D. Yin, J. Feng, N.-R. Jiang, R. Ma, Y.-F. Liu, H.-B. Sun, *ACS Appl. Mater. Interfaces* **2016**, *8*, 31166.
[147] D.-H. Jiang, Y.-C. Liao, C.-J. Cho, L. Veeramuthu, F.-C. Liang, T.-C. Wang, C.-C. Chueh, T. Satoh, S.-H. Tung, C.-C. Kuo, *ACS Appl. Mater. Interfaces* **2020**, *12*, 14408.
[148] T. Yokota, P. Zalar, M. Kaltenbrunner, H. Jinno, N. Matsuhisa, H. Kitanosako, Y. Tachibana, W. Yukita, M. Koizumi, T. Someya, *Sci. Adv.* **2016**, *2*, e1501856.
[149] J. H. Koo, S. Jeong, H. J. Shim, D. Son, J. Kim, D. C. Kim, S. Choi, J.-I. Hong, D.-H. Kim, *ACS Nano* **2017**, *11*, 10032.
[150] J. Kim, H. J. Shim, J. Yang, M. K. Choi, D. C. Kim, J. Kim, T. Hyeon, D. H. Kim, *Adv. Mater.* **2017**, *29*, 1700217.
[151] H. Ding, X. Shu, Y. Jin, T. Fan, H. Zhang, *Nanoscale* **2019**, *11*, 5839.
[152] A. R. Barnard, D. M. Jenkins, T. A. Brungart, T. M. McDevitt, B. L. Kline, *J. Acoust. Soc. Am.* **2013**, *134*, EL276.
[153] S. Xu, B. Man, S. Jiang, C. Chen, C. Yang, M. Liu, X. Gao, Z. Sun, C. Zhang, *Appl. Phys. Lett.* **2013**, *102*, 151902.
[154] S. W. Jin, J. Park, S. Y. Hong, H. Park, Y. R. Jeong, J. Park, S.-S. Lee, J. S. Ha, *Sci. Rep.* **2015**, *5*, 11695.
[155] K.-Y. Shin, J.-Y. Hong, J. Jang, *Chem. Commun.* **2011**, *47*, 8527.
[156] Q.-Y. Xie, Z.-Y. Ju, H. Tian, Q.-T. Xue, Y.-Q. Chen, L.-Q. Tao, M. A. Mohammad, X.-Y. Zhang, Y. Yang, T.-L. Ren, *Nanoscale* **2016**, *8*, 5516.
[157] H. Tian, D. Xie, Y. Yang, T.-L. Ren, Y.-F. Wang, C.-J. Zhou, P.-G. Peng, L.-G. Wang, L.-T. Liu, *Appl. Phys. Lett.* **2011**, *99*, 043503.
[158] C. Keplinger, J.-Y. Sun, C. C. Foo, P. Rothemund, G. M. Whitesides, Z. Suo, *Science* **2013**, *341*, 984.
[159] H. Tian, D. Xie, Y. Yang, T.-L. Ren, T.-T. Feng, Y.-F. Wang, C.-J. Zhou, P.-G. Peng, L.-G. Wang, L.-T. Liu, *Appl. Phys. Lett.* **2011**, *99*, 233503.
[160] L. Xiao, Z. Chen, C. Feng, L. Liu, Z.-Q. Bai, Y. Wang, L. Qian, Y. Zhang, Q. Li, K. Jiang, S. Fan, *Nano Lett.* **2008**, *8*, 4539.
[161] S. Biswas, Y. Visell, *Adv. Mater. Technol.* **2019**, *4*, 1900042.
[162] a) I. M. Koo, K. Jung, J. C. Koo, J.-D. Nam, Y. K. Lee, H. R. Choi, *IEEE Trans. Rob.* **2008**, *24*, 549; b) I. Koo, K. Jung, J. Koo, Y. Lee, H. R. Choi, in *Proc. of the 2006 IEEE Int. Conf. on Robotics and Automation, ICRA 2006*, IEEE, Florida **2006**, pp. 2220–2225.
[163] a) A. Withana, D. Groeger, J. Steimle, in *Proc. of the 31st Annual ACM Symp. on User Interface Software and Technology*, ACM, Berlin **2018**, pp. 365–378; b) S. Mun, S. Yun, S. Nam, S. K. Park, S. Park, B. J. Park, J. M. Lim, K.-U. Kyung, *IEEE Trans. Haptics* **2018**, *11*, 15.
[164] a) C. W. Carpenter, M. G. Malinao, T. A. Rafeedi, D. Rodriquez, S. T. M. Tan, N. B. Root, K. Skelil, J. Ramírez, B. Polat, S. E. Root, *Adv. Mater. Technol.* **2020**, *5*, 1901119; b) E. Leroy, R. Hinchet, H. Shea, *Adv. Mater.* **2020**, *32*, 2002564.
[165] X. Yu, Z. Xie, Y. Yu, J. Lee, A. Vazquez-Guardado, H. Luan, J. Ruban, X. Ning, A. Akhtar, D. Li, B. Ji, Y. Liu, R. Sun, J. Cao, Q. Huo, Y. Zhong, C. Lee, S. Kim, P. Gutruf, C. Zhang, Y. Xue, Q. Guo, A. Chempakasseril, P. Tian, W. Lu, J. Jeong, Y. Yu, J. Cornman, C. Tan, B. Kim, et al., *Nature* **2019**, *575*, 473.
[166] Y. Shao, S. Ma, S. H. Yoon, Y. Visell, J. Holbery, in *2020 IEEE Haptics Symp. (HAPTICS)*, IEEE, Piscataway, NJ **2020**, pp. 815–820.
[167] a) S. Choi, J. Park, W. Hyun, J. Kim, J. Kim, Y. B. Lee, C. Song, H. J. Hwang, J. H. Kim, T. Hyeon, *ACS Nano* **2015**, *9*, 6626; b) R. Zhou, P. Li, Z. Fan, D. Du, J. Ouyang, *J. Mater. Chem. C* **2017**, *5*, 1544.
[168] Y. Cheng, H. Zhang, R. Wang, X. Wang, H. Zhai, T. Wang, Q. Jin, J. Sun, *ACS Appl. Mater. Interfaces* **2016**, *8*, 32925.
[169] E.-H. Ko, H.-J. Kim, S.-M. Lee, T.-W. Kim, H.-K. Kim, *Sci. Rep.* **2017**, *7*, 46739.
[170] H. Lin, J. Tan, J. Zhu, S. Lin, Y. Zhao, W. Yu, H. Hojaiji, B. Wang, S. Yang, X. Cheng, *Nat. Commun.* **2020**, *11*, 4405.
[171] Y. Wang, Z. Yu, G. Mao, Y. Liu, G. Liu, J. Shang, S. Qu, Q. Chen, R. W. Li, *Adv. Mater. Technol.* **2019**, *4*, 1800435.
[172] Q. Huang, K. N. Al-Milaji, H. Zhao, *ACS Appl. Nano Mater.* **2018**, *1*, 4528.
[173] C. Yeon, G. Kim, J. Lim, S. Yun, *RSC Adv.* **2017**, *7*, 5888.
[174] W.-J. Sun, L. Xu, L.-C. Jia, C.-G. Zhou, Y. Xiang, R.-H. Yin, D.-X. Yan, J.-H. Tang, Z.-M. Li, *Compos. Sci. Technol.* **2019**, *181*, 107695.
[175] R. Wang, Z. Xu, J. Zhuang, Z. Liu, L. Peng, Z. Li, Y. Liu, W. Gao, C. Gao, *Adv. Electron. Mater.* **2017**, *3*, 1600425.
[176] a) J. Ahn, J. Gu, B. Hwang, H. Kang, S. Hwang, S. Jeon, J. Jeong, I. Park, *Nanotechnology* **2019**, *30*, 455707; b) B.-Y. Hwang, S.-H. Choi, K.-W. Lee, J.-Y. Kim, *Composites, Part B* **2018**, *151*, 1; c) P. Li, J. Ma, H. Xu, X. Xue, Y. Liu, *J. Mater. Chem. C* **2016**, *4*, 3581; d) S. Wang, Y. Tian, C. Wang, C. Hang, Y. Huang, C. Liao, *Compos. Sci. Technol.* **2019**, *174*, 76.
[177] a) H. Zhai, R. Wang, X. Wang, Y. Cheng, L. Shi, J. Sun, *Nano Res.* **2016**, *9*, 3924; b) S. J. Lee, J.-W. Kim, J. H. Park, Y. Porte, J.-H. Kim, J.-W. Park, S. Kim, J.-M. Myoung, *J. Mater. Sci.* **2018**, *53*, 12284; c) J.-H. Park, H.-J. Seok, E. Kamaraj, S. Park, H.-K. Kim, *RSC Adv.* **2020**, *10*, 31856.
[178] B. W. An, E.-J. Gwak, K. Kim, Y.-C. Kim, J. Jang, J.-Y. Kim, J.-U. Park, *Nano Lett.* **2016**, *16*, 471.
[179] M. Zhao, D. Li, J. Huang, D. Wang, A. Mensah, Q. Wei, *J. Mater. Chem. C* **2019**, *7*, 13468.
[180] S. Hong, H. Lee, J. Lee, J. Kwon, S. Han, Y. D. Suh, H. Cho, J. Shin, J. Yeo, S. H. Ko, *Adv. Mater.* **2015**, *27*, 4744.
[181] Y. Li, Z. Zhang, X. Li, J. Zhang, H. Lou, X. Shi, X. Cheng, H. Peng, *J. Mater. Chem. C* **2017**, *5*, 41.
[182] J.-G. Lee, J.-H. Lee, S. An, D.-Y. Kim, T.-G. Kim, S. S. Al-Deyab, A. L. Yarin, S. S. Yoon, *J. Mater. Chem. A* **2017**, *5*, 6677.
[183] a) J. Jang, B. G. Hyun, S. Ji, E. Cho, B. W. An, W. H. Cheong, J.-U. Park, *NPG Asia Mater.* **2017**, *9*, e432; b) D. Han, Y. Li, X. Jiang, W. Zhao, F. Wang, W. Lan, E. Xie, W. Han, *Compos. Sci. Technol.* **2018**, *168*, 460.
[184] M. Zhang, C. Wang, X. Liang, Z. Yin, K. Xia, H. Wang, M. Jian, Y. Zhang, *Adv. Electron. Mater.* **2017**, *3*, 1700193.
[185] a) Y. Xu, B. Sun, Y. Ling, Q. Fei, Z. Chen, X. Li, P. Guo, N. Jeon, S. Goswami, Y. Liao, *Proc. Natl. Acad. Sci. USA* **2020**, *117*, 205; b) P.-C. Hsu, A. Y. Song, P. B. Catrysse, C. Liu, Y. Peng, J. Xie, S. Fan, Y. Cui, *Science* **2016**, *353*, 1019.
[186] a) A. Nozariasbmarz, H. Collins, K. Dsouza, M. H. Polash, M. Hosseini, M. Hyland, J. Liu, A. Malhotra, F. M. Ortiz, F. Mohaddes, *Appl. Energy* **2020**, *258*, 114069; b) W. He, G. Zhang, X. Zhang, J. Ji, G. Li, X. Zhao, *Appl. Energy* **2015**, *143*, 1.
[187] A. R. M. Siddique, S. Mahmud, B. Van Heyst, *Renewable Sustainable Energy Rev.* **2017**, *73*, 730.
[188] G. Zhang, X. Zhang, H. Huang, J. Wang, Q. Li, L. Q. Chen, Q. Wang, *Adv. Mater.* **2016**, *28*, 4811.
[189] G. Agarwal, N. Besuchet, B. Audergon, J. Paik, *Sci. Rep.* **2016**, *6*, 34224.
[190] P. Brochu, Q. Pei, *Electroactivity in Polymeric Materials*, Springer, New York **2012**, p. 1.

[191] B. Chen, Y. Bai, F. Xiang, J. Y. Sun, Y. M. Chen, H. Wang, J. Zhou, Z. Suo, *J. Polym. Sci., Part B: Polym. Phys.* **2014**, *52*, 1055.
[192] A. Miriyev, K. Stack, H. Lipson, *Nat. Commun.* **2017**, *8*, 596.
[193] W. Zheng, G. Alici, P. R. Clingan, B. J. Munro, G. M. Spinks, J. R. Steele, G. G. Wallace, *J. Polym. Sci., Part B: Polym. Phys.* **2013**, *51*, 57.
[194] U. Kim, J. Kang, C. Lee, H. Y. Kwon, S. Hwang, H. Moon, J. C. Koo, J.-D. Nam, B. H. Hong, J.-B. Choi, *Nanotechnology* **2013**, *24*, 145501.
[195] Z. Zhou, Q. Li, L. Chen, C. Liu, S. Fan, *J. Mater. Chem. B* **2016**, *4*, 1228.
[196] X. Ji, A. E. l. Haitami, F. Sorba, S. Rosset, G. T. Nguyen, C. Plesse, F. Vidal, H. R. Shea, S. Cantin, *Sens. Actuators, B* **2018**, *261*, 135.
[197] N. Besse, S. Rosset, J. J. Zarate, H. Shea, *Adv. Mater. Technol.* **2017**, *2*, 1700102.
[198] W.-E. Ju, Y.-J. Moon, C.-H. Park, S. T. Choi, *Smart Mater. Struct.* **2014**, *23*, 074004.
[199] H. R. Choi, D. Kim, N. H. Chuc, N. H. L. Vuong, J. Koo, J.-D. Nam, Y. Lee, *Electroactive Polymer Actuators and Devices (EAPAD)*, Proc. SPIE, Vol. *7287*, SPIE, Bellingham, WA **2009**.
[200] C. Son, K. Ko, H. J. Lee, K. Na, J. Han, K.-S. Yun, E.-S. Yoon, E. Kim, I.-J. Cho, *Microsyst. Technol.* **2016**, *22*, 2587.
[201] S. Saga, K. Deguchi, in *2010 IEEE Haptics Symp.*, IEEE, Waltham, MA, USA **2010**, pp. 309–312.
[202] G. Bubak, A. Ansaldo, L. Ceseracciu, K. Hata, D. Ricci, *Electroactive Polymer Actuators and Devices (EAPAD) 2014*, Proc. SPIE, Vol. *9056*, SPIE, Bellingham, WA **2014**.
[203] a) P. Polygerinos, Z. Wang, K. C. Galloway, R. J. Wood, C. J. Walsh, *Rob. Auton. Syst.* **2015**, *73*, 135; b) A. T. Asbeck, K. Schmidt, C. J. Walsh, *Rob. Auton. Syst.* **2015**, *73*, 102; c) E. T. Roche, R. Wohlfarth, J. T. Overvelde, N. V. Vasilyev, F. A. Pigula, D. J. Mooney, K. Bertoldi, C. J. Walsh, *Adv. Mater.* **2014**, *26*, 1200; d) X. de Tinguy, T. Howard, C. Pacchierotti, M. Marchal, A. Lécuyer, in *WeATaViX: WEarable Actuated TAngibles for VIrtual reality eXperiences*, Springer, Cham **2020**, pp. 262–270; e) B. Kim, J. Ryu, K.-J. Cho, *Sensors* **2020**, *20*, 2852.
[204] S. Rosset, H. R. Shea, *Appl. Phys. A* **2013**, *110*, 281.
[205] J.-B. Chossat, D. K. Chen, Y.-L. Park, P. B. Shull, *IEEE Trans. Haptics* **2019**, *12*, 521.
[206] M. T. Thai, T. T. Hoang, P. T. Phan, N. H. Lovell, T. N. Do, *IEEE Access* **2020**, *8*, 157878.
[207] S. J. Varma, K. Sambath Kumar, S. Seal, S. Rajaraman, J. Thomas, *Adv. Sci.* **2018**, *5*, 1800340.
[208] Y. Wang, S. Gong, S. J. Wang, G. P. Simon, W. Cheng, *Mater. Horiz.* **2016**, *3*, 208.
[209] B. Zhu, Y. Ling, L. W. Yap, M. Yang, F. Lin, S. Gong, Y. Wang, T. An, Y. Zhao, W. Cheng, *ACS Appl. Mater. Interfaces* **2019**, *11*, 29014.
[210] D.-J. Chou, *U.S. Patent 6,151,968*, **2000**.
[211] D. B. McCombie, A. T. Reisner, H. H. Asada, in *2006 Int. Conf. of the IEEE Engineering in Medicine and Biology Society*, IEEE, New York **2006**, pp. 3521–3524.
[212] S. Park, K. Fukuda, M. Wang, C. Lee, T. Yokota, H. Jin, H. Jinno, H. Kimura, P. Zalar, N. Matsuhisa, *Adv. Mater.* **2018**, *30*, 1802359.
[213] Q. Zhai, S. Gong, Y. Wang, Q. Lyu, Y. Liu, Y. Ling, J. Wang, G. P. Simon, W. Cheng, *ACS Appl. Mater. Interfaces* **2019**, *11*, 9724.
[214] K. S. Ling, A. J. Ringrose, P. J. Markan, G. Amit, D. J. Clifton, E. K. Askin, *U.S. Patent Application 29/521,264*, **2016**.
[215] a) X. Liu, H. Gao, J. E. Ward, X. Liu, B. Yin, T. Fu, J. Chen, D. R. Lovley, J. Yao, *Nature* **2020**, *578*, 550; b) C. Yang, Y. Huang, H. Cheng, L. Jiang, L. Qu, *Adv. Mater.* **2019**, *31*, 1805705; c) F. Zhao, H. Cheng, Z. Zhang, L. Jiang, L. Qu, *Adv. Mater.* **2015**, *27*, 4351; d) Y. Xu, G. Zhao, L. Zhu, Q. Fei, Z. Zhang, Z. Chen, F. An, Y. Chen, Y. Ling, P. Guo, *Proc. Natl. Acad. Sci. USA* **2020**, *117*, 18292.
[216] a) A. Bandodkar, S. Lee, I. Huang, W. Li, S. Wang, C.-J. Su, W. Jeang, T. Hang, S. Mehta, N. Nyberg, *Nat. Electron.* **2020**, *3*, 554; b) Y. Song, J. Min, Y. Yu, H. Wang, Y. Yang, H. Zhang, W. Gao, *Sci. Adv.* **2020**, *6*, eaay9842.
[217] A. J. Bandodkar, *J. Electrochem. Soc.* **2016**, *164*, H3007.
[218] I. Jeerapan, J. R. Sempionatto, J. Wang, *Adv. Funct. Mater.* **2019**, *30*, 1906243.
[219] J. Kim, I. Jeerapan, J. R. Sempionatto, A. Barfidokht, R. K. Mishra, A. S. Campbell, L. J. Hubble, J. Wang, *Acc. Chem. Res.* **2018**, *51*, 2820.
[220] a) F. C. Sales, R. M. Iost, M. V. Martins, M. C. Almeida, F. N. Crespilho, *Lab Chip* **2013**, *13*, 468; b) L. Fu, J. Liu, Z. Hu, M. Zhou, *Electroanalysis* **2018**, *30*, 2535.
[221] W. Jia, G. Valdés-Ramírez, A. J. Bandodkar, J. R. Windmiller, J. Wang, *Angew. Chem., Int. Ed.* **2013**, *52*, 7233.
[222] A. J. Bandodkar, I. Jeerapan, J.-M. You, R. Nuñez-Flores, J. Wang, *Nano Lett.* **2016**, *16*, 721.
[223] A. J. Bandodkar, J.-M. You, N.-H. Kim, Y. Gu, R. Kumar, A. V. Mohan, J. Kurniawan, S. Imani, T. Nakagawa, B. Parish, *Energy Environ. Sci.* **2017**, *10*, 1581.
[224] a) G. M. Olyveira, J. H. Kim, M. V. Martins, R. M. Iost, K. N. Chaudhari, J.-S. Yu, F. N. Crespilho, *J. Nanosci. Nanotechnol.* **2012**, *12*, 356; b) E. Cho, M. Mohammadifar, S. Choi, *Micromachines* **2017**, *8*, 265.
[225] I. Jeerapan, J. R. Sempionatto, A. Pavinatto, J.-M. You, J. Wang, *J. Mater. Chem. A* **2016**, *4*, 18342.
[226] S. Cosnier, A. J. Gross, A. L. Goff, M. Holzinger, *J. Power Sources* **2016**, *325*, 252.
[227] A. Zebda, J.-P. Alcaraz, P. Vadgama, S. Shleev, S. D. Minteer, F. Boucher, P. Cinquin, D. K. Martin, *Bioelectrochemistry* **2018**, *124*, 57.
[228] Z. Liu, H. Li, B. Shi, Y. Fan, Z. L. Wang, Z. Li, *Adv. Funct. Mater.* **2019**, *29*, 1808820.
[229] Z. Lin, B. Zhang, H. Guo, Z. Wu, H. Zou, J. Yang, Z. L. Wang, *Nano Energy* **2019**, *64*, 103908.
[230] S. S. Kwak, H. J. Yoon, S. W. Kim, *Adv. Funct. Mater.* **2019**, *29*, 1804533.
[231] a) Z. Lin, J. Chen, J. Yang, *J. Nanomater.* **2016**, *2016*, 5651613; b) J. Chen, S. K. Oh, N. Nabulsi, H. Johnson, W. Wang, J.-H. Ryou, *Nano Energy* **2019**, *57*, 670; c) H. Chu, H. Jang, Y. Lee, Y. Chae, J.-H. Ahn, *Nano Energy* **2016**, *27*, 298.
[232] Y. Wang, C. Chen, H. Xie, T. Gao, Y. Yao, G. Pastel, X. Han, Y. Li, J. Zhao, K. Fu, *Adv. Funct. Mater.* **2017**, *27*, 1703140.
[233] J. Yu, X. Hou, M. Cui, S. Zhang, J. He, W. Geng, J. Mu, X. Chou, *Nano Energy* **2019**, *64*, 103923.
[234] K. N. Kim, J. Chun, J. W. Kim, K. Y. Lee, J.-U. Park, S.-W. Kim, Z. L. Wang, J. M. Baik, *ACS Nano* **2015**, *9*, 6394.
[235] T. Zhou, C. Zhang, C. B. Han, F. R. Fan, W. Tang, Z. L. Wang, *ACS Appl. Mater. Interfaces* **2014**, *6*, 14695.
[236] a) S. Li, J. Wang, W. Peng, L. Lin, Y. Zi, S. Wang, G. Zhang, Z. L. Wang, *Adv. Energy Mater.* **2017**, *7*, 1602832; b) Z. Wen, Y. Yang, N. Sun, G. Li, Y. Liu, C. Chen, J. Shi, L. Xie, H. Jiang, D. Bao, *Adv. Funct. Mater.* **2018**, *28*, 1803684; c) Z. Li, J. Shen, I. Abdalla, J. Yu, B. Ding, *Nano Energy* **2017**, *36*, 341; d) X. Pu, W. Song, M. Liu, C. Sun, C. Du, C. Jiang, X. Huang, D. Zou, W. Hu, Z. L. Wang, *Adv. Energy Mater.* **2016**, *6*, 1601048.
[237] W. Seung, M. K. Gupta, K. Y. Lee, K.-S. Shin, J.-H. Lee, T. Y. Kim, S. Kim, J. Lin, J. H. Kim, S.-W. Kim, *ACS Nano* **2015**, *9*, 3501.
[238] Y. Yang, N. Sun, Z. Wen, P. Cheng, H. Zheng, H. Shao, Y. Xia, C. Chen, H. Lan, X. Xie, *ACS Nano* **2018**, *12*, 2027.
[239] a) T. Huang, C. Wang, H. Yu, H. Wang, Q. Zhang, M. Zhu, *Nano Energy* **2015**, *14*, 226; b) S. Lee, W. Ko, Y. Oh, J. Lee, G. Baek, Y. Lee, J. Sohn, S. Cha, J. Kim, J. Park, *Nano Energy* **2015**, *12*, 410.
[240] X. He, Y. Zi, H. Guo, H. Zheng, Y. Xi, C. Wu, J. Wang, W. Zhang, C. Lu, Z. L. Wang, *Adv. Funct. Mater.* **2017**, *27*, 1604378.
[241] a) X. Pu, L. Li, M. Liu, C. Jiang, C. Du, Z. Zhao, W. Hu, Z. L. Wang, *Adv. Mater.* **2016**, *28*, 98; b) X. Pu, W. Hu, Z. L. Wang, *Small* **2018**, *14*, 1702817.

[242] a) X.-S. Zhang, M. Han, B. Kim, J.-F. Bao, J. Brugger, H. Zhang, *Nano Energy* **2018**, *47*, 410; b) K. Dong, X. Peng, Z. L. Wang, *Adv. Mater.* **2020**, *32*, 1902549.
[243] a) Y. Qiu, D. Yang, B. Li, S. Shao, L. Hu, *RSC Adv.* **2018**, *8*, 26243; b) L. Dhakar, P. Pitchappa, F. E. H. Tay, C. Lee, *Nano Energy* **2016**, *19*, 532.
[244] a) M. Salauddin, R. Toyabur, P. Maharjan, M. Rasel, J. Kim, H. Cho, J. Y. Park, *Nano Energy* **2018**, *51*, 61; b) U. J. Yang, J. W. Lee, J. P. Lee, J. M. Baik, *Nano Energy* **2019**, *57*, 293; c) T. Kim, S. Jeon, S. Lone, S. J. Doh, D.-M. Shin, H. K. Kim, Y.-H. Hwang, S. W. Hong, *Nano Energy* **2018**, *54*, 209.
[245] A. R. Mule, B. Dudem, H. Patnam, S. A. Graham, J. S. Yu, *ACS Sustainable Chem. Eng.* **2019**, *7*, 16450.
[246] a) S. Niu, Y. Liu, X. Chen, S. Wang, Y. S. Zhou, L. Lin, Y. Xie, Z. L. Wang, *Nano Energy* **2015**, *12*, 760; b) T. Huang, J. Zhang, B. Yu, H. Yu, H. Long, H. Wang, Q. Zhang, M. Zhu, *Nano Energy* **2019**, *58*, 375; c) A. Yu, X. Pu, R. Wen, M. Liu, T. Zhou, K. Zhang, Y. Zhang, J. Zhai, W. Hu, Z. L. Wang, *ACS Nano* **2017**, *11*, 12764.
[247] B. Dudem, A. R. Mule, H. R. Patnam, J. S. Yu, *Nano Energy* **2019**, *55*, 305.
[248] a) V. Jella, S. Ippili, J.-H. Eom, S. Pammi, J.-S. Jung, V.-D. Tran, V. H. Nguyen, A. Kirakosyan, S. Yun, D. Kim, *Nano Energy* **2019**, *57*, 74; b) H. Yuan, T. Lei, Y. Qin, R. Yang, *Nano Energy* **2019**, *59*, 84; c) M. Wu, Y. Wang, S. Gao, R. Wang, C. Ma, Z. Tang, N. Bao, W. Wu, F. Fan, W. Wu, *Nano Energy* **2019**, *56*, 693.
[249] Z. L. Wang, *Adv. Funct. Mater.* **2008**, *18*, 3553.
[250] W. Wu, C. Pan, Y. Zhang, X. Wen, Z. L. Wang, *Nano Today* **2013**, *8*, 619.
[251] W. Wu, Z. L. Wang, *Nat. Rev. Mater.* **2016**, *1*, 16031.
[252] a) Z. Zhang, Y. Chen, J. Guo, *Phys. E* **2019**, *105*, 212; b) Y. Qiu, J. Lei, D. Yang, B. Yin, H. Zhang, J. Bian, J. Ji, Y. Liu, Y. Zhao, Y. Luo, *Appl. Phys. Lett.* **2014**, *104*, 113903.
[253] D. Zhang, Z. Yang, P. Li, M. Pang, Q. Xue, *Nano Energy* **2019**, *65*, 103974.
[254] a) J. Yu, X. Hou, M. Cui, N. Zhang, S. Zhang, J. He, X. Chou, *Mater. Lett.* **2020**, *269*, 127686; b) X. Guan, B. Xu, J. Gong, *Nano Energy* **2020**, *70*, 104516.
[255] a) W. Wu, S. Bai, M. Yuan, Y. Qin, Z. L. Wang, T. Jing, *ACS Nano* **2012**, *6*, 6231; b) X. Niu, W. Jia, S. Qian, J. Zhu, J. Zhang, X. Hou, J. Mu, W. Geng, J. Cho, J. He, *ACS Sustainable Chem. Eng.* **2018**, *7*, 979.
[256] X. Chen, X. Li, J. Shao, N. An, H. Tian, C. Wang, T. Han, L. Wang, B. Lu, *Small* **2017**, *13*, 1604245.
[257] a) S. K. Ghosh, D. Mandal, *Nano Energy* **2018**, *53*, 245; b) M. Kim, Y. S. Wu, E. C. Kan, J. Fan, *Polymers* **2018**, *10*, 745.
[258] a) S. You, L. Zhang, J. Gui, H. Cui, S. Guo, *Micromachines* **2019**, *10*, 302; b) S. Ye, C. Cheng, X. Chen, X. Chen, J. Shao, J. Zhang, H. Hu, H. Tian, X. Li, L. Ma, *Nano Energy* **2019**, *60*, 701.
[259] a) J. Liu, B. Yang, L. Lu, X. Wang, X. Li, X. Chen, J. Liu, *Sens. Actuators, A* **2020**, *303*, 111796; b) D. Ponnamma, H. Parangusan, A. Tanvir, M. A. A. AlMa'adeed, *Mater. Des.* **2019**, *184*, 108176; c) Y. Lu, Y. Jiang, Z. Lou, R. Shi, D. Chen, G. Shen, *Prog. Nat. Sci.: Mater. Int.* **2020**, *30*, 174.
[260] H. Gao, P. T. Minh, H. Wang, S. Minko, J. Locklin, T. Nguyen, S. Sharma, *Smart Mater. Struct.* **2018**, *27*, 095018.
[261] a) M. Lee, C. Y. Chen, S. Wang, S. N. Cha, Y. J. Park, J. M. Kim, L. J. Chou, Z. L. Wang, *Adv. Mater.* **2012**, *24*, 1759; b) A. S. Dahiya, F. Morini, S. Boubenia, K. Nadaud, D. Alquier, G. Poulin-Vittrant, *Adv. Mater. Technol.* **2018**, *3*, 1700249; c) M. Zhang, T. Gao, J. Wang, J. Liao, Y. Qiu, Q. Yang, H. Xue, Z. Shi, Y. Zhao, Z. Xiong, *Nano Energy* **2015**, *13*, 298.
[262] S. Siddiqui, H. B. Lee, D. I. Kim, L. T. Duy, A. Hanif, N. E. Lee, *Adv. Energy Mater.* **2018**, *8*, 1701520.
[263] a) X. Fu, L. Xu, J. Li, X. Sun, H. Peng, *Carbon* **2018**, *139*, 1063; b) E. G. Jeong, Y. Jeon, S. H. Cho, K. C. Choi, *Energy Environ. Sci.* **2019**, *12*, 1878; c) S. A. Hashemi, S. Ramakrishna, A. G. Aberle, *Energy Environ. Sci.* **2020**, *13*, 685; d) L. Qiu, J. Deng, X. Lu, Z. Yang, H. Peng, *Angew. Chem., Int. Ed.* **2014**, *53*, 10425; e) R. Tang, H. Huang, H. Tu, H. Liang, M. Liang, Z. Song, Y. Xu, H. Jiang, H. Yu, *Appl. Phys. Lett.* **2014**, *104*, 083501.
[264] a) K. Yu, S. Rich, S. Lee, K. Fukuda, T. Yokota, T. Someya, *Proc. IEEE* **2019**, *107*, 2137; b) K. Fukuda, K. Yu, T. Someya, *Adv. Energy Mater.* **2020**, *10*, 2000765; c) C. Wu, T. W. Kim, T. Guo, F. Li, *Nano. Energy* **2017**, *32*, 367; d) S. Arumugam, Y. Li, S. Senthilarasu, R. Torah, A. Kanibolotsky, A. Inigo, P. Skabara, S. Beeby, *J. Mater. Chem. A* **2016**, *4*, 5561.
[265] a) D. Yang, R. Yang, S. Priya, S. Liu, *Angew. Chem., Int. Ed.* **2019**, *58*, 4466; b) Z. Wu, P. Li, Y. Zhang, Z. Zheng, *Small Methods* **2018**, *2*, 1800031; c) Z. Liu, P. You, C. Xie, G. Tang, F. Yan, *Nano Energy* **2016**, *28*, 151; d) X. Wang, Z. Li, W. Xu, S. A. Kulkarni, S. K. Batabyal, S. Zhang, A. Cao, L. H. Wong, *Nano Energy* **2015**, *11*, 728.
[266] a) M. J. Yun, S. I. Cha, S. H. Seo, D. Y. Lee, *Sci. Rep.* **2015**, *5*, 11022; b) S. Pan, Z. Yang, P. Chen, J. Deng, H. Li, H. Peng, *Angew. Chem., Int. Ed.* **2014**, *126*, 6224; c) N. Zhang, J. Chen, Y. Huang, W. Guo, J. Yang, J. Du, X. Fan, C. Tao, *Adv. Mater.* **2016**, *28*, 263.
[267] a) X. Xu, K. Fukuda, A. Karki, S. Park, H. Kimura, H. Jinno, N. Watanabe, S. Yamamoto, S. Shimomura, D. Kitazawa, *Proc. Natl. Acad. Sci. USA* **2018**, *115*, 4589; b) Z. Jiang, K. Fukuda, X. Xu, S. Park, D. Inoue, H. Jin, M. Saito, I. Osaka, K. Takimiya, T. Someya, *Adv. Mater.* **2018**, *30*, 1707526; c) R. Liu, M. Takakuwa, A. Li, D. Inoue, D. Hashizume, K. Yu, S. Umezu, K. Fukuda, T. Someya, *Adv. Energy Mater.* **2020**, *10*, 2000523; d) T. Kim, J.-H. Kim, T. E. Kang, C. Lee, H. Kang, M. Shin, C. Wang, B. Ma, U. Jeong, T.-S. Kim, *Nat. Commun.* **2015**, *6*, 2015; e) J. G. Tait, B. J. Worfolk, S. A. Maloney, T. C. Hauger, A. L. Elias, J. M. Buriak, K. D. Harris, *Sol. Energy Mater. Sol. Cells* **2013**, *110*, 98.
[268] S. Xiong, L. Hu, L. Hu, L. Sun, F. Qin, X. Liu, M. Fahlman, Y. Zhou, *Adv. Mater.* **2019**, *31*, 1806616.
[269] M. Kaltenbrunner, M. S. White, E. D. Głowacki, T. Sekitani, T. Someya, N. S. Sariciftci, S. Bauer, *Nat. Commun.* **2012**, *3*, 770.
[270] H. Jinno, K. Fukuda, X. Xu, S. Park, Y. Suzuki, M. Koizumi, T. Yokota, I. Osaka, K. Takimiya, T. Someya, *Nat. Energy* **2017**, *2*, 780.
[271] a) M. A. Green, A. Ho-Baillie, H. J. Snaith, *Nat. Photonics* **2014**, *8*, 506; b) N.-G. Park, *Mater. Today* **2015**, *18*, 65.
[272] a) R. Li, X. Xiang, X. Tong, J. Zou, Q. Li, *Adv. Mater.* **2015**, *27*, 3831; b) B. J. Kim, D. H. Kim, Y. Y. Lee, H. W. Shin, G. S. Han, J. S. Hong, K. Mahmood, T. K. Ahn, Y. C. Joo, K. S. Hong, *Energy Environ. Sci.* **2015**, *8*, 916; c) Y. Li, L. Meng, Y. M. Yang, G. Xu, Z. Hong, Q. Chen, J. You, G. Li, Y. Yang, Y. Li, *Nat. Commun.* **2016**, *7*, 10214.
[273] C. Bi, B. Chen, H. Wei, S. DeLuca, J. Huang, *Adv. Mater.* **2017**, *29*, 1605900.
[274] J. Feng, X. Zhu, Z. Yang, X. Zhang, J. Niu, Z. Wang, S. Zuo, S. Priya, S. Liu, D. Yang, *Adv. Mater.* **2018**, *30*, 1801418.
[275] Z. Yang, J. Deng, X. Sun, H. Li, H. Peng, *Adv. Mater.* **2014**, *26*, 2643.
[276] a) X. Fan, Z. Chu, F. Wang, C. Zhang, L. Chen, Y. Tang, D. Zou, *Adv. Mater.* **2008**, *20*, 592; b) R. Zhou, W. Guo, R. Yu, C. Pan, *J. Mater. Chem. A* **2015**, *3*, 23028.
[277] a) D. Kuang, J. Brillet, P. Chen, M. Takata, S. Uchida, H. Miura, K. Sumioka, S. M. Zakeeruddin, M. Grätzel, *ACS Nano* **2008**, *2*, 1113; b) S. Ito, G. Rothenberger, P. Liska, P. Comte, S. M. Zakeeruddin, P. Péchy, M. K. Nazeeruddin, M. Grätzel, *Chem. Commun.* **2006**, 4004.
[278] S. Pan, Z. Yang, H. Li, L. Qiu, H. Sun, H. Peng, *J. Am. Chem. Soc.* **2013**, *135*, 10622.
[279] X. Fu, H. Sun, S. Xie, J. Zhang, Z. Pan, M. Liao, L. Xu, Z. Li, B. Wang, X. Sun, *J. Mater. Chem. A* **2018**, *6*, 45.
[280] a) Q. Xue, J. Sun, Y. Huang, M. Zhu, Z. Pei, H. Li, Y. Wang, N. Li, H. Zhang, C. Zhi, *Small* **2017**, *13*, 1701827; b) D. P. Dubal, N. R. Chodankar, D.-H. Kim, P. Gomez-Romero, *Chem. Soc. Rev.* **2018**, *47*, 2065.

[281] L. Dong, C. Xu, Y. Li, Z.-H. Huang, F. Kang, Q.-H. Yang, X. Zhao, *J. Mater. Chem. A* **2016**, *4*, 4659.
[282] C. V. M. Gopi, R. Vinodh, S. Sambasivam, I. M. Obaidat, H.-J. Kim, *J. Energy Storage* **2020**, *27*, 101035.
[283] a) C. Yu, C. Masarapu, J. Rong, B. Wei, H. Jiang, *Adv. Mater.* **2009**, *21*, 4793; b) T. Chen, Y. Xue, A. K. Roy, L. Dai, *ACS Nano* **2014**, *8*, 1039; c) T. Lv, Y. Yao, N. Li, T. Chen, *Nano Today* **2016**, *11*, 644.
[284] a) Y. Wang, Y. Song, Y. Xia, *Chem. Soc. Rev.* **2016**, *45*, 5925; b) V. Augustyn, P. Simon, B. Dunn, *Energy Environ. Sci.* **2014**, *7*, 1597.
[285] a) Y. Shi, L. Pan, B. Liu, Y. Wang, Y. Cui, Z. Bao, G. Yu, *J. Mater. Chem. A* **2014**, *2*, 6086; b) I. Shown, A. Ganguly, L. C. Chen, K. H. Chen, *Energy Sci. Eng.* **2015**, *3*, 2.
[286] a) T. An, Y. Ling, S. Gong, B. Zhu, Y. Zhao, D. Dong, L. W. Yap, Y. Wang, W. Cheng, *Adv. Mater. Technol.* **2019**, *4*, 1800473; b) Y. He, W. Chen, X. Li, Z. Zhang, J. Fu, C. Zhao, E. Xie, *ACS Nano* **2013**, *7*, 174.
[287] a) Y. Zhao, D. Dong, Y. Wang, S. Gong, T. An, L. W. Yap, W. Cheng, *ACS Appl. Mater. Interfaces* **2018**, *10*, 42612; b) L. Kou, T. Huang, B. Zheng, Y. Han, X. Zhao, K. Gopalsamy, H. Sun, C. Gao, *Nat. Commun.* **2014**, *5*, 3754; c) Y. Meng, Y. Zhao, C. Hu, H. Cheng, Y. Hu, Z. Zhang, G. Shi, L. Qu, *Adv. Mater.* **2013**, *25*, 2326.
[288] a) Y. Fu, X. Cai, H. Wu, Z. Lv, S. Hou, M. Peng, X. Yu, D. Zou, *Adv. Mater.* **2012**, *24*, 5713; b) L. Liu, Y. Yu, C. Yan, K. Li, Z. Zheng, *Nat. Commun.* **2015**, *6*, 7260.
[289] L. Lim, Y. Liu, W. Liu, R. Tjandra, L. Rasenthiram, Z. Chen, A. Yu, *ACS Appl. Mater. Interfaces* **2017**, *9*, 39576.
[290] a) Y. Wang, S. Gong, S. J. Wang, X. Yang, Y. Ling, L. W. Yap, D. Dong, G. P. Simon, W. Cheng, *ACS Nano* **2018**, *12*, 9742; b) Z. Zhang, L. Wang, Y. Li, Y. Wang, J. Zhang, G. Guan, Z. Pan, G. Zheng, H. Peng, *Adv. Energy Mater.* **2017**, *7*, 1601814.
[291] Y. Zhao, J. Liu, Y. Hu, H. Cheng, C. Hu, C. Jiang, L. Jiang, A. Cao, L. Qu, *Adv. Mater.* **2013**, *25*, 591.
[292] a) T. Chen, H. Peng, M. Durstock, L. Dai, *Sci. Rep.* **2014**, *4*, 3612; b) F. Li, J. Chen, X. Wang, M. Xue, G. Chen, *Adv. Funct. Mater.* **2015**, *25*, 4601; c) C. Zhao, C. Wang, Z. Yue, K. Shu, G. G. Wallace, *ACS Appl. Mater. Interfaces* **2013**, *5*, 9008.
[293] a) P. Xu, J. Kang, J.-B. Choi, J. Suhr, J. Yu, F. Li, J.-H. Byun, B.-S. Kim, T.-W. Chou, *ACS Nano* **2014**, *8*, 9437; b) A. Lamberti, F. Clerici, M. Fontana, L. Scaltrito, *Adv. Energy Mater.* **2016**, *6*, 1600050; c) H. Lee, S. Hong, J. Lee, Y. D. Suh, J. Kwon, H. Moon, H. Kim, J. Yeo, S. H. Ko, *ACS Appl. Mater. Interfaces* **2016**, *8*, 15449.
[294] A. Ramadoss, K.-Y. Yoon, M.-J. Kwak, S.-I. Kim, S.-T. Ryu, J.-H. Jang, *J. Power Sources* **2017**, *337*, 159.
[295] a) S. Gong, Y. Zhao, Q. Shi, Y. Wang, L. W. Yap, W. Cheng, *Electroanalysis* **2016**, *28*, 1298; b) Y. Wang, S. Gong, D. Dong, Y. Zhao, L. W. Yap, Q. Shi, T. An, Y. Ling, G. P. Simon, W. Cheng, *Nanoscale* **2018**, *10*, 15948.
[296] Z. Su, C. Yang, B. Xie, Z. Lin, Z. Zhang, J. Liu, B. Li, F. Kang, C. P. Wong, *Energy Environ. Sci.* **2014**, *7*, 2652.
[297] Y. Yang, Q. Huang, L. Niu, D. Wang, C. Yan, Y. She, Z. Zheng, *Adv. Mater.* **2017**, *29*, 1606679.
[298] Y. Huang, M. Zhong, Y. Huang, M. Zhu, Z. Pei, Z. Wang, Q. Xue, X. Xie, C. Zhi, *Nat. Commun.* **2015**, *6*, 10310.
[299] G. Zhou, F. Li, H.-M. Cheng, *Energy Environ. Sci.* **2014**, *7*, 1307.
[300] W. Liu, M. S. Song, B. Kong, Y. Cui, *Adv. Mater.* **2017**, *29*, 1603436.
[301] W. J. Song, S. Yoo, G. Song, S. Lee, M. Kong, J. Rim, U. Jeong, S. Park, *Batteries Supercaps* **2019**, *2*, 181.
[302] H. Li, Y. Ding, H. Ha, Y. Shi, L. Peng, X. Zhang, C. J. Ellison, G. Yu, *Adv. Mater.* **2017**, *29*, 1700898.
[303] a) W. Weng, Q. Sun, Y. Zhang, H. Lin, J. Ren, X. Lu, M. Wang, H. Peng, *Nano Lett.* **2014**, *14*, 3432; b) Y. Zhang, W. Bai, J. Ren, W. Weng, H. Lin, Z. Zhang, H. Peng, *J. Mater. Chem. A* **2014**, *2*, 11054.
[304] W. Liu, J. Chen, Z. Chen, K. Liu, G. Zhou, Y. Sun, M. S. Song, Z. Bao, Y. Cui, *Adv. Energy Mater.* **2017**, *7*, 1701076.
[305] J. Ren, Y. Zhang, W. Bai, X. Chen, Z. Zhang, X. Fang, W. Weng, Y. Wang, H. Peng, *Angew. Chem.* **2014**, *126*, 7998.
[306] M. Xie, J. Wang, X. Wang, M. Yin, C. Wang, D. Chao, X. Liu, *Macromol. Res.* **2016**, *24*, 965.
[307] a) W. Weng, Q. Sun, Y. Zhang, S. He, Q. Wu, J. Deng, X. Fang, G. Guan, J. Ren, H. Peng, *Adv. Mater.* **2015**, *27*, 1363; b) T. Liu, J. J. Xu, Q. C. Liu, Z. W. Chang, Y. B. Yin, X. Y. Yang, X. B. Zhang, *Small* **2017**, *13*, 1602952; c) D. Chen, Z. Lou, K. Jiang, G. Shen, *Adv. Funct. Mater.* **2018**, *28*, 1805596.
[308] a) R. Kumar, J. Shin, L. Yin, J. M. You, Y. S. Meng, J. Wang, *Adv. Energy Mater.* **2017**, *7*, 1602096; b) Y. Xu, Y. Zhang, Z. Guo, J. Ren, Y. Wang, H. Peng, *Angew. Chem.* **2015**, *127*, 15610; c) H.-J. Peng, J.-Q. Huang, Q. Zhang, *Chem. Soc. Rev.* **2017**, *46*, 5237.
[309] a) W. Gao, S. Emaminejad, H. Y. Y. Nyein, S. Challa, K. Chen, A. Peck, H. M. Fahad, H. Ota, H. Shiraki, D. Kiriya, D. H. Lien, G. A. Brooks, R. W. Davis, A. Javey, *Nature* **2016**, *529*, 509; b) S. Emaminejad, W. Gao, E. Wu, Z. A. Davies, H. Yin Yin Nyein, S. Challa, S. P. Ryan, H. M. Fahad, K. Chen, Z. Shahpar, S. Talebi, C. Milla, A. Javey, R. W. Davis, *Proc. Natl. Acad. Sci. USA* **2017**, *114*, 4625; c) Z. Huang, Y. Hao, Y. Li, H. Hu, C. Wang, A. Nomoto, T. Pan, Y. Gu, Y. Chen, T. Zhang, W. Li, Y. Lei, N. Kim, C. Wang, L. Zhang, J. W. Ward, A. Maralani, X. Li, M. F. Durstock, A. Pisano, Y. Lin, S. Xu, *Nat. Electron.* **2018**, *1*, 473; d) K. I. Jang, K. Li, H. U. Chung, S. Xu, H. N. Jung, Y. Yang, J. W. Kwak, H. H. Jung, J. Song, C. Yang, A. Wang, Z. Liu, J. Y. Lee, B. H. Kim, J. H. Kim, J. Lee, Y. Yu, B. J. Kim, H. Jang, K. J. Yu, J. Kim, J. W. Lee, J. W. Jeong, Y. M. Song, Y. Huang, Y. Zhang, J. A. Rogers, *Nat. Commun.* **2017**, *8*, 15894; e) J. Kim, P. Gutruf, A. M. Chiarelli, S. Y. Heo, K. Cho, Z. Xie, A. Banks, S. Han, K. I. Jang, J. W. Lee, K. T. Lee, X. Feng, Y. Huang, M. Fabiani, G. Gratton, U. Paik, J. A. Rogers, *Adv. Funct. Mater.* **2017**, *27*, 1604373; f) Y. Yu, J. Nassar, C. Xu, J. Min, Y. Yang, A. Dai, R. Doshi, A. Huang, Y. Song, R. Gehlhar, *Sci. Rob.* **2020**, *5*, eaaz7946; g) J. Kim, G. A. Salvatore, H. Araki, A. M. Chiarelli, Z. Xie, A. Banks, X. Sheng, Y. Liu, J. W. Lee, K.-I. Jang, *Sci. Adv.* **2016**, *2*, e1600418.
[310] X. Yu, Z. Xie, Y. Yu, J. Lee, A. Vazquez-Guardado, H. Luan, J. Ruban, X. Ning, A. Akhtar, D. Li, B. Ji, Y. Liu, R. Sun, J. Cao, Q. Huo, Y. Zhong, C. Lee, S. Kim, P. Gutruf, C. Zhang, Y. Xue, Q. Guo, A. Chempakasseril, P. Tian, W. Lu, J. Jeong, Y. Yu, J. Cornman, C. Tan, B. Kim, K. Lee, X. Feng, Y. Huang, J. A. Rogers, *Nature* **2019**, *575*, 473.
[311] a) J. A. Rogers, M. G. Lagally, R. G. Nuzzo, *Nature* **2011**, *477*, 45; b) S. Wagner, S. Bauer, *MRS Bull.* **2012**, *37*, 207; c) J. Lee, J. Wu, M. Shi, J. Yoon, S. I. Park, M. Li, Z. Liu, Y. Huang, J. A. Rogers, *Adv. Mater.* **2011**, *23*, 986.
[312] S. Xu, Y. Zhang, L. Jia, K. E. Mathewson, K.-I. Jang, J. Kim, H. Fu, X. Huang, P. Chava, R. Wang, *Science* **2014**, *344*, 70.
[313] M. Chen, L. Zhang, S. Duan, S. Jing, H. Jiang, M. Luo, C. Li, *Nanoscale* **2014**, *6*, 3796.
[314] Y. Zhao, B. Wang, H. Hojaiji, Z. Wang, S. Lin, C. Yeung, H. Lin, P. Nguyen, K. Chiu, K. Salahi, *Sci. Adv.* **2020**, *6*, eaaz0007.
[315] a) T. Sekitani, T. Yokota, K. Kuribara, M. Kaltenbrunner, T. Fukushima, Y. Inoue, M. Sekino, T. Isoyama, Y. Abe, H. Onodera, T. Someya, *Nat. Commun.* **2016**, *7*, 11425; b) S. Wang, J. Xu, W. Wang, G. N. Wang, R. Rastak, F. Molina-Lopez, J. W. Chung, S. Niu, V. R. Feig, J. Lopez, T. Lei, S. K. Kwon, Y. Kim, A. M. Foudeh, A. Ehrlich, A. Gasperini, Y. Yun, B. Murmann, J. B. Tok, Z. Bao, *Nature* **2018**, *555*, 83; c) M. Sugiyama, T. Uemura, M. Kondo, M. Akiyama, N. Namba, S. Yoshimoto, Y. Noda, T. Araki, T. Sekitani, *Nat. Electron.* **2019**, *2*, 351.
[316] S. Park, S. W. Heo, W. Lee, D. Inoue, Z. Jiang, K. Yu, H. Jinno, D. Hashizume, M. Sekino, T. Yokota, K. Fukuda, K. Tajima, T. Someya, *Nature* **2018**, *561*, 516.
[317] B.-U. Hwang, J.-H. Lee, T. Q. Trung, E. Roh, D.-I. Kim, S.-W. Kim, N.-E. Lee, *ACS Nano* **2015**, *9*, 8801.

[318] a) C.-Y. Lin, C.-H. Tsai, H.-T. Lin, L.-C. Chang, Y.-H. Yeh, Z. Pei, Y.-R. Peng, C.-C. Wu, *Org. Electron.* **2011**, *12*, 1777; b) D. D. Wen, F. Y. Yue, G. X. Li, G. X. Zheng, K. L. Chan, S. M. Chen, M. Chen, K. L. Li, P. W. H. Wong, K. W. Cheah, E. Y. B. Pun, S. Zhang, X. Z. Chen, *Nat. Commun.* **2015**, *6*, 8241; c) Y. Zhang, Z. Mei, T. Wang, W. Huo, S. Cui, H. Liang, X. Du, *Nano Energy* **2017**, *40*, 289.
[319] A. Rasheed, W. He, Y. Qian, H. Park, D. J. Kang, *ACS Appl. Mater. Interfaces* **2020**, *12*, 20891.
[320] A. M. Zamarayeva, A. E. Ostfeld, M. Wang, J. K. Duey, I. Deckman, B. P. Lechêne, G. Davies, D. A. Steingart, A. C. Arias, *Sci. Adv.* **2017**, *3*, e1602051.
[321] C. S. Kim, H. M. Yang, J. Lee, G. S. Lee, H. Choi, Y. J. Kim, S. H. Lim, S. H. Cho, B. J. Cho, *ACS Energy Lett.* **2018**, *3*, 501.
[322] A. Kurs, A. Karalis, R. Moffatt, J. D. Joannopoulos, P. Fisher, M. Soljačić, *Science* **2007**, *317*, 83.
[323] J. S. Ho, A. J. Yeh, E. Neofytou, S. Kim, Y. Tanabe, B. Patlolla, R. E. Beygui, A. S. Poon, *Proc. Natl. Acad. Sci. USA* **2014**, *111*, 7974.
[324] a) T. Le, K. Mayaram, T. Fiez, *IEEE J. Solid-State Circuits* **2008**, *43*, 1287; b) X. Huang, Y. Liu, G. W. Kong, J. H. Seo, Y. Ma, K. I. Jang, J. A. Fan, S. Mao, Q. Chen, D. Li, H. Liu, C. Wang, D. Patnaik, L. Tian, G. A. Salvatore, X. Feng, Z. Ma, Y. Huang, J. A. Rogers, *Microsyst. Nanoeng.* **2016**, *2*, 16052; c) S. I. Park, D. S. Brenner, G. Shin, C. D. Morgan, B. A. Copits, H. U. Chung, M. Y. Pullen, K. N. Noh, S. Davidson, S. J. Oh, J. Yoon, K. I. Jang, V. K. Samineni, M. Norman, J. G. Grajales-Reyes, S. K. Vogt, S. S. Sundaram, K. M. Wilson, J. S. Ha, R. Xu, T. Pan, T. I. Kim, Y. Huang, M. C. Montana, J. P. Golden, M. R. Bruchas, R. W. Gereau, J. A. Rogers, *Nat. Biotechnol.* **2015**, *33*, 1280.
[325] a) S. Niu, N. Matsuhisa, L. Beker, J. Li, S. Wang, J. Wang, Y. Jiang, X. Yan, Y. Yun, W. Burnett, A. S. Y. Poon, J. B. H. Tok, X. Chen, Z. Bao, *Nat. Electron.* **2019**, *2*, 361; b) D. P. Rose, M. E. Ratterman, D. K. Griffin, L. Hou, N. Kelley-Loughnane, R. R. Naik, J. A. Hagen, I. Papautsky, J. C. Heikenfeld, *IEEE Trans. Biomed. Eng.* **2015**, *62*, 1457.
[326] A. J. Bandodkar, P. Gutruf, J. Choi, K. Lee, Y. Sekine, J. T. Reeder, W. J. Jeang, A. J. Aranyosi, S. P. Lee, J. B. Model, *Sci. Adv.* **2019**, *5*, eaav3294.
[327] S. Imani, A. J. Bandodkar, A. M. Mohan, R. Kumar, S. Yu, J. Wang, P. P. Mercier, *Nat. Commun.* **2016**, *7*, 11650.
[328] X. Tian, P. M. Lee, Y. J. Tan, T. L. Wu, H. Yao, M. Zhang, Z. Li, K. A. Ng, B. C. Tee, J. S. Ho, *Nat. Electron.* **2019**, *2*, 243.
[329] a) J. Jeon, H. B. Lee, Z. Bao, *Adv. Mater.* **2013**, *25*, 850; b) L. Y. Chen, B. C. Tee, A. L. Chortos, G. Schwartz, V. Tse, D. J. Lipomi, H. S. Wong, M. V. McConnell, Z. Bao, *Nat. Commun.* **2014**, *5*, 5028; c) X. Huang, Y. Liu, H. Cheng, W.-J. Shin, J. A. Fan, Z. Liu, C.-J. Lu, G.-W. Kong, K. Chen, D. Patnaik, S.-H. Lee, S. Hage-Ali, Y. Huang, J. A. Rogers, *Adv. Funct. Mater.* **2014**, *24*, 3846.
[330] B. Chu, W. Burnett, J. W. Chung, Z. Bao, *Nature* **2017**, *549*, 328.
[331] R. Lin, H. J. Kim, S. Achavananthadith, S. A. Kurt, S. C. C. Tan, H. Yao, B. C. K. Tee, J. K. W. Lee, J. S. Ho, *Nat. Commun.* **2020**, *11*, 444.
[332] S. Liu, K. Ma, B. Yang, H. Li, X. Tao, *Adv. Funct. Mater.* **2020**, *2007254*, 1.
[333] Y. H. Jung, J.-H. Kim, J. A. Rogers, *Adv. Funct. Mater.* **2020**, *2008805*, 1.
[334] H. Kim, Y. T. Kwon, H. R. Lim, J. H. Kim, Y. S. Kim, W. H. Yeo, *Adv. Funct. Mater.* **2020**, *2005692*, 1.

Jae Joon Kim is currently a postdoctoral researcher in the Department of Electrical Engineering and Information Systems at the University of Tokyo, Tokyo, Japan. He received his Ph.D. degree at Nuclear and Quantum Engineering from Korea Advanced Institute of Science and Technology (KAIST) in 2015. From 2015 to 2019, he worked as a postdoctoral research fellow in the Polymer Science and Engineering, and Chemistry departments in the University of Massachusetts Amherst. His current research interests are bioelectronics including plant, microbe, and on-skin sensors.

Yan Wang is currently a postdoctoral researcher in the Department of Electrical Engineering and Information Systems at the University of Tokyo, Tokyo, Japan. She received her Ph.D. degree majoring in chemical engineering from Monash University in 2018. Her current research interests include stretchable conductors, wearable sensors, and soft energy devices.

Haoyang Wang is currently a Ph.D. candidate in the Department of Electrical Engineering and Information Systems at the University of Tokyo, Japan. He received his master's degree from the same department in 2020. His current research interests are mainly flexible sensors and devices.

Sunghoon Lee received his B.S. degree from the Department of Applied Physics, the University of Tokyo, Tokyo, Japan, in 2009, and his M.S. and Ph.D. degrees from the Department of Electrical and Electronic Engineering, the University of Tokyo, in 2011 and 2017, respectively. Since 2019, he has been a project assistant professor and a lecturer at the University of Tokyo. His current research interests include organic electronics, soft electronics, and flexible electronics.

Tomoyuki Yokota was born in Tochigi, Japan, in 1985. He received his Ph.D. degree from the Department of Applied Physics, the University of Tokyo, Tokyo, Japan, in 2013. Since 2019, he has been an associate professor at the Department of Electrical and Electronic Engineering, the University of Tokyo. His current research interests include organic photonic devices, flexible electronics, printed electronics, large-area sensors, and wearable electronics.

Takao Someya is a professor and dean of the Graduate School of Engineering, the University of Tokyo, Tokyo, Japan. He received his Ph.D. degree in electrical engineering from the University of Tokyo in 1997. From 2001 to 2003, he was a visiting scholar with the Nanocenter (NSEC), Columbia University, New York, NY, USA, and Bell Labs, Lucent Technologies, Murray Hill, NJ, USA. Since 2009, he has been a professor at the Department of Electrical and Electronic Engineering, the University of Tokyo. He has also been the team Leader at the Center for Emergent Matter Science in RIKEN since 2015.